NOAA Technical Report NESDIS 142-1

Regional Climate Trends and Scenarios for the U.S. National Climate Assessment

Part 1. Climate of the Northeast U.S.

Washington, D.C.
January 2013

U.S. DEPARTMENT OF COMMERCE
National Oceanic and Atmospheric Administration
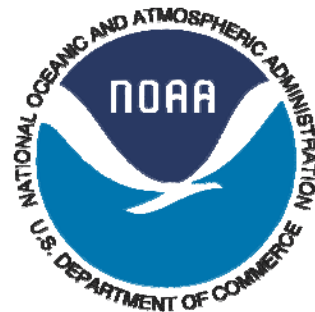National Environmental Satellite, Data, and Information Service

NOAA TECHNICAL REPORTS
National Environmental Satellite, Data, and Information Service

The National Environmental Satellite, Data, and Information Service (NESDIS) manages the Nation's civil Earth-observing satellite systems, as well as global national data bases for meteorology, oceanography, geophysics, and solar-terrestrial sciences. From these sources, it develops and disseminates environmental data and information products critical to the protection of life and property, national defense, the national economy, energy development and distribution, global food supplies, and the development of natural resources.

Publication in the NOAA Technical Report series does not preclude later publication in scientific journals in expanded or modified form. The NESDIS series of NOAA Technical Reports is a continuation of the former NESS and EDIS series of NOAA Technical Reports and the NESC and EDS series of Environmental Science Services Administration (ESSA) Technical Reports.

Copies of earlier reports may be available by contacting NESDIS Chief of Staff, NOAA/ NESDIS, 1335 East-West Highway, SSMC1, Silver Spring, MD 20910, (301) 713-3578.

Regional Climate Trends and Scenarios for the U.S. National Climate Assessment

Part 1. Climate of the Northeast U.S.

Kenneth E. Kunkel, Laura E. Stevens, Scott E. Stevens, and Liqiang Sun

Cooperative Institute for Climate and Satellites (CICS), North Carolina State University and NOAA's National Climatic Data Center (NCDC)
Asheville, NC

Emily Janssen and Donald Wuebbles

University of Illinois at Urbana-Champaign
Champaign, IL

Jessica Rennells and Art DeGaetano

Northeast Regional Climate Center
Cornell University
Ithaca, NY

J. Greg Dobson

National Environmental Modeling and Analysis Center
University of North Carolina at Asheville
Asheville, NC

PREFACE

This document is one of series of regional climate descriptions designed to provide input that can be used in the development of the National Climate Assessment (NCA). As part of a sustained assessment approach, it is intended that these documents will be updated as new and well-vetted model results are available and as new climate scenario needs become clear. It is also hoped that these documents (and associated data and resources) are of direct benefit to decision makers and communities seeking to use this information in developing adaptation plans.

There are nine reports in this series, one each for eight regions defined by the NCA, and one for the contiguous U.S. The eight NCA regions are the Northeast, Southeast, Midwest, Great Plains, Northwest, Southwest, Alaska, and Hawai'i/Pacific Islands.

These documents include a description of the observed historical climate conditions for each region and a set of climate scenarios as plausible futures – these components are described in more detail below.

While the datasets and simulations in these regional climate documents are not, by themselves, new, (they have been previously published in various sources), these documents represent a more complete and targeted synthesis of historical and plausible future climate conditions around the specific regions of the NCA.

There are two components of these descriptions. One component is a description of the historical climate conditions in the region. The other component is a description of the climate conditions associated with two future pathways of greenhouse gas emissions.

Historical Climate

The description of the historical climate conditions was based on an analysis of core climate data (the data sources are available and described in each document). However, to help understand, prioritize, and describe the importance and significance of different climate conditions, additional input was derived from climate experts in each region, some of whom are authors on these reports. In particular, input was sought from the NOAA Regional Climate Centers and from the American Association of State Climatologists. The historical climate conditions are meant to provide a perspective on what has been happening in each region and what types of extreme events have historically been noteworthy, to provide a context for assessment of future impacts.

Future Scenarios

The future climate scenarios are intended to provide an internally consistent set of climate conditions that can serve as inputs to analyses of potential impacts of climate change. The scenarios are not intended as projections as there are no established probabilities for their future realization. They simply represent an internally consistent climate picture using certain assumptions about the future pathway of greenhouse gas emissions. By "consistent" we mean that the relationships among different climate variables and the spatial patterns of these variables are derived directly from the same set of climate model simulations and are therefore physically plausible.

These future climate scenarios are based on well-established sources of information. No new climate model simulations or downscaled data sets were produced for use in these regional climate reports.

The use of the climate scenario information should take into account the following considerations:

1. All of the maps of climate variables contain information related to statistical significance of changes and model agreement. This information is crucial to appropriate application of the information. Three types of conditions are illustrated in these maps:

    a. The first condition is where most or all of the models simulate statistically significant changes and agree on the direction (whether increasing or decreasing) of the change. If this condition is present, then analyses of future impacts and vulnerabilities can more confidently incorporate this direction of change. It should be noted that the models may still produce a significant range of magnitude associated with the change, so the manner of incorporating these results into decision models will still depend to a large degree on the risk tolerance of the impacted system.

    b. The second condition is where the most or all of the models simulate changes that are too small to be statistically significant. If this condition is present, then assessment of impacts should be conducted on the basis that the future conditions could represent a small change from present or could be similar to current conditions and that the normal year-to-year fluctuations in climate dominate over any underlying long-term changes.

    c. The third condition is where most or all of the models simulate statistically significant changes but do not agree on the direction of the change, i.e. a sizeable fraction of the models simulate increases while another sizeable fraction simulate decreases. If this condition is present, there is little basis for a definitive assessment of impacts, and, separate assessments of potential impacts under an increasing scenario and under a decreasing scenario would be most prudent.

2. The range of conditions produced in climate model simulations is quite large. Several figures and tables provide quantification for this range. Impacts assessments should consider not only the mean changes, but also the range of these changes.

3. Several graphics compare historical observed mean temperature and total precipitation with model simulations for the same historical period. These should be examined since they provide one basis for assessing confidence in the model simulated future changes in climate.

    a. Temperature Changes: Magnitude. In most regions, the model simulations of the past century simulate the magnitude of change in temperature from observations; the southeast region being an exception where the lack of century-scale observed warming is not simulated in any model.

    b. Temperature Changes: Rate. The *rate* of warming over the last 40 years is well simulated in all regions.

    c. Precipitation Changes: Magnitude. Model simulations of precipitation generally simulate the overall observed trend but the observed decade-to-decade variations are greater than the model observations.

In general, for impacts assessments, this information suggests that the model simulations of temperature conditions for these scenarios are likely reliable, but users of precipitation simulations may want to consider the likelihood of decadal-scale variations larger than simulated by the models. It should also be noted that accompanying these documents will be a web-based resource with downloadable graphics, metadata about each, and more information and links to the datasets and overall descriptions of the process.

1. INTRODUCTION

The Global Change Research Act of 1990[1] mandated that national assessments of climate change be prepared not less frequently than every four years. The last national assessment was published in 2009 (Karl et al. 2009). To meet the requirements of the act, the Third National Climate Assessment (NCA) report is now being prepared. The National Climate Assessment Development and Advisory Committee (NCADAC), a federal advisory committee established in the spring of 2011, will produce the report. The NCADAC Scenarios Working Group (SWG) developed a set of specifications with regard to scenarios to provide a uniform framework for the chapter authors of the NCA report.

This climate document was prepared to provide a resource for authors of the Third National Climate Assessment report, pertinent to the states of Maine, New Hampshire, Vermont, Massachusetts, Rhode Island, Connecticut, New York, New Jersey, Pennsylvania, Delaware, Maryland, and West Virginia, as well as Washington DC; hereafter referred to collectively as the Northeast. The specifications of the NCADAC SWG, along with anticipated needs for historical information, guided the choices of information included in this description of Northeast climate. While guided by these specifications, the material herein is solely the responsibility of the authors and usage of this material is at the discretion of the 2013 NCA report authors.

This document has two main sections: one on historical conditions and trends, and the other on future conditions as simulated by climate models. The historical section concentrates on temperature and precipitation, primarily based on analyses of data from the National Weather Service's (NWS) Cooperative Observer Network, which has been in operation since the late 19th century. Additional climate features are discussed based on the availability of information. The future simulations section is exclusively focused on temperature and precipitation.

With regard to the future, the NCADAC, at its May 20, 2011 meeting, decided that scenarios should be prepared to provide an overall context for assessment of impacts, adaptation, and mitigation, and to coordinate any additional modeling used in synthesizing or analyzing the literature. Scenario information for climate, sea-level change, changes in other environmental factors (such as land cover), and changes in socioeconomic conditions (such as population growth and migration) have been prepared. This document provides an overall description of the climate information.

In order to complete this document in time for use by the NCA report authors, it was necessary to restrict its scope in the following ways. Firstly, this document does not include a comprehensive description of all climate aspects of relevance and interest to a national assessment. We restricted our discussion to climate conditions for which data were readily available. Secondly, the choice of climate model simulations was also restricted to readily available sources. Lastly, the document does not provide a comprehensive analysis of climate model performance for historical climate conditions, although a few selected analyses are included.

The NCADAC directed the "use of simulations forced by the A2 emissions scenario as the primary basis for the high climate future and by the B1 emissions scenario as the primary basis for the low climate future for the 2013 report" for climate scenarios. These emissions scenarios were generated by the Intergovernmental Panel on Climate Change (IPCC) and are described in the IPCC Special

---

[1] http://thomas.loc.gov/cgi-bin/bdquery/z?d101:SN00169:|TOM:/bss/d101query.html

Report on Emissions Scenarios (SRES) (IPCC 2000). These scenarios were selected because they incorporate much of the range of potential future human impacts on the climate system and because there is a large body of literature that uses climate and other scenarios based on them to evaluate potential impacts and adaptation options. These scenarios represent different narrative storylines about possible future social, economic, technological, and demographic developments. These SRES scenarios have internally consistent relationships that were used to describe future pathways of greenhouse gas emissions. The A2 scenario "describes a very heterogeneous world. The underlying theme is self-reliance and preservation of local identities. Fertility patterns across regions converge very slowly, which results in continuously increasing global population. Economic development is primarily regionally oriented and per capita economic growth and technological change are more fragmented and slower than in the other storylines" (IPCC 2000). The B1 scenario describes "a convergent world with…global population that peaks in mid-century and declines thereafter…but with rapid changes in economic structures toward a service and information economy, with reductions in material intensity, and the introduction of clean and resource-efficient technologies. The emphasis is on global solutions to economic, social, and environmental sustainability, including improved equity, but without additional climate initiatives" (IPCC 2000).

The temporal changes of emissions under these two scenarios are illustrated in Fig. 1 (left panel). Emissions under the A2 scenario continually rise during the 21st century from about 40 gigatons (Gt) CO_2-equivalent per year in the year 2000 to about 140 Gt CO_2-equivalent per year by 2100. By contrast, under the B1 scenario, emissions rise from about 40 Gt CO_2-equivalent per year in the year 2000 to a maximum of slightly more than 50 Gt CO_2-equivalent per year by mid-century, then falling to less than 30 Gt CO_2-equivalent per year by 2100. Under both scenarios, CO_2 concentrations rise throughout the 21st century. However, under the A2 scenario, there is an acceleration in concentration trends, and by 2100 the estimated concentration is above 800 ppm. Under the B1 scenario, the rate of increase gradually slows and concentrations level off at about 500 ppm by 2100. An increase of 1 ppm is equivalent to about 8 Gt of CO_2. The increase in concentration is considerably smaller than the rate of emissions because a sizeable fraction of the emitted CO_2 is absorbed by the oceans.

The projected CO_2 concentrations are used to estimate the effects on the earth's radiative energy budget, and this is the key forcing input used in global climate model simulations of the future. These simulations provide the primary source of information about how the future climate could evolve in response to the changing composition of the earth's atmosphere. A large number of modeling groups performed simulations of the 21st century in support of the IPCC's Fourth Assessment Report (AR4), using these two scenarios. The associated changes in global mean temperature by the year 2100 (relative to the average temperature during the late 20th century) are about +6.5°F (3.6°C) under the A2 scenario and +3.2°F (1.8°C) under the B1 scenario with considerable variations among models (Fig. 1, right panel).
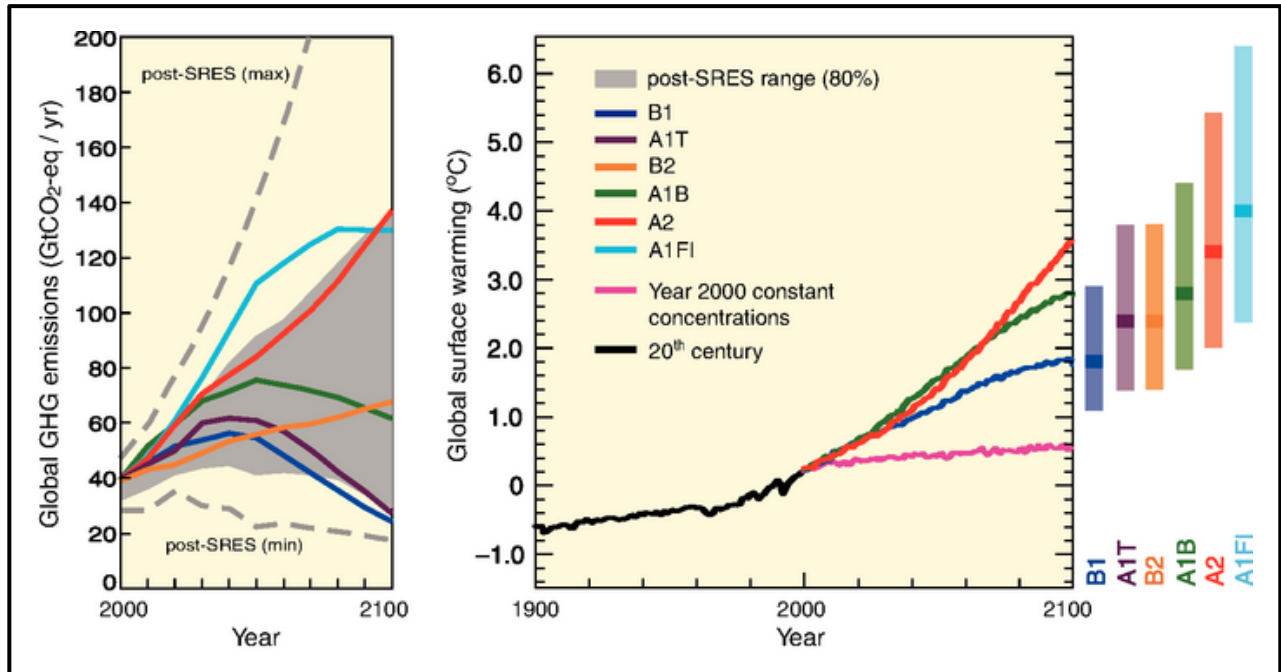
Figure 1. Left Panel: Global GHG emissions (in GtCO₂-eq) in the absence of climate policies: six illustrative SRES marker scenarios (colored lines) and the 80ᵗʰ percentile range of recent scenarios published since SRES (post-SRES) (gray shaded area). Dashed lines show the full range of post-SRES scenarios. The emissions include CO₂, CH₄, N₂O and F-gases. Right Panel: Solid lines are multi-model global averages of surface warming for scenarios A2, A1B and B1, shown as continuations of the 20ᵗʰ-century simulations. These projections also take into account emissions of short-lived GHGs and aerosols. The pink line is not a scenario, but is for Atmosphere-Ocean General Circulation Model (AOGCM) simulations where atmospheric concentrations are held constant at year 2000 values. The bars at the right of the figure indicate the best estimate (solid line within each bar) and the likely range assessed for the six SRES marker scenarios at 2090-2099. All temperatures are relative to the period 1980-1999. From IPCC AR4, Sections 3.1 and 3.2, Figures 3.1 and 3.2, IPCC (2007b).

In addition to the direct output of the global climate model simulations, the NCADAC approved "the use of both statistically- and dynamically-downscaled data sets". "Downscaling" refers to the process of producing higher-resolution simulations of climate from the low-resolution outputs of the global models. The motivation for use of these types of data sets is the spatial resolution of global climate models. While the spatial resolution of available global climate model simulations varies widely, many models have resolutions in the range of 100-200 km (~60-120 miles). Such scales are very large compared to local and regional features important to many applications. For example, at these scales mountain ranges are not resolved sufficiently to provide a reasonably accurate representation of the sharp gradients in temperature, precipitation, and wind that typically exist in these areas.

Statistical downscaling achieves higher-resolution simulations through the development of statistical relationships between large-scale atmospheric features that are well-resolved by global models and the local climate conditions that are not well-resolved. The statistical relationships are developed by comparing observed local climate data with model simulations of the recent historical climate. These relationships are then applied to the simulations of the future to obtain local high-

resolution projections. Statistical downscaling approaches are relatively economical from a computational perspective, and thus they can be easily applied to many global climate model simulations. One underlying assumption is that the relationships between large-scale features and local climate conditions in the present climate will not change in the future (Wilby and Wigley 1997). Careful consideration must also be given when deciding how to choose the appropriate predictors because statistical downscaling is extremely sensitive to the choice of predictors (Norton et al. 2011).

Dynamical downscaling is much more computationally intensive but avoids assumptions about constant relationships between present and future. Dynamical downscaling uses a climate model, similar in most respects to the global climate models. However, the climate model is run at a much higher resolution but only for a small region of the earth (such as North America) and is termed a "regional climate model (RCM)". A global climate model simulation is needed to provide the boundary conditions (e.g., temperature, wind, pressure, and humidity) on the lateral boundaries of the region. Typically, the spatial resolution of an RCM is 3 or more times higher than the global model used to provide the boundary conditions. With this higher resolution, topographic features and smaller-scale weather phenomena are better represented. The major downside of dynamical downscaling is that a simulation for a region can take as much computer time as a global climate model simulation for the entire globe. As a result, the availability of such simulations is limited, both in terms of global models used for boundary conditions and time periods of the simulations (Hayhoe 2010).

Section 3 of this document (Future Regional Climate Scenarios) responds to the NCADAC directives by incorporating analyses from multiple sources. The core source is the set of global climate model simulations performed for the IPCC AR4, also referred to as the Climate Model Intercomparison Project phase 3 (CMIP3) suite. These have undergone extensive evaluation and analysis by many research groups. A second source is a set of statistically-downscaled data sets based on the CMIP3 simulations. A third source is a set of dynamically-downscaled simulations, driven by CMIP3 models. A new set of global climate model simulations is being generated for the IPCC Fifth Assessment Report (AR5). This new set of simulations is referred to as the Climate Model Intercomparison Project phase 5 (CMIP5). These scenarios do not incorporate any CMIP5 simulations as relatively few were available at the time the data analyses were initiated.
As noted earlier, the information included in this document is primarily concentrated around analyses of temperature and precipitation. This is explicitly the case for the future scenarios sections; due in large part to the short time frame and limited resources, we capitalized on the work of other groups on future climate simulations, and these groups have devoted a greater effort to the analysis of temperature and precipitation than other surface climate variables.

Climate models have generally exhibited a high level of ability to simulate the large-scale circulation patterns of the atmosphere. These include the seasonal progression of the position of the jet stream and associated storm tracks, the overall patterns of temperature and precipitation, the occasional occurrence of droughts and extreme temperature events, and the influence of geography on climatic patterns. There are also important processes that are less successfully simulated by models, as noted by the following selected examples.

Climate model simulation of clouds is problematic. Probably the greatest uncertainty in model simulations arises from clouds and their interactions with radiative energy fluxes (Dufresne and Bony 2008). Uncertainties related to clouds are largely responsible for the substantial range of

global temperature change in response to specified greenhouse gas forcing (Randall et al. 2007). Climate model simulation of precipitation shows considerable sensitivities to cloud parameterization schemes (Arakawa 2004). Cloud parameterizations remain inadequate in current GCMs. Consequently, climate models have large biases in simulating precipitation, particularly in the tropics. Models typically simulate too much light precipitation and too little heavy precipitation in both the tropics and middle latitudes, creating potential biases when studying extreme events (Bader et al. 2008).

Climate models also have biases in simulation of some important climate modes of variability. The El Niño-Southern Oscillation (ENSO) is a prominent example. In some parts of the U.S., El Niño and La Niña events make important contributions to year-to-year variations in conditions. Climate models have difficulty capturing the correct phase locking between the annual cycle and ENSO (AchutaRao and Sperber 2002). Some climate models also fail to represent the spatial and temporal structure of the El Niño - La Niña asymmetry (Monahan and Dai 2004). Climate simulations over the U.S. are affected adversely by these deficiencies in ENSO simulations.

The model biases listed above add additional layers of uncertainty to the information presented herein and should be kept in mind when using the climate information in this document.

The representation of the results of the suite of climate model simulations has been a subject of active discussion in the scientific literature. In many recent assessments, including AR4, the results of climate model simulations have been shown as multi-model mean maps (e.g., Figs. 10.8 and 10.9 in Meehl et al. 2007). Such maps give equal weight to all models, which is thought to better represent the present-day climate than any single model (Overland et al. 2011). However, models do not represent the current climate with equal fidelity. Knutti (2010) raises several issues about the multi-model mean approach. These include: (a) some model parameterizations may be tuned to observations, which reduces the spread of the results and may lead to underestimation of the true uncertainty; (b) many models share code and expertise and thus are not independent, leading to a reduction in the true number of independent simulations of the future climate; (c) all models have some processes that are not accurately simulated, and thus a greater number of models does not necessarily lead to a better projection of the future; and (d) there is no consensus on how to define a metric of model fidelity, and this is likely to depend on the application. Despite these issues, there is no clear superior alternative to the multi-model mean map presentation for general use. Tebaldi et al. (2011) propose a method for incorporating information about model variability and consensus. This method is adopted here where data availability make it possible. In this method, multi-model mean values at a grid point are put into one of three categories: (1) models agree on the statistical significance of changes and the sign of the changes; (2) models agree that the changes are not statistically significant; and (3) models agree that the changes are statistically significant but disagree on the sign of the changes. The details on specifying the categories are included in Section 3.

2. REGIONAL CLIMATE TRENDS AND IMPORTANT CLIMATE FACTORS

2.1. Description of Data Sources

One of the core data sets used in the United States for climate analysis is the National Weather Service's Cooperative Observer Network (COOP), which has been in operation since the late 19th century. The resulting data can be used to examine long-term trends. The typical COOP observer takes daily observations of various climate elements that might include precipitation, maximum temperature, minimum temperature, snowfall, and snow depth. While most observers are volunteers, standard equipment is provided by the National Weather Service (NWS), as well as training in standard observational practices. Diligent efforts are made by the NWS to find replacement volunteers when needed to ensure the continuity of stations whenever possible. Over a thousand of these stations have been in operation continuously for many decades (NOAA 2012a).

For examination of U.S. long-term trends in temperature and precipitation, the COOP data is the best available resource. Its central purpose is climate description (although it has many other applications as well); the number of stations is large, there have been relatively few changes in instrumentation and procedures, and it has been in existence for over 100 years. However, there are some sources of temporal inhomogeneities in station records, described as follows:

- One instrumental change is important. For much of the COOP history, the standard temperature system was a pair of liquid-in-glass (LIG) thermometers placed in a radiation shield known as the Cotton Region Shelter (CRS). In the 1980s, the NWS began replacing this system with an electronic maximum-minimum temperature system (MMTS). Inter-comparison experiments indicated that there is a systematic difference between these two instrument systems, with the newer electronic system recording lower daily maximum temperatures (T_{max}) and higher daily minimum temperatures (T_{min}) (Quayle et al. 1991; Hubbard and Lin 2006; Menne et al. 2009). Menne et al. (2009) estimate that the mean shift (going from CRS/LIG to MMTS) is -0.52K for T_{max} and +0.37K for T_{min}. Adjustments for these differences can be applied to monthly mean temperature to create homogeneous time series.

- Changes in the characteristics and/or locations of sites can introduce artificial shifts or trends in the data. In the COOP network, a station is generally not given a new name or identifier unless it moves at least 5 miles and/or changes elevation by at least 100 feet (NWS 1993). Site characteristics can change over time and affect a station's record, even if no move is involved (and even small moves << 5 miles can have substantial impacts). A common source of such changes is urbanization around the station, which will generally cause artificial warming, primarily in T_{min} (Karl et al. 1988), the magnitude of which can be several degrees in the largest urban areas. Most research suggests that the overall effect on national and global temperature trends is rather small because of the large number of rural stations included in such analyses (Karl et al. 1988; Jones et al. 1990) and because homogenization procedures reduce the urban signal (Menne et al. 2009).

- Station siting can cause biases. Recent research by Menne et al. (2010) and Fall et al. (2011) examined this issue in great detail. The effects on mean trends was found to be small in both studies, but Fall et al. (2011) found that stations with poor siting overestimate (underestimate) minimum (maximum) temperature trends.

- Changes in the time that observations are taken can also introduce artificial shifts or trends in the data (Karl et al. 1986; Vose et al. 2003). In the COOP network, typical observation times are early morning or late afternoon, near the usual times of the daily minimum and maximum temperatures. Because observations occur near the times of the daily extremes, a change in observation time can have a measurable effect on averages, irrespective of real changes. The study by Karl et al. (1986) indicates that the difference in monthly mean temperatures between early morning and late afternoon observers can be in excess of 2°C. There has, in fact, been a major shift from a preponderance of afternoon observers in the early and middle part of the 20th century to a preponderance of morning observers at the present time. In the 1930s, nearly 80% of the COOP stations were afternoon observers (Karl et al. 1986). By the early 2000s, the number of early morning observers was more than double the number of late afternoon observers (Menne et al. 2009). This shift tends to introduce an artificial cooling trend in the data.

A recent study by Williams et al. (2011) found that correction of known and estimated inhomogeneities lead to a larger warming trend in average temperature, principally arising from correction of the biases introduced by the changeover to the MMTS and from the biases introduced by the shift from mostly afternoon observers to mostly morning observers.

Much of the following analysis on temperature, precipitation, and snow is based on COOP data. Nationally, data for approximately 10,000 stations for temperature and 14,000 stations for precipitation were used in the general descriptions of temperature and precipitation conditions. For some of these analyses, a subset of 726 COOP stations with long periods of record was used, specifically less than 10% missing data for the period of 1895-2011; of these 726 stations, 52 are located in the Northeast region. The use of a consistent network is important when examining trends in order to minimize artificial shifts arising from a changing mix of stations.

2.2.   General Description of Northeast Climate

The Northeast region is characterized by a highly diverse climate with large spatial variations. Several geographic factors contribute to this. The moderating effects of the Atlantic Ocean affect coastal areas, and the inland regions are also influenced by large water bodies such as the Great Lakes and Lake Champlain. During much of the year, the prevailing westerly flow brings air masses from the interior North American continent across the entire region, bringing bitter cold to the region during winter. The polar jet stream is often located near or over the region during the winter, with frequent storm systems bringing cloudy skies, windy conditions, and precipitation. In the southern portions of the region, the Appalachian Mountains act to partially shield coastal regions from these interior air masses, while also shielding the western part of the region from the warm, humid air masses characteristic of the western Atlantic Ocean, although there is no barrier to humid air masses from the Gulf of Mexico. The local representations of the Appalachians (e.g., the Green Mountains of Vermont and the White Mountains of New Hampshire) also influence the climates of northern New England in ways that lead to significant differences vis-à-vis the climates of southern New England. All of the mountain ranges act as orographic barriers leading to the local enhancement of precipitation during storms through forced ascent of air flow.

Northeast summers are characteristically warm and humid in the southern part of the region due to a semi-permanent high-pressure system over the subtropical Atlantic Ocean that draws warm, humid

maritime air into the area. In the north, summers are considerably more moderate due to their latitude and the frequent intrusions of cooler air masses from Canada.

The Northeast is subject to a strong seasonal cycle and is often affected by extreme events such as ice storms, floods, droughts, heat waves, hurricanes and nor'easters. Its landscape is diverse, ranging from agricultural land to mountains to coastal beaches and estuaries. Other parts of the region are densely populated and highly urbanized. Thus, it is no surprise that the economy of the Northeastern United States is also sensitive to a range of climate influences. The agriculture, fisheries, forestry, recreation, and tourism sectors are particularly sensitive to climate (Hayhoe 2010).

The average annual temperatures in the Northeast (Fig. 2) are comparable to the Northwest region and cooler than the other four contiguous U.S. regions. The average annual temperature in the coastal regions, especially the more southern areas, is in the 50°F to 60°F range. The coldest average temperatures (between 35°F and 40°F) are observed along the northern border of Maine. Average temperatures in the Northeast generally decrease to the north and with elevation and distance from the coast.

Annual average precipitation ranges from less than 35 inches in parts of New York to over 50 inches along the New England coast. However, orographic effects produce localized amounts in excess of 60 inches at inland locations, particularly in West Virginia and New York. This orographic enhancement also leads to pockets of higher precipitation along the spines of the Green and White Mountains. Some lower elevation areas away from the coast that are partially blocked by mountains from oceanic moisture sources receive less than 40 inches. As with temperature, the amount of precipitation tends to decrease further inland.

During winter, blizzards and ice storms can be particularly crippling to local economies. A particularly disruptive phenomenon in the Northeast is the east coast winter storm, popularly known as the nor'easter. These storms derive their energy from the strong contrast in temperature between the interior of North America and the western Atlantic. The unique juxtaposition of the cold air to the northwest and warm and moist air to the southeast creates optimum conditions for the occasional explosive development of extratropical cyclones. With an abundant supply of moisture, these storms can produce crippling snowfall, flood-producing rainfall, hurricane-force winds, and dangerous cold. Major economic losses and loss of life can occur in the strongest of the storms. Lake-effect snows are another phenomenon affecting areas adjacent to the Great Lakes. Arctic air masses moving over the eastern Great Lakes are warmed, humidified and destabilized, often leading to intense bands of heavy snowfall over land areas downwind of Lakes Ontario and Erie.
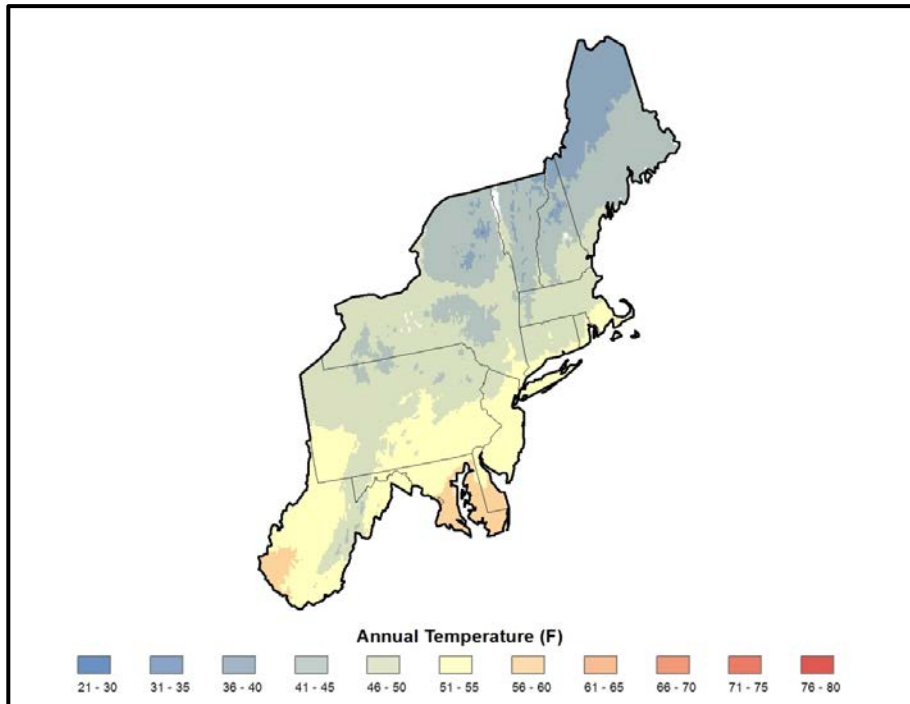
Figure 2. Average (1981-2010) annual temperature (°F) for the Northeast region. Based on a new gridded version of COOP data from the National Climatic Data Center, the CDDv2 data set (R. Vose, personal communication, July 27, 2012).
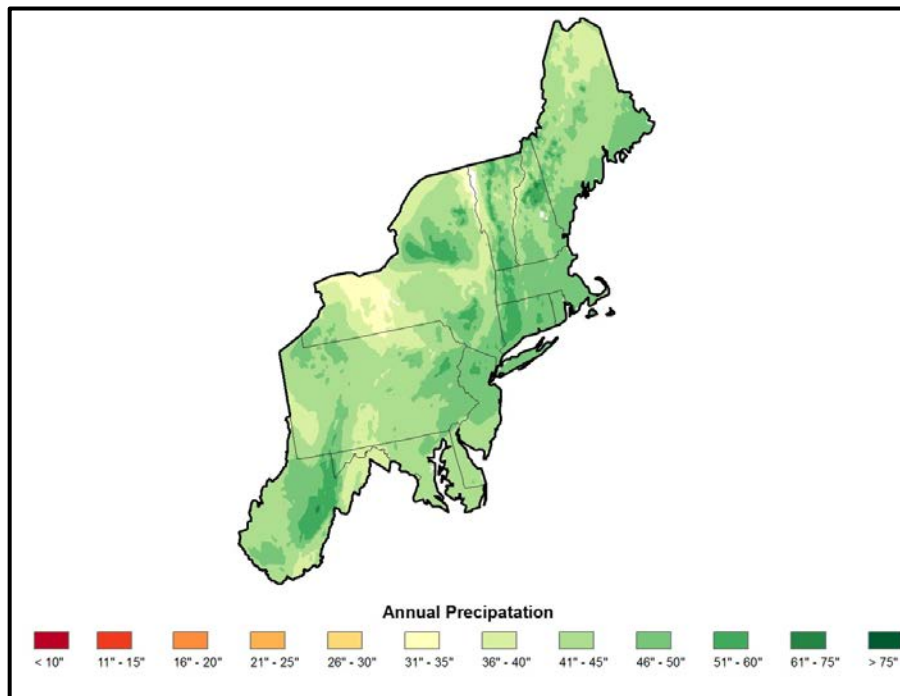

Figure 3. Average (1981-2010) annual precipitation (inches) for the Northeast region. Based on a new gridded version of COOP data from the National Climatic Data Center, the CDDv2 data set (R. Vose, personal communication, July 27, 2012).

The Northeast is the most urbanized assessment region. Its population density of 306 persons per square mile is more than double that of the second most urbanized region, the Southeast at 131 persons per square mile. Major urban centers in the region, ranked in the top 30 by population (U.S. Census Bureau 2011), include New York City (rank #1), Philadelphia (#6), Washington, DC (#7), Boston (#10), Baltimore (#20), and Pittsburgh (#22). These urban centers experience particular sensitivities that are unique to specific characteristics of the urban environment. Temperature extremes can have large impacts on human health, particularly in the urban core where the urban heat island effect raises summer temperatures. Severe storms, both winter and summer, result in major disruptions to surface and air transportation. Extreme rainfall causes a host of problems, including storm sewer overflow, flooding of homes and roadways, and contamination of municipal water supplies. Climate extremes, combined with urban pollution sources, can create air quality conditions that are detrimental to human health.

2.3. Important Climate Factors

The Northeast region experiences a wide range of extreme weather and climate events that affect human society, ecosystems, and infrastructure. This discussion is meant to provide general information about these types of weather and climate phenomena. These include:

2.3.1. Flood-Producing Extreme Precipitation

Frontal systems, thunderstorms, coastal storms, nor'easters, snowmelt, ice jams, and tropical storms all contribute to flooding in the Northeast. Coastal areas are also susceptible to storm surges. Taking the state of Vermont as an example, rarely does a year elapse without a flooding event of a significant magnitude being reported in at least one of Vermont's fourteen counties or perhaps statewide, making this the number-one weather-related hazard across that state. Between 1955 and 1999, floods accounted for $16.97 million in damage annually in Vermont (Dupigny-Giroux 2002).

On the region's largest rivers, spring snowmelt is a major cause of flooding. In Maine, record floods on the Kennebec occurred in 1936 and 1987 in association with melting snow and ice jams. Likewise on the Hudson near Albany, NY, record floods in the early 20th century, and more recently in 1977, resulted from snowmelt and ice jamming. At Pittsburgh, PA, both tropical storms and snowmelt have been responsible for floods on the Monongahela, with the flood of record being a March 1936 rain-on-snow event. The Potomac at Little Falls, MD, also reached its peak crest in this event. On the Susquehanna near Harrisburg, PA, five of the nine major floods since 1786 have occurred since 1972. Three of these floods occurred with tropical cyclones, one was due to precipitation associated with a stationary frontal boundary, and one was a rain-on-snow event. Similar mechanisms have been responsible for historical flooding in West Virginia. For instance, in 1985 the interaction between the remnants of Hurricane Juan and a secondary low-pressure system produced record floods in West Virginia that killed 47 people.

The region's smaller streams and tributaries are prone to flash flooding. Such floods typically occur during summer in association with intense convective rainfall. Land surface features such as the steep narrow drainages that characterize areas along and adjacent to the Appalachian Mountains contribute to flash flood risk. A recent flash flood in 1977 in Johnstown, PA killed 84 people and caused millions of dollars in damages. Nearly 12 inches of rain were measured in 10 hours within

the Conemaugh Valley, leading to the failure of several dams. Johnstown was also the site of the Great Flood of 1889 in which 2000 people lost their lives.

Urban flooding is also prevalent in the Northeast, because the development and proliferation of impervious paved surfaces limit the infiltration of water into the soil. During intense rainfall, the resulting runoff floods streets and underpasses, impacting traffic. Outside of urban areas, frozen ground and wet antecedent soil conditions also limit infiltration. In the case of rain on frozen ground, downward percolation is inhibited, leading to surface runoff, as occurred during the ice storm of January 1998 (Dupigny-Giroux 2002).

2.3.2. East Coast Winter Storms (Nor'easters)

Winter storms are common occurrences in the Northeast. There have been 45 high-impact storms since 1947 (Kocin and Uccellini 2004a), with the impacts of many documented by Kocin and Uccellini (2004b). The Blizzard of '96 was a classic nor'easter with record-breaking snowfall that resulted in 96 deaths as well as many closures and cancellations. In the middle-Atlantic region, the winters of 2009-2010 and 2010-2011 saw many locations break daily and seasonal snowfall records as the result of frequent nor'easters. These events resulted in power outages, motor vehicle accidents, and school and event cancellations. Transportation was severely disrupted with widespread economic effects.

2.3.3. Lake-Effect Snow

Like nor'easters, lake-effect snows also cause frequent winter climate impacts in portions of the Northeast. These events occur when air masses move off of relatively warm, unfrozen lakes, into a much colder area onshore, so longer ice-free periods have the potential to extend the period when lake-effect snows are possible. Although the impacts of lake-effect snowstorms are not as widespread as nor'easters, they can be just as significant. In December of 1995, lake-effect snow fell at a rate of 2 to 4 inches per hour, totaling 28-38" in Buffalo, NY.

2.3.4. Ice Storms

The Northeast is also prone to freezing rain. Cortinas et al. (2004) show that across the United States, the annual number of hours with freezing rain is maximized in the Northeast, largely due to the region's proximity to winter storm tracks and topography. Ice accumulations from freezing rain can cause dangerous situations. In January of 1998 a massive ice storm affected portions of upstate New York, northern New England and eastern Canada. The extent, thickness of accumulated ice (as much as 2 – 3 inches), duration, and overall impact of the storm are considered the most severe of any ice storm to hit eastern North America in recent history (DeGaetano 2000). Over 350,000 U.S. homes lost power for as long as 25 days. Ice storms can also cause significant disturbance to forest ecosystems. Forestry losses for this storm exceeded 57 million dollars.

2.3.5. Heat Waves

High temperatures, combined with high humidity, can create dangerous heat index values, particularly in the major metropolitan areas of the Northeast. Strings of three or more consecutive days above 90°F are common, occurring almost every year. Three-day runs of 100°F are rare, occurring only twice in over 130 years of record at Central Park, New York and twice in 70 years in

Philadelphia, PA and Washington, DC. Two-day runs of 100°F have occurred 10 times in Washington, DC, with five of these occurrences observed since 1990.

In the heat wave of July 1995 temperatures reached or exceeded 90° on all but one of 25 consecutive days in Washington, DC, which resulted in 19 deaths there as well as 11 deaths in New York City. In addition to negative effects on human health, heat waves cause high power usage and brown or blackouts as a result of increased demand from air conditioner use.

2.3.6. Drought

In the Northeast, droughts lasting one to three months occur every two or three years. The drought of the 1960's is the benchmark drought that lasted from the fall of 1961 to the spring of 1967, affecting the entire Northeast. Almost 50% of the Northeast was in extreme or severe drought from 1964-1967. Short-lived drought periods also punctuated the 1980s through early 2000s, most notably in 1985-1986, 1988, 1992-1993, and 2000-2003. In addition to agricultural impacts, these droughts have affected water resources. Water use restrictions, and in some cases water rationing, were common during drought periods in the metropolitan and suburban areas of the Northeast.

2.3.7. Tropical Cyclones

Since 1900, coastal counties in the Northeast have experienced between 1 and 8 hurricane strikes, with the highest frequencies occurring in Massachusetts (Cape Cod, Nantucket and Martha's Vineyard) and New York's Long Island (Fig. 4). Major hurricanes have struck Suffolk County on the eastern end of Long Island five times since 1900. The most notable storm to strike Long Island was a Category 3 hurricane in 1938. It brought a greater than 13-foot storm surge to Rhode Island and claimed more than 600 lives in New York and New England. As the storm tracked inland through New England, considerable flooding and wind damage were reported throughout Massachusetts, Vermont and New Hampshire. In terms of 2010 dollars this storm was the 19th most costly hurricane to affect the United States, with estimated damages totaling 6.3 billion dollars (Blake et al. 2011). In August 2011, Hurricane Irene made landfall along the southern New Jersey coast as a tropical storm and then continuing northward over New York City as a tropical storm. Rainfall from Irene caused extensive flooding inland in New Jersey, New York and Vermont, where 2-day rainfall totals exceeded ten inches in some locations. Wind and coastal storm surge damage also accompanied the storm, leaving millions of homes and businesses without power. Hundreds of thousands of tourists and residents were ordered to evacuate coastal areas of the Delmarva Peninsula, New Jersey and New York. Public transportation systems were shut down. There were 45 fatalities and damage is estimated at near 10 billion dollars.

Often persistent rain from the remnants of tropical systems have produced widespread, and at times, catastrophic flooding in the region. For example, the Great Flood of 1927 in Vermont resulted from record rainfall totals produced by tropical storm remnants on November 3, following October precipitation totals that had been 50 percent above normal. Agnes in 1972 also produced catastrophic flooding damage in parts of Pennsylvania and southern New York.
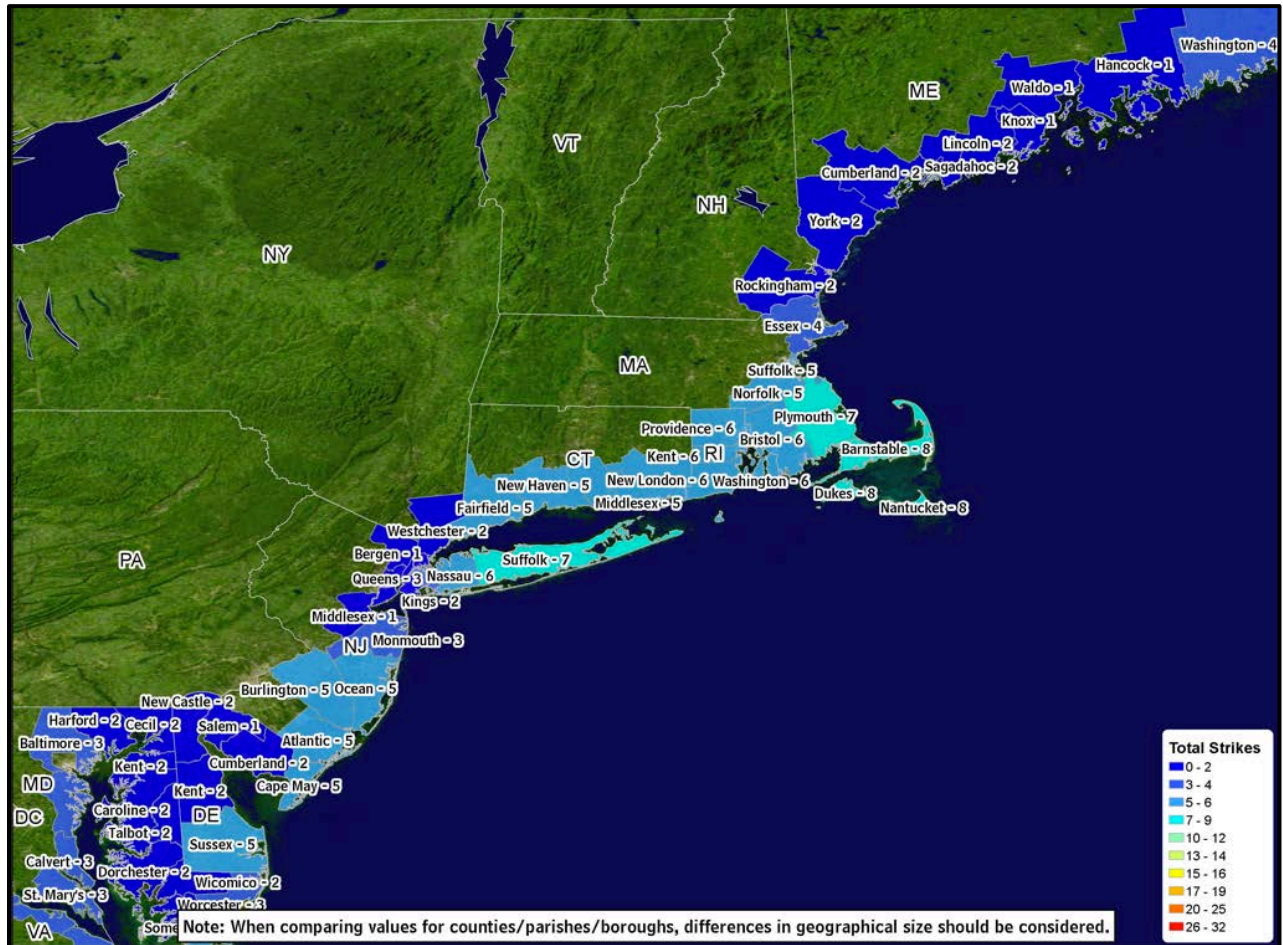
Figure 4. Number of hurricane strikes per county along the Northeast coast 1900-2010. Figure courtesy of the National Hurricane Center (NWS 2012b), from Jarrell et al. (1992) and updates.

2.3.8. Fog

Fog is a common occurrence, especially mornings during the fall and spring seasons in the Northeast. Radiation fog is common in the mountains and valleys due to rapid overnight cooling, while coastal fog is common during early mornings in winter. Dense fog reduces visibility, causing deadly traffic accidents and creating hazardous navigation conditions for aviation and mariners.

2.4. Climatic Trends

The temperature and precipitation data sets used to examine trends were obtained from NOAA's National Climatic Data Center (NCDC). The NCDC data is based on NWS Cooperative Observer Network (COOP) observations, as descibed in Section 2.1. Some analyses use daily observations for selected stations from the COOP network. Other analyses use a new national gridded monthly data set at a resolution of 5 x 5 km, for the time period of 1895-2011. This gridded data set is derived from bias-corrected monthly station data and is named the "Climate Division Database version 2 beta" (CDDv2) and is scheduled for public release in January 2013 (R. Vose, NCDC, personal communication, July 27, 2012).

The COOP data were processed using 1901-1960 as the reference period to calculate anomalies. In Section 3, this period is used for comparing net warming between model simulations and observations. There were two considerations in choosing this period for this purpose. Firstly, while some gradually-increasing anthropogenic forcing was present in the early and middle part of the 20th century, there is a pronounced acceleration of the forcing after 1960 (Meehl et al. 2003). Thus, there is an expectation that the effects of that forcing on surface climate conditions should accelerate after 1960. This year was therefore chosen as the ending year of the reference period. Secondly, in order to average out the natural fluctuations in climate as much as possible, it is desirable to use the longest practical reference period. Both observational and climate model data are generally available starting around the turn of the 20th century, thus motivating the use of 1901 as the beginning year of the reference period. We use this period as the reference for historical time series appearing in this section in order to be consistent with related figures in Section 3.

2.4.1. Temperature

Figure 5 shows annual and seasonal time series of temperature anomalies for the period of 1895-2011. Across the Northeast temperatures have generally remained above the 1901-1960 average for the last 30 years, both annually and especially during the winter. The warmest year on record through 2011 is 1998. The warmest winter on record for the region is 2001-2002. Fifteen of the last twenty winters from 1992-2011 have been above average. Warming has been more pronounced during the winter and spring seasons.

Table 1 shows temperature trends for the period of 1895-2011, using the CDDv2 data set. Values are only displayed for trends that are statistically significant at the 95% confidence level. Temperature trends are upward and statistically significant for each season, as well as the year as a whole, with magnitudes ranging from +0.11 to +0.24°F/decade.

Table 1. 1895-2011 trends in temperature anomaly (°F/decade) and precipitation anomaly (inches/decade) based on a new gridded version of COOP data from the National Climatic Data Center, the CDDv2 data set (R. Vose, personal communication, July 27, 2012) for the Northeast U.S., for each season as well as the year as a whole. Only values statistically significant at the 95% confidence level are displayed. Statistical significance of trends was assessed using Kendall's tau coefficient. The test using tau is a non-parametric hypothesis test.

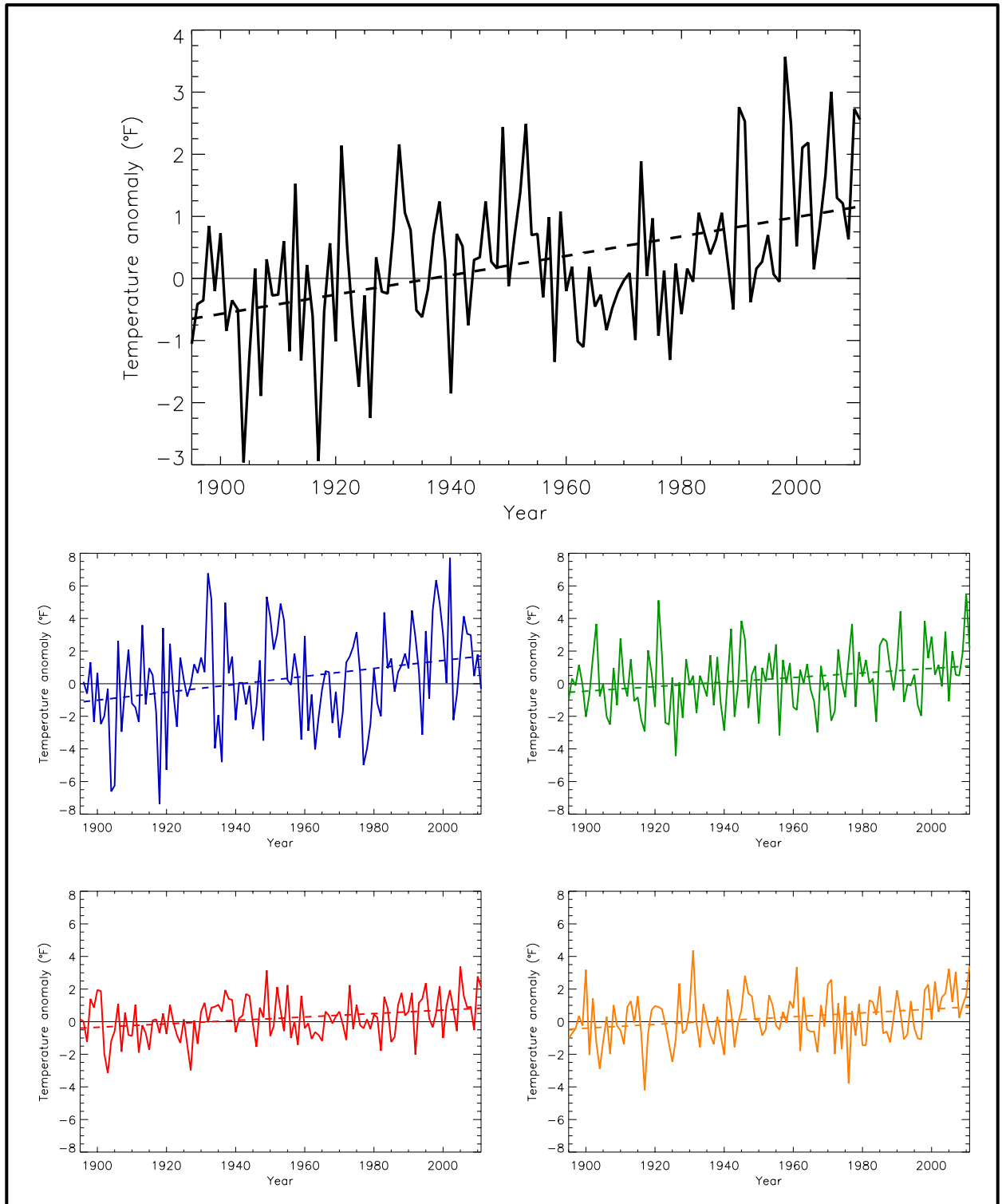| Season	Temperature (°F/decade)	Precipitation (inches/decade)
Winter	+0.24	—
Spring	+0.14	—
Summer	+0.11	—
Fall	+0.12	+0.24
Annual	+0.16	+0.39

Figure 5. Temperature anomaly (deviations from the 1901-1960 average, °F) for annual (black), winter (blue), spring (green), summer (red), and fall (orange), for the Northeast U.S. Dashed lines indicate the best fit by minimizing the chi-square error statistic. Based on a new gridded version of COOP data from the National Climatic Data Center, the CDDv2 data set (R. Vose, personal communication, July 27, 2012). Note that the annual time series is on a unique scale. Trends are upward and statistically significant annually and for all seasons.

2.4.2. *Precipitation*

Figure 6 shows annual and seasonal time series of precipitation anomalies for the period of 1895-2011, again calculated using the CDDv2 data set. Annual precipitation has varied over time, showing a clear shift towards greater variability and higher totals since 1970. The wettest year since 1895 was 2011, while the 2nd driest year occurred in 1996. The 1960s were characterized by a very severe, long-term drought that was particularly intense in the New England region, where it spanned almost the entire decade. The Northeast's three driest years were 1930, 1941, and 1965. Summer precipitation does not exhibit an overall trend, but, over the past 10 years, there have been a few very wet summers, including 2006 (wettest on record) and 2009 (second wettest on record).

Trends in precipitation for the period of 1895-2011 can be seen in Table 1. Precipitation trends are not statistically significant for winter, spring, or summer, however, the upward annual and fall trends (as seen in Fig. 6) are statistically significant, with magnitudes of +0.39 and +0.24 inches/decade, respectively.

See http://charts.srcc.lsu.edu/trends/ (LSU 2012) for a comparative seasonal or annual climate trend analysis of a specified state from the Northeast, which uses National Climate Data Center (NCDC) monthly and annual temperature and precipitation datasets.

2.4.3. *Extreme Heat and Cold*

Large spatial variations in the temperature climatology of this region result in analogous spatial variations in the definition of "extreme temperature". We define here extremes as relative to a location's overall temperature climatology, in terms of local frequency of occurrence.

Figure 7 shows time series of an index intended to represent heat and cold wave events. This index specifically reflects the number of 4-day duration episodes with extreme hot and cold temperatures, exceeding a threshold for a 1 in 5-year recurrence interval, calculated using daily COOP data from long-term stations. Extreme events are first identified for each individual climate observing station. Then, annual values of the index are gridding the station values and averaging the grid box values.

There is a large amount of interannual variability in extreme cold periods and extreme hot periods, reflecting the fact that, when they occur, such events affect large areas and thus large numbers of stations in the region simultaneously experience an extreme event exceeding the 1 in 5-year threshold.

The occurrence of heat waves, as shown in Fig. 7 (top), can be divided into 3 epochs. The period from the late 19th century into the 1950s was characterized by a moderately high number of heat waves. From the late 1950s into the early 1980s, there were few intense heat waves. Since the late 1980s, the frequency of heat waves has been similar to the early half of the 20th century. The highest value of the index occurred in 1988, which was a year of intense drought and heat throughout much of the nation. More recently, the years of 2001, 2002, 2010, and 2011 were characterized by moderately high values of the heat wave index.
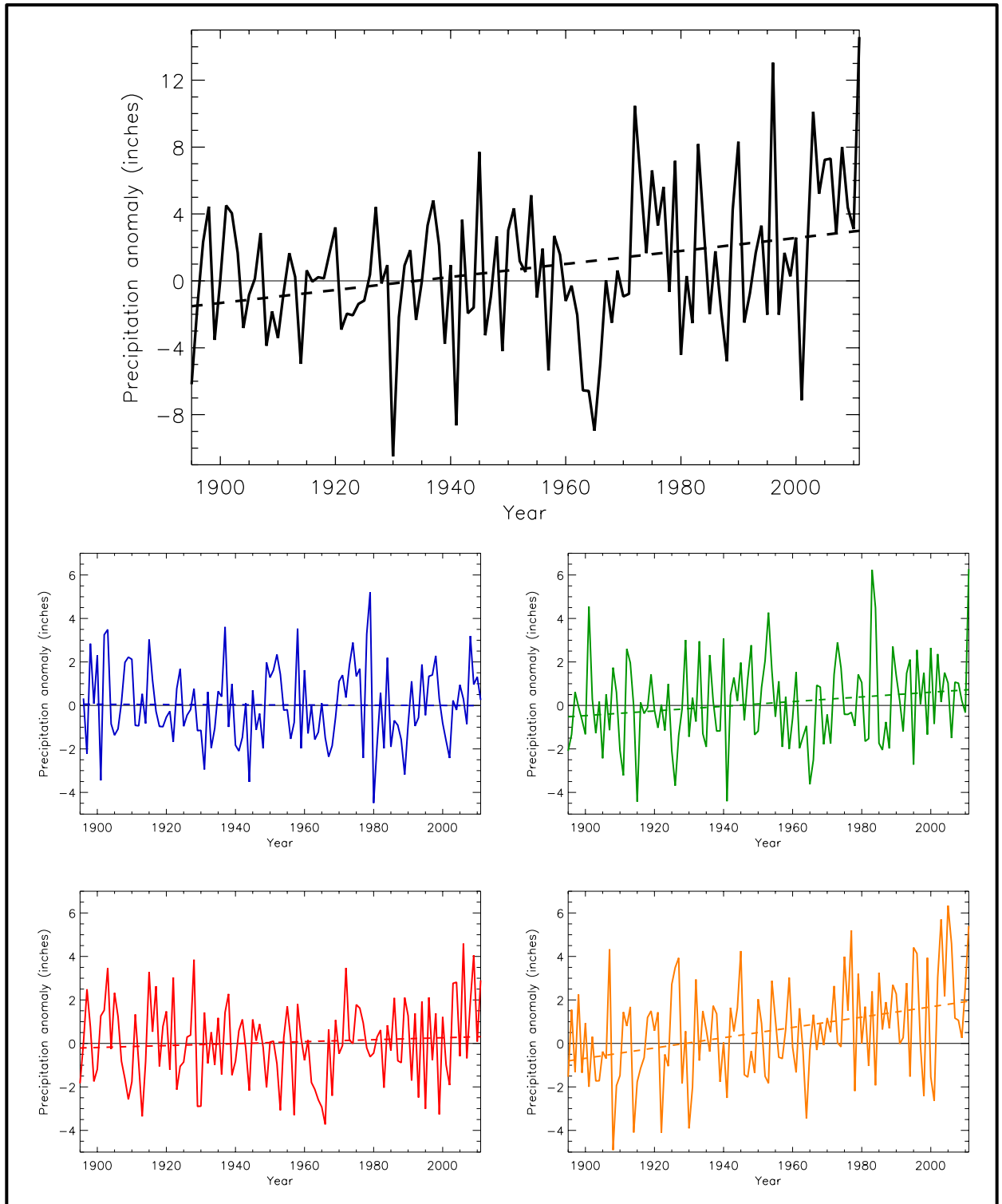
Figure 6. Precipitation anomaly (deviations from the 1901-1960 average, inches) for annual (black), winter (blue), spring (green), summer (red), and fall (orange), for the Northeast U.S. Dashed lines indicate the best fit by minimizing the chi-square error statistic. Based on a new gridded version of COOP data from the National Climatic Data Center, the CDDv2 data set (R. Vose, personal communication, July 27, 2012). Note that the annual time series is on a unique scale. Trends are upward and statistically significant annually and for the fall season.
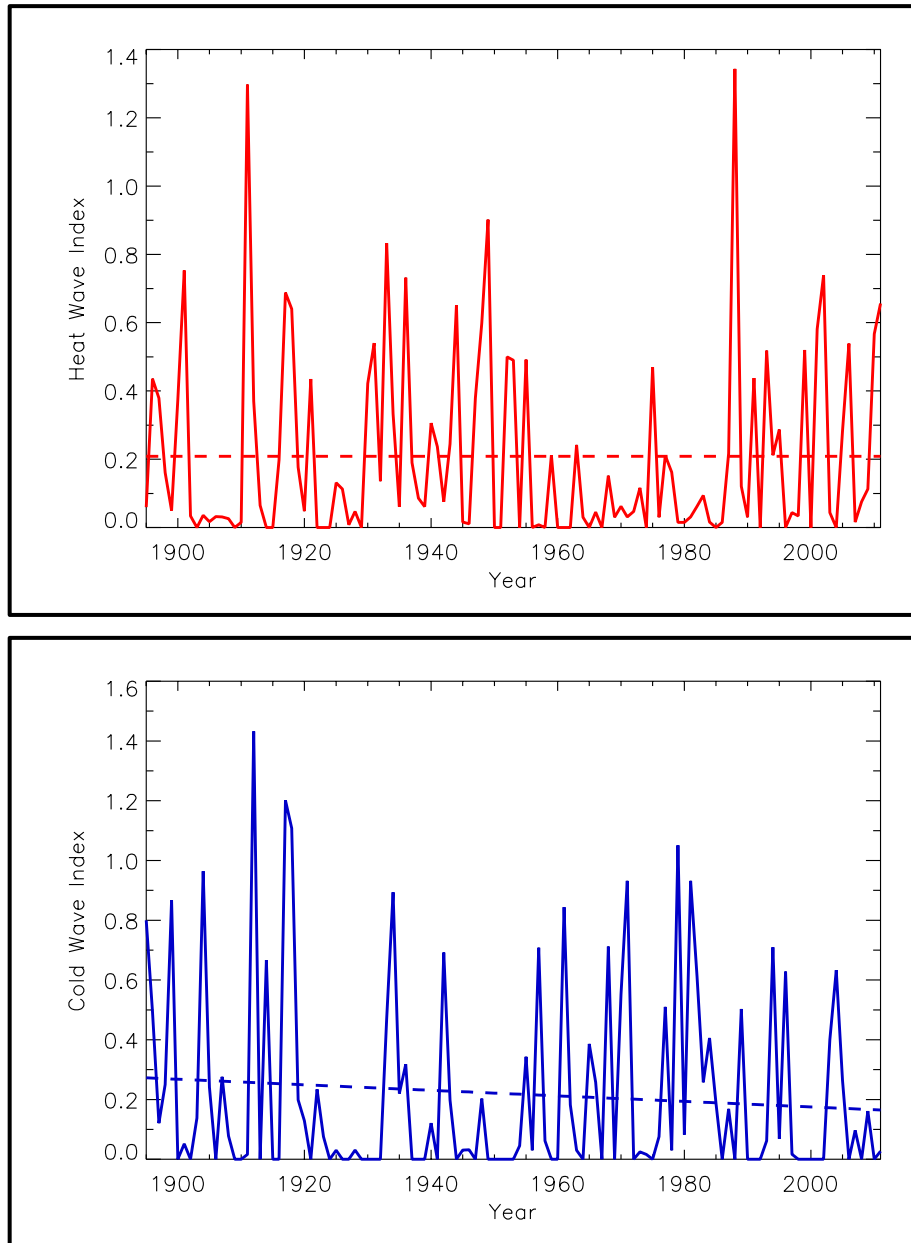
Figure 7. Time series of an index for the occurrence of heat waves (top) and cold waves (bottom), defined as 4-day periods that are hotter and colder, respectively, than the threshold for a 1 in 5-year recurrence, for the Northeast region. The dashed line is a linear fit. Based on daily COOP data from long-term stations in the National Climatic Data Center's Global Historical Climate Network data set. Only stations with less than 10% missing daily temperature data for the period 1895-2011 are used in this analysis. Events are first identified for each individual station by ranking all 4-day period mean temperature values and choosing the highest (heat waves) and lowest (cold waves) non-overlapping N/5 events, where N is the number of years of data for that particular station. Then, event numbers for each year are averaged for all stations in each 1x1° grid box. Finally, a regional average is determined by averaging the values for the individual grid boxes. This regional average is the index. The most intense heat waves occurred in the 1910s and 1980s, with moderate values in recent years. There is no overall trend in heat waves. Cold wave events were most intense in the 1910s and the 1970s/80s and have been low during the last few years. The overall trend in cold waves is not statistically significant.

22

The frequency of extreme cold periods was high early in the record, followed by a quieter period and has been generally less than average since a peak in the 1970s and early 1980s (Fig. 7, bottom). During the period of 1977-1984, the index averaged more than double the 1895-2011 average, while since 1985 the index has averaged about 30% below the long-term average, although there is no statistically significant long-term trend. The highest value for the 4-day index occurred in 1912. The period of the 1920s/early 1930s was characterized by very low values of the index.

2.4.4. *Extreme Precipitation*

There are many different metrics that have been used in research studies to examine temporal changes in extreme precipitation. Here, we define the threshold for an extreme event based on a recurrence interval. This type of definition is commonly used for design applications, for example, in the design of runoff control structures. The analysis was performed using daily COOP data from long-term stations for a range of recurrence intervals, from one to twenty years. The results were not very sensitive to the exact choice. Results are presented for the five-year threshold, as an intermediate value. The duration of the extreme event is another choice for a metric. A range of durations was analyzed, from one to ten days, but the results were also not very sensitive to the choice. Results are presented (Fig. 8) for 1-day duration events, which is the shortest duration possible because of the daily time resolution of the COOP data.

There is substantial decadal-scale variability in the number of extreme precipitation events since around 1935. The index was quite high in the 1990s up to the present time. The highest index value occurred in 1996. The index remained below 0.2 between 1961 and 1968, coinciding well with the drought that affected the Northeast during the 1960's.

The recent elevated level in extreme precipitation also manifests itself in estimates of shorter rainfall recurrence intervals. These values are used extensively in engineering design and governmental regulations (e.g., building codes). Commonly these rainfall extremes are known as the 50- or 100-year storm and represent the amount of rainfall that can be expected to occur on average once in 50 (or 100) years. In terms of these design specifications, an increase in extreme rainfall lowers the expected recurrence interval of a specific precipitation amount. Thus the amount of rain that was expected to occur once in 100 years, may now occur on average once every 60 years. This could lead to the premature failure of infrastructure or more frequent infrastructure disruptions. DeGaetano (2009) shows that what would be expected to be a 100-year event based on 1950-1979 data, occurs with an average return interval of 60 years when data from the 1978-2007 period are considered. Similarly, the amount of rain that constituted a 50-year event during 1950-1979 is expected to occur on average once every 30 years based on the more recent data.
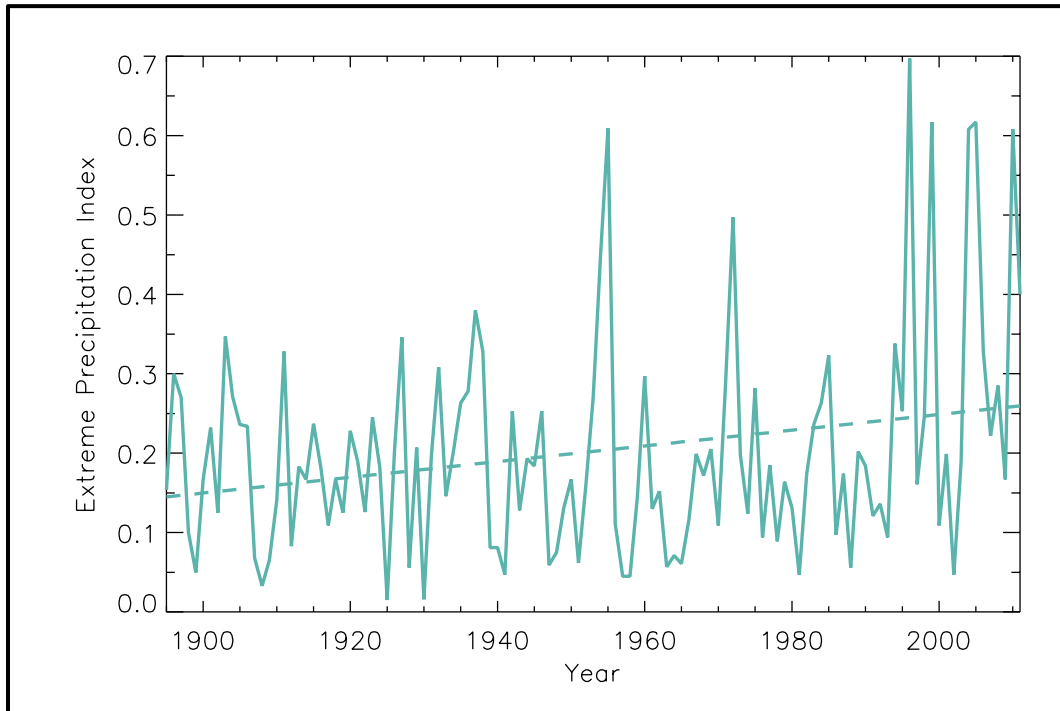
Figure 8. Time series of extreme precipitation index for the occurrence of 1-day, 1 in 5-year extreme precipitation, for the Northeast region. The dashed line is a linear fit. Based on daily COOP data from long-term stations in the National Climatic Data Center's Global Historical Climate Network data set. Only stations with less than 10% missing daily precipitation data for the period 1895-2011 are used in this analysis. Events are first identified for each individual station by ranking all daily precipitation values and choosing the top N/5 events, where N is the number of years of data for that particular station. Then, event numbers for each year are averaged for all stations in each 1x1° grid box. Finally, a regional average is determined by averaging the values for the individual grid boxes. This regional average is the extreme precipitation index. There is no statistically significant trend.

2.4.5. Freeze-Free Season

Figure 9 shows time series of freeze-free season length, calculated using daily COOP data from long-term stations. The freeze-free season length exhibited relatively minor fluctuations in the decadal-scale average from the beginning of the record (1895) into the 1980s. There has been a generally increasing trend since the mid-1980s in freeze-free season length. The last occurrence of 32°F in the spring has been occurring earlier and the first occurrence of 32°F in the fall has been happening later. The longest and second longest freeze-free seasons occurred in 2007 and 2004, respectively. The average freeze-free season length during 1991-2010 was about 10 days longer than during 1961-1990, which included a 5-year sequence of years (1963-1967) with very short freeze-free seasons. Over the entire time period of 1895-2011 there is a statistically significant upward trend in freeze-free season length.
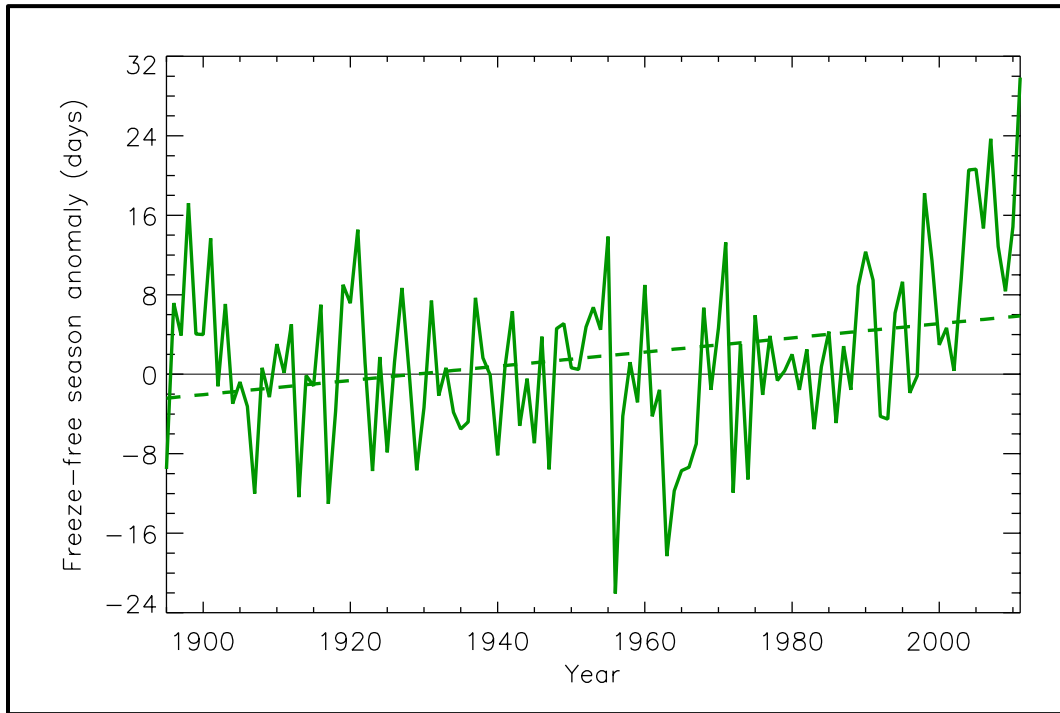
Figure 9. Time series of freeze-free season anomalies shown as the number of days per year, for the Northeast region. Length of the freeze-free season is defined as the period between the last occurrence of 32°F in the spring and first occurrence of 32°F in the fall. The dashed line is a linear fit. Based on daily COOP data from long-term stations in the National Climatic Data Center's Global Historical Climate Network data set. Only stations with less than 10% missing daily temperature data for the period 1895-2011 are used in this analysis. Freeze events are first identified for each individual station. Then, event dates for each year are averaged for 1x1° grid boxes. Finally, a regional average is determined by averaging the values for the individual grid boxes. There is an overall statistically significant upward trend.

2.4.6. Inland Hydrology

The spring center of volume date is a measure of the seasonality of river flow volume. It defines the date on which half of the total river flow volume over the period from January through May passes a point. In terms of climate, this is an integrative measure as the volume of river flow is a function of temperature, particularly with regard to snowmelt, precipitation, and antecedent soil moisture. Hodgkins et al. (2003) analyzed spring center of volume data from 27 rural, unregulated river-gauging stations in New England (Fig. 10). On all streams, the spring center of volume date has become earlier. This is especially true on the eleven streams where spring flow is most affected by runoff from snowmelt. On average, over the last 30 years, these dates have occurred one to two weeks earlier in the year. Such changes in the timing of spring stream flow affect fish and other aquatic organisms in both the streams and coastal estuaries. Human activities including water-supply management strategies are also affected.
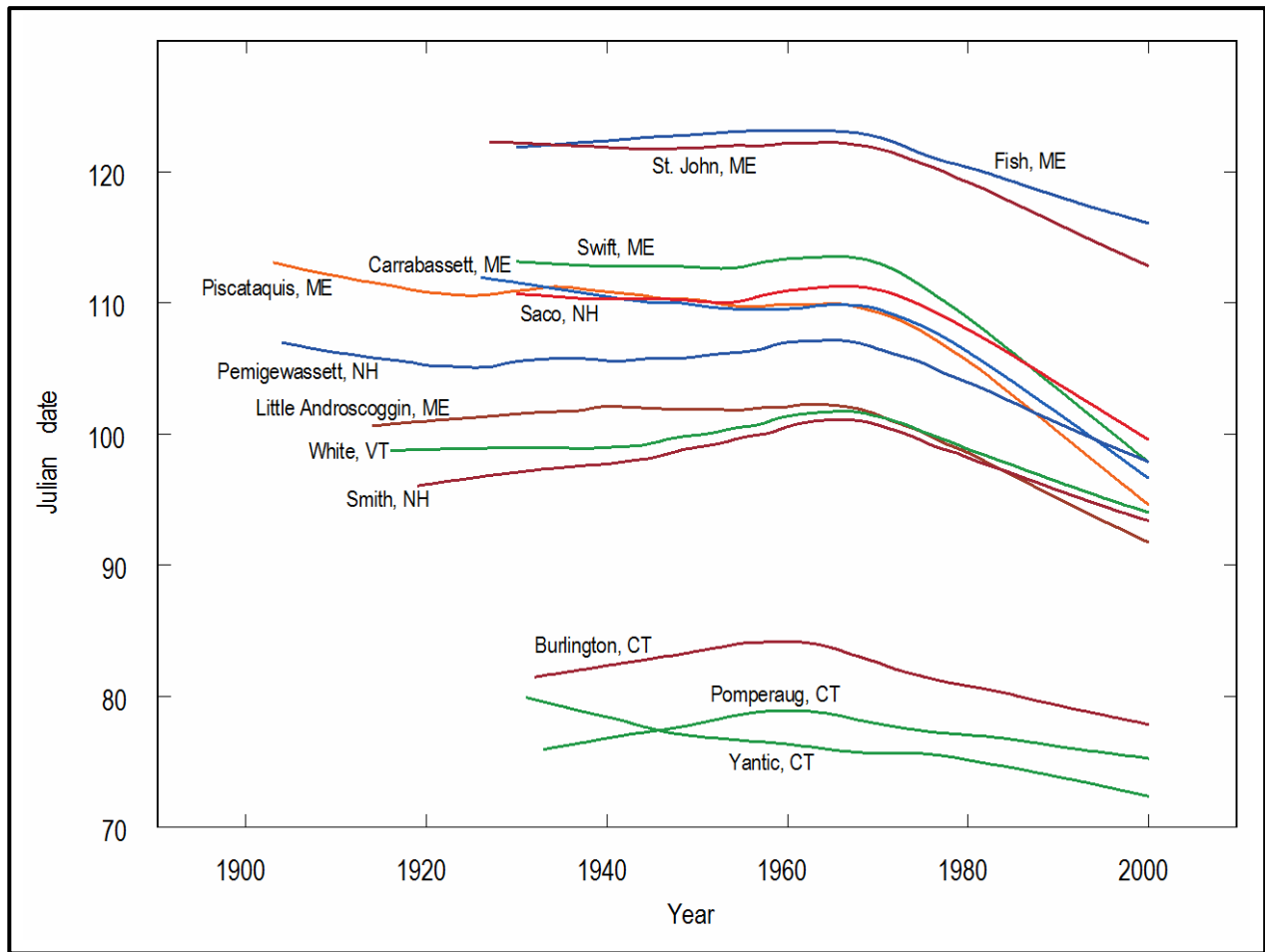
Figure 10. Smoothed winter/spring center of volume dates for the 13 longest-record rural, unregulated rivers in New England (Hodgkins et al. 2003).

2.4.7. Lake Ice Cover

A long-term record of the date of ice-in on Lake Champlain in Vermont shows that the lake now freezes approximately two weeks later than it did in the early 1800s and over a week later than it did 100 years ago (Fig. 11). Later ice-in dates are an indication of warmer lake temperatures, as it takes longer for the warmer water to freeze in winter. Prior to 1950, the absence of winter ice cover on Lake Champlain was rare, occurring three times in the 1800s and another three times between 1900 and 1940. Since 1970 Lake Champlain has remained ice-free during 18 winters.

2.4.8. Snow Depth

Like these other winter phenomena, snow depth has also shown decreases over recent decades. In Maine, Hodgkins and Dudley (2006) analyzed snow depth data from 23 long-term snow course sites. Eighteen of the sites had statistically significant decreases in snow depth (Fig. 12). At mountainous sites along the Maine-New Hampshire border, average snow depth decreased by approximately 16% from 1926-2004. Across the region, snow depth data from Historical Climatology Network stations show a decrease in the number of days with at least an inch of snow on the ground.
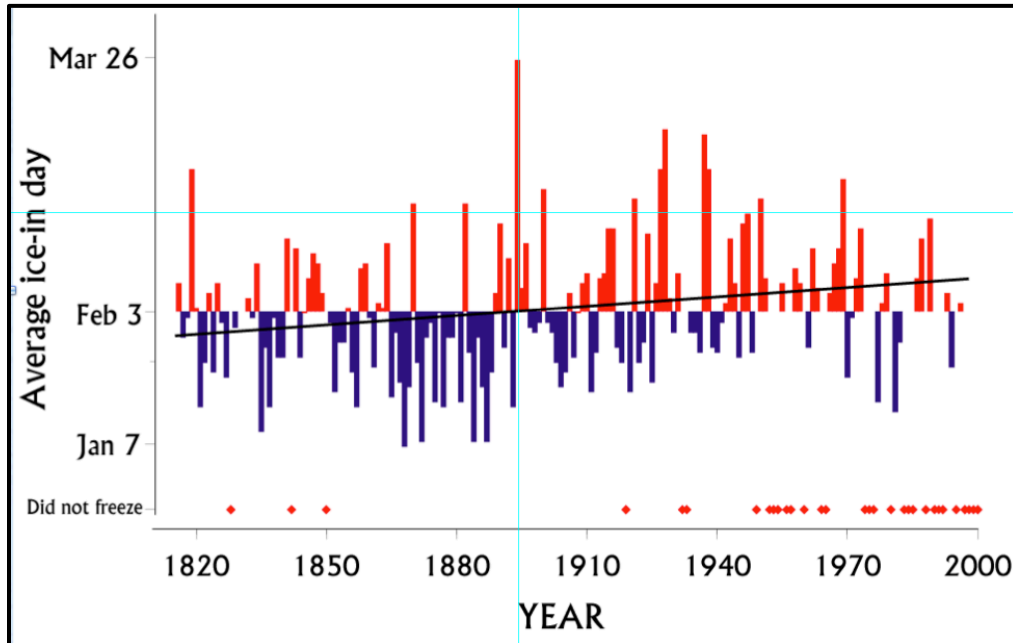
Figure 11. Date of ice-in on the main portion of Lake Champlain. Asterisks denote years in which the Lake remained ice-fee. Data from NWS (2012a).
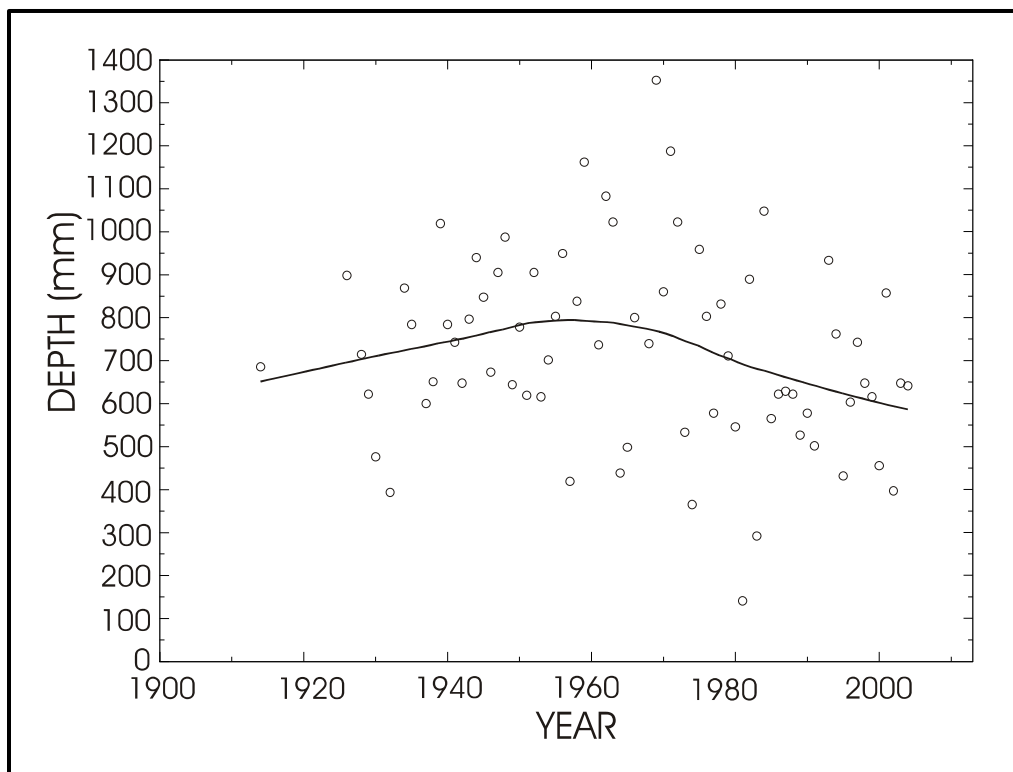

Figure 12. Time series of average snow depth at 23 snow course sites in Maine. Data from Hodgkins and Dudley (2006). Solid line is a smoothed representation of the data using a LOESS (LOcally Estimated Scatterplot Smoothing) filter.
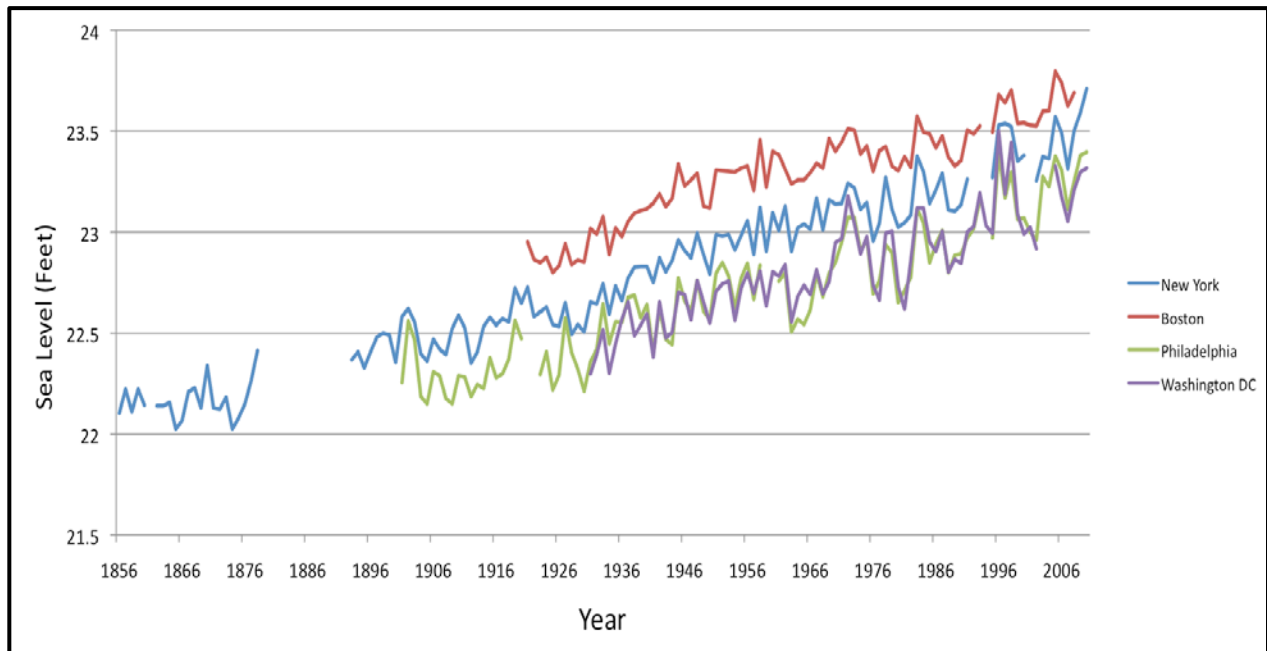
27

Figure 13. Annual mean sea level for gauges at four major Northeast coastal cities. Data from PSMSL (2012).

2.4.9. Sea Level Rise

Historically, the rise in sea level along the Northeast Coast has varied through time but has accelerated during the 20th century. Over the past thousand years, regional sea level was rising at a rate of 0.34 to 0.43 inch per decade. This change was primarily the result of slow geological processes. During the last ice age, land areas near the southern periphery of the ice sheets were forced upward by the weight of ice to their north. These areas now continue to slowly sink in response to the melting of the ice sheets many thousands of years ago. More recently, the rate of sea level rise along the Northeast Coast has increased. On average during the 20th century, sea level rose by 1.2 inches per decade. This reflects the increase in ocean water volume as the oceans warm as well as the melting of glaciers and ice sheets, and changes in Atlantic Ocean circulation, along with the geological processes. Figure 13 shows the change in sea level at four major northeast coastal cities. The rate of change at each site has been similar in recent decades.

2.4.10. Great Lakes

One fifth of the world's fresh water resides in the Great Lakes. Lakes Erie and Ontario border the Northeast to the north and west. They are an important resource for water supply, hydropower generation, recreation, and transportation (particularly via the St Lawrence Seaway).

Long-term water levels in Lake Ontario and Lake Erie have remained fairly constant through time, in part because the levels can be manually regulated. Nonetheless, Lake levels show marked variability from year to year and decade to decade (Fig. 14). The major drought that characterized the early 1960s in the Northeast is reflected in the Lake level record.
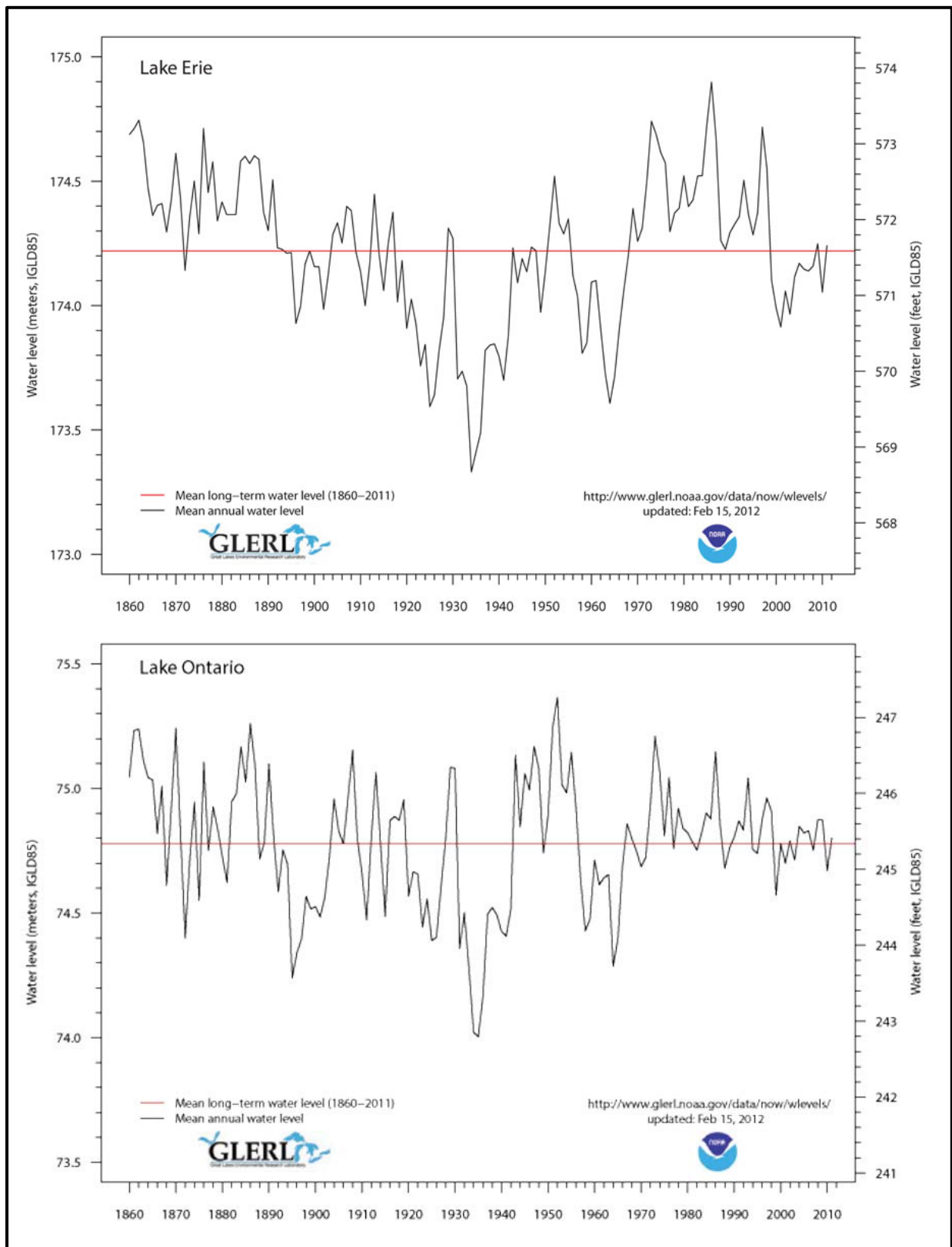
Figure 14. Time series of water levels in Lake Erie and Lake Ontario. Data from NOAA GLERL (2012).
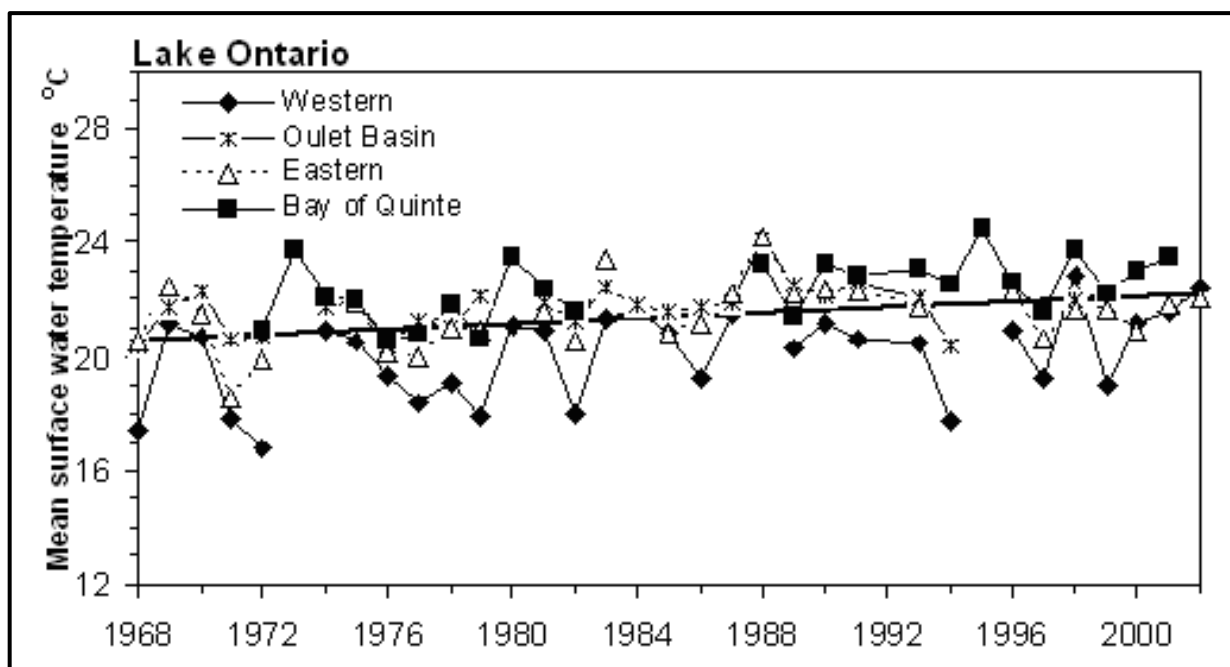
Figure 15. Surface water temperatures in four sub-basins of Lake Ontario in August. Republished with permission of Elsevier, from Dobiesz and Lester (2009); permission conveyed through Copyright Clearance Center, Inc.

Lake water temperatures are also an important climate indicator for the Lakes. They affect the health of the Lake's ecosystems, the cooling capacity of lakeshore power generation plants and influence the potential for winter lake-effect snow. Figure 15 shows a time series (1968-2002) of surface water temperature from different sections of Lake Ontario (Dobiesz and Lester 2009). Significant trends toward warmer lake temperatures are apparent in three of the four sub basins. Across the four basins, temperatures have increased by more than 5°F. Surface water temperatures in Lake Erie have also increased, but at a much lower rate.

3. FUTURE REGIONAL CLIMATE SCENARIOS

As noted above, the physical climate framework for the 2013 NCA report is based on climate model simulations of the future using the high (A2) and low (B1) SRES emissions scenarios. The resulting climate conditions are to be viewed as scenarios, not forecasts, and there are no explicit or implicit assumptions about the probability of occurrence of either scenario.

3.1. Description of Data Sources

This summary of future regional climate scenarios is based on the following model data sets:

- **Coupled Model Intercomparison Project phase 3 (CMIP3)** – Fifteen coupled Atmosphere-Ocean General Circulation Models (AOGCMs) from the World Climate Research Programme (WCRP) CMIP3 multi-model dataset (PCMDI 2012), as identified in the 2009 NCA report (Karl et al. 2009), were used (see Table 2). The spatial resolution of the great majority of these model simulations was 2-3° (a grid point spacing of approximately 100-200 miles), with a few slightly greater or smaller. All model data were re-gridded to a common resolution before processing (see below). The simulations from all of these models include:

  a) Simulations of the 20th century using best estimates of the temporal variations in external forcing factors (such as greenhouse gas concentrations, solar output, volcanic aerosol concentrations); and

  b) Simulations of the 21st century assuming changing greenhouse gas concentrations following both the A2 and B1 emissions scenarios. One of the fifteen models did not have a B1 simulation.

  These model simulations also serve as the basis for the following downscaled data set.

- **Downscaled CMIP3 (Daily_CMIP3)** – These temperature and precipitation data are at 1/8° (~8.6 miles latitude and ~6.0-7.5 miles longitude) resolution. The CMIP3 model data were initially downscaled on a monthly timescale using the bias-corrected spatial disaggregation (BCSD) method, for the period of 1961-2100. The starting point for this downscaling was an observationally-based gridded data set produced by Maurer et al. (2002). The climate model output was adjusted for biases through a comparison between this observational gridded data set and the model's simulation of the 20th century. Then, high-resolution gridded data for the future were obtained by applying change factors calculated as the difference between the model's present and future simulations (the so-called "delta" method).

  Daily statistically-downscaled data were then created by randomly sampling historical months and adjusting the values using the "delta" method (Hayhoe et al. 2004; 2008). Eight models with complete data for 1961-2100 were available and used in the Daily_CMIP3 analyses (Table 2).

- **North American Regional Climate Change Assessment Program (NARCCAP)** – This multi-institutional program is producing regional climate model (RCM) simulations in a coordinated experimental approach (NARCCAP 2012). At the time that this data analysis was initiated, simulations were available for 9 different combinations of an RCM driven by a general circulation model (GCM); during the development of these documents, two additional simulations became available and were incorporated into selected products. These 11 combinations involved four different GCMs and six different RCMs (see Table 3). The mean temperature and precipitation maps include all 11 combinations. For calculations and graphics

involving the distribution of NARCCAP models, analyses of only the original 9 model combinations were used. For graphics of the number of days exceeding thresholds and the number of degree days, the values were obtained from the Northeast Regional Climate Center, where only 8 of the model combinations were analyzed.

Each GCM-RCM combination performed simulations for the periods of 1971-2000, 1979-2004 and 2041-2070 for the high (A2) emissions scenario only. These simulations are at a resolution of approximately 50 km (~30 miles), covering much of North America and adjacent ocean areas. The simulations for 1971-2000 and 2041-2070 are "driven" (time-dependent conditions on the lateral boundaries of the domain of the RCM are provided) by global climate model simulations. The 1979-2004 simulations are driven by the NCEP/DOE Reanalysis II data set, which is an estimate of the actual time-dependent state of the atmosphere using a model that incorporates observations; thus the resulting simulations are the RCM's representation of historical observations. From this 1979-2004 simulation, the interval of 1980-2000 was selected for analysis.

Table 2. Listing of the 15 models used for the CMIP3 simulations (left column). The 8 models used in the daily statistically-downscaled (Daily_CMIP3) analyses are indicated (right column).

CMIP3 Models	Daily_CMIP3
CCSM3	X
CGCM3.1 (T47)	X
CNRM-CM3	
CSIRO-Mk3.0	
ECHAM5/MPI-OM	X
ECHO-G	X
GFDL-CM2.0	
GFDL-CM2.1	
INM-CM3.0	
IPSL-CM4	X
MIROC3.2 (medres)	X
MRI-CGCM2.3.2	X
PCM	X
UKMO-HadCM3	
UKMO-HadGEM1[2]	

---

[2] Simulations from this model are for the A2 scenario only.

Table 3. Combinations of the 4 GCMs and 6 RCMs that make up the 11 NARCCAP dynamically-downscaled model simulations.

		GCMs			
		CCSM3	CGCM3.1	GFDL-CM2.1	UKMO-HadCM3
RCMs	CRCM	X	X		
	ECPC			X^3	
	HRM3			X^4	X
	MM5I	X			X^3
	RCM3		X	X	
	WRFG	X	X		

3.2. Analyses

Analyses are provided for the periods of 2021-2050, 2041-2070, and 2070-2099, with changes calculated with respect to an historical climate reference period (either 1971-1999, 1971-2000, or 1980-2000). These future periods will sometimes be denoted in the text by their midpoints of 2035, 2055, and 2085, respectively.

As noted above, three different intervals are used as the reference period for the historical climatology. Although a uniform reference period would be ideal, there were variations in data availability and in the needs of the author teams. For the NARCCAP maps of mean temperature and precipitation, the 1971-2000 period was used as the reference because that represents the full historical simulation period. The 1971-1999 period (rather than 1971-2000) was used as the reference for CMIP3 maps because some of the CMIP3 models' 20th century simulations ended in 1999, but we wanted to keep the same starting date of 1971 for both CMIP3 and NARCCAP mean temperature and precipitation maps. The 1980-2000 period was used as the historical reference for some of the NARCCAP maps (days over thresholds and degree days) because this is the analyzed period of the reanalysis-driven simulation, and we were requested to provide maps of the actual values of these variables, for both the historical period and the future period, and not just a difference map. A U.S.-wide climatology based on actual observations was not readily available for all of these variables and we chose to use the reanalysis-driven model simulation as an alternative. Since the reanalysis data set approximates observations, the reanalysis-driven RCM simulation will be free from biases arising from a driving GCM. To produce the future climatology map of actual values, we added the (future minus historical) differences to the 1980-2000 map values. For consistency then, the differences between future and present were calculated using the 1980-2000 subset of the 1971-2000 GCM-driven simulation.

Three different types of analyses are represented, described as follows:

---

[3] Data from this model combination were not used for simulations of the number of days exceeding thresholds or degree days.

[4] Data from these model combinations were not used for simulations of the number of days exceeding thresholds or degree days, or calculations and graphics involving the distribution of NARCCAP models.

- **Multi-model mean maps** – Model simulations of future climate conditions typically exhibit considerable model-to-model variability. In most cases, the future climate scenario information is presented as multi-model mean maps. To produce these, each model's data is first re-gridded to a common grid of approximately 2.8° latitude (~190 miles) by 2.8° longitude (~130-170 miles). Then, each grid point value is calculated as the mean of all available model values at that grid point. Finally, the mean grid point values are mapped. This type of analysis weights all models equally. Although an equal weighting does not incorporate known differences among models in their fidelity in reproducing various climatic conditions, a number of research studies have found that the multi-model mean with equal weighting is superior to any single model in reproducing the present-day climate (Overland et al. 2011). In most cases, the multi-model mean maps include information about the variability of the model simulations. In addition, there are several graphs that show the variability of individual model results. These should be examined to gain an awareness of the magnitude of the uncertainties in each scenario's future values.

- **Spatially-averaged products** – To produce these, all the grid point values within the Northeast region boundaries are averaged and represented as a single value. This is useful for general comparisons of different models, periods, and data sources. Because of the spatial aggregation, this product may not be suitable for many types of impacts analyses.

- **Probability density functions (pdfs)** – These are used here to illustrate the differences among models. To produce these, spatially-averaged values are calculated for each model simulation. Then, the distribution of these spatially-averaged values is displayed. This product provides an estimate of the uncertainty of future changes in a tabular form. As noted above, this information should be used as a complement to the multi-model mean maps.

3.3. Mean Temperature

Figure 16 shows the spatial distribution of multi-model mean simulated differences in average annual temperature for the three future time periods (2035, 2055, 2085) relative to the model reference period of 1971-1999, for both emissions scenarios, for the 14 (B1) or 15 (A2) CMIP3 models. The statistical significance regarding the change in temperature between each future time period and the model reference period was determined using a 2-sample t-test assuming unequal variances for those two samples. For each period (present and future climate), the mean and standard deviation were calculated using the 29 or 30 annual values. These were then used to calculate t. In order to assess the agreement between models, the following three categories were determined for each grid point, similar to that described in Tebaldi et al. (2011):

- *Category 1*: If less than 50% of the models indicate a statistically significant change then the multi-model mean is shown in color. Model results are in general agreement that simulated changes are within historical variations;
- *Category 2*: If more than 50% of the models indicate a statistically significant change, and less than 67% of the significant models agree on the sign of the change, then the grid points are masked out, indicating that the models are in disagreement about the direction of change;
- *Category 3*: If more than 50% of the models indicate a statistically significant change, and more than 67% of the significant models agree on the sign of the change, then the multi-model mean is shown in color with hatching. Model results are in agreement that simulated changes are statistically significant and in a particular direction.

It can be seen from Fig. 16 that all three periods indicate an increase in temperature with respect to the reference period. Little spatial variation is simulated, especially for the low (B1) emissions scenario. Changes along the coastal areas are slightly smaller than inland areas. Also, the warming tends to be slightly larger in the north, from the Great Lakes along the Canadian border into Maine. This is consistent with global analyses that show relatively gradual spatial changes on a global scale (Meehl et al. 2007), a probable consequence of the generally high instantaneous spatial coherence of temperature and the smoothing effect of multi-model averaging. Changes are simulated to increase for each future time period, and the differences between the A2 and B1 scenarios are also simulated to increase over time. For 2035, B1 values range between 1.5 and 3.5°F and A2 values range slightly higher from about 2.5 to 3.5°F. For 2055, warming ranges between 2.5 and 4.5°F for B1 and from 3.5 to 5.5°F for A2. Simulated temperature increases in 2085 range from 3.5 to 5.5°F for B1 and 6.5 to 8.5°F for A2. The CMIP3 models indicate that temperature changes across the Northeast U.S., for all three future time periods and both emissions scenarios, are statistically significant. The models also agree on the sign of change, with all grid points satisfying category 3 above, i.e. the models are in agreement on temperature increases throughout the region for each future time period and scenario.

Figure 17 shows the multi-model mean simulated annual and seasonal 30-year average temperature changes between 2041-2070 and 1971-2000 for the high (A2) emissions scenario, for 11 NARCCAP regional climate model simulations. The simulated annual changes increase with latitude, ranging from 4.0 to 5.0°F across the region. Seasonal changes show more spatial variability, with winter increases ranging from 4.0°F in the southwestern part of the region to 6.0°F in the north. Springtime increases are smaller in magnitude, ranging from 3.0 in the southwestern part of the region to 4.5°F in Maine. Summer and fall show a reversed spatial pattern, with the greatest increases simulated to be in the southwestern part of the region. Summer shows a maximum increase of 5.0 to 5.5°F in Pennsylvania and West Virginia, and the smallest changes in Maine of 4.0 to 4.5°F. Fall shows less spatial variability, with values ranging between 4.0 and 4.5°F in New England to between 4.5 and 5.0°F over the remainder of the region. The agreement between models was again assessed using the three categories described in Fig. 16. The models agree on the sign of change, with all grid points satisfying category 3, annually, and for all seasons.

Figure 18 shows the simulated change in annual mean temperature for each future time period with respect to 1971-1999, for both emissions scenarios, averaged over the entire Northeast region for the 14 (B1) or 15 (A2) CMIP3 models. In addition, values for 9 of the NARCCAP simulations and the 4 GCMs used in the NARCCAP experiment are shown for 2055 (A2 scenario only) with respect to 1971-2000. Both the multi-model mean and individual model values are shown. For the high (A2) emissions scenario, the CMIP3 models simulate average temperature increases of 3.0°F by 2035, 4.8°F by 2055, and 8.0°F by 2085. The difference between the two emissions scenarios widens over time, with average increases for the low (B1) emissions scenario of 2.7°F by 2035, 3.6°F by 2055, and 4.7°F by 2085. For 2055, the average temperature change simulated by the NARCCAP models is comparable to that of the average of all of the CMIP3 GCMs and the average of the 4 NARCCAP GCMs.
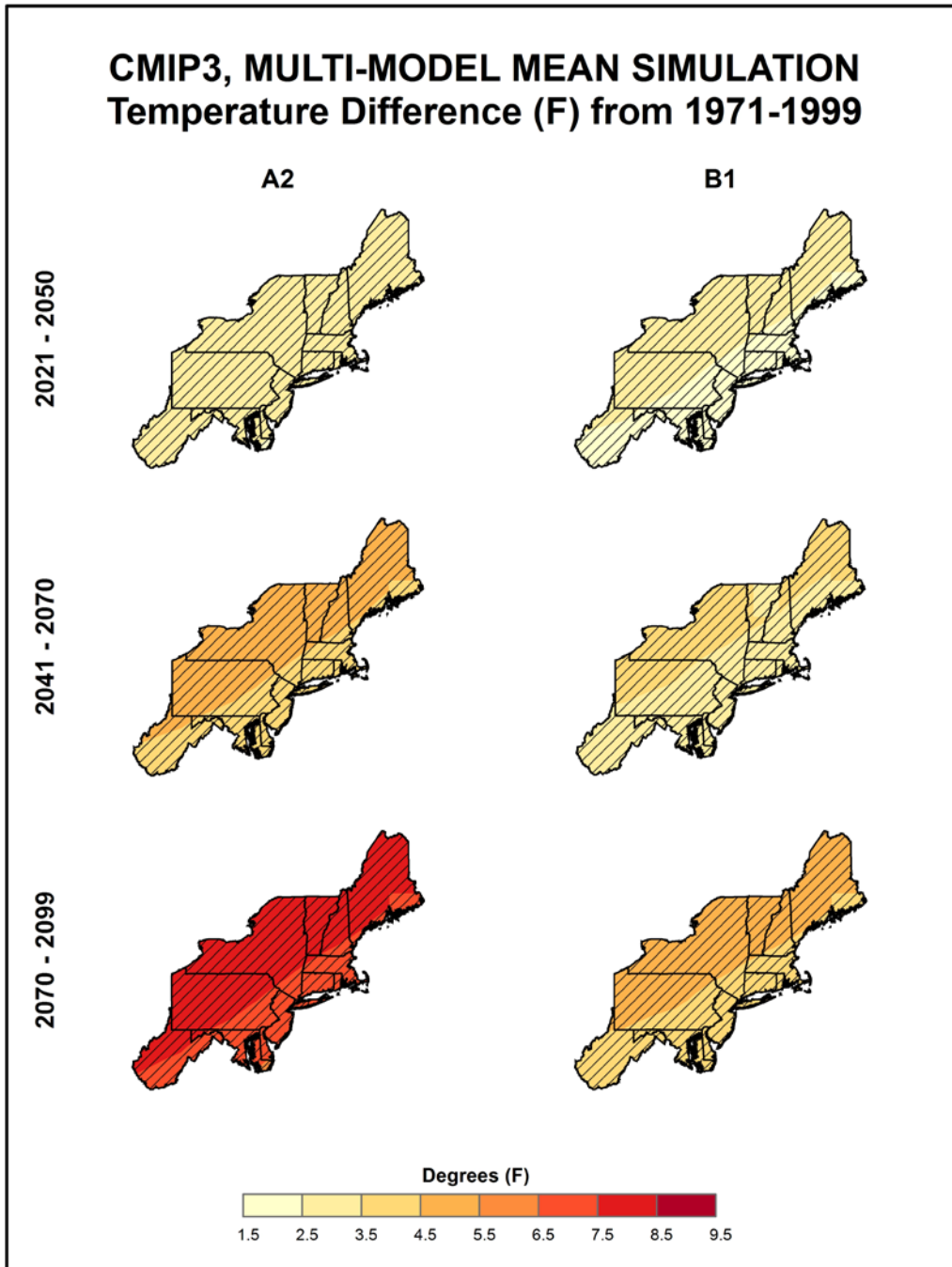
Figure 16. Simulated difference in annual mean temperature (°F) for the Northeast region, for each future time period (2021-2050, 2041-2070, and 2070-2099) with respect to the reference period of 1971-1999. These are multi-model means for the high (A2) and low (B1) emissions scenarios from the 14 (B1) or 15 (A2) CMIP3 global climate simulations. Color with hatching (category 3) indicates that more than 50% of the models show a statistically significant change in temperature, and more than 67% agree on the sign of the change (see text). Temperature changes increase throughout the 21st century, more rapidly for the high emissions scenario.
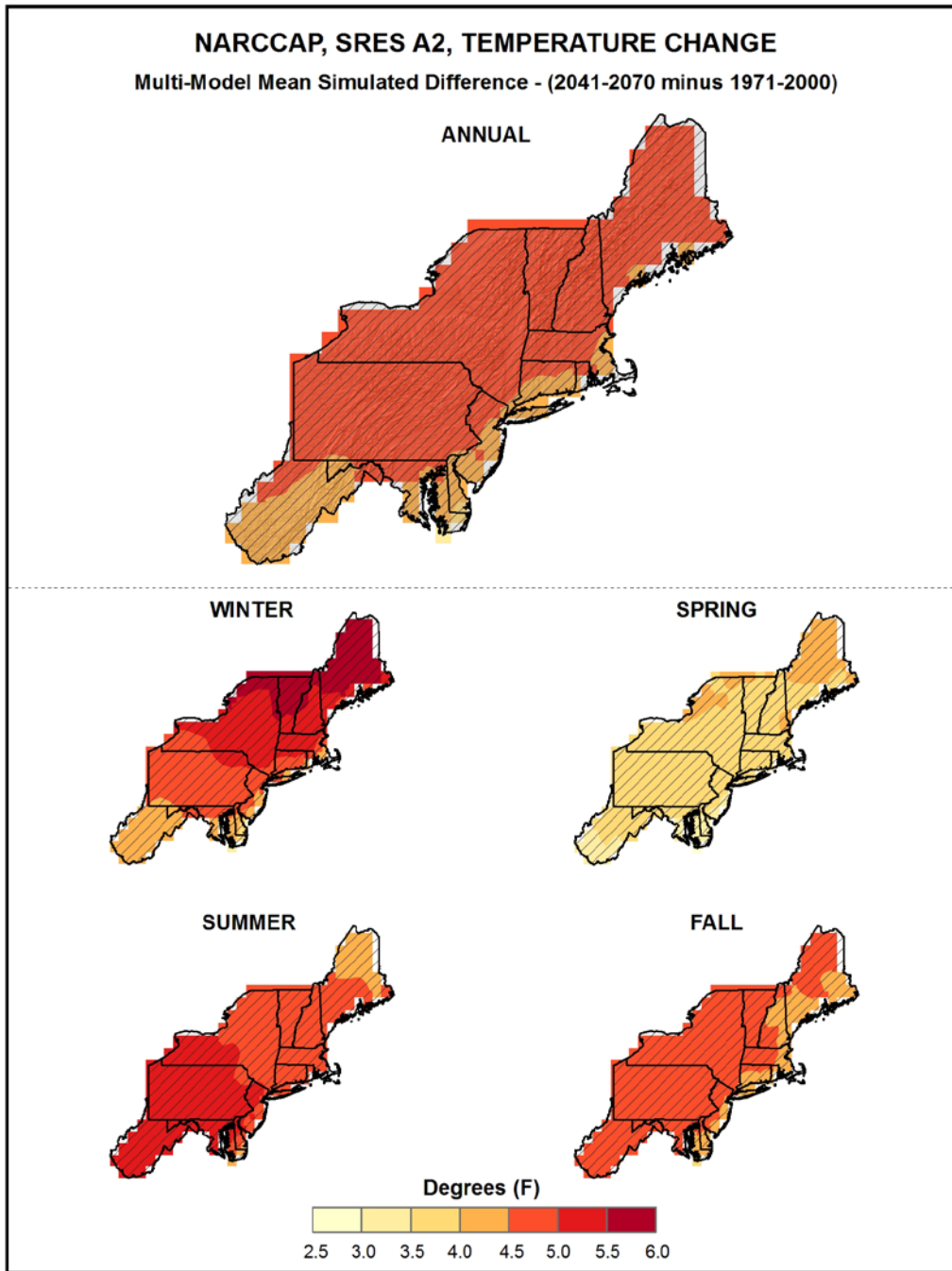
Figure 17. Simulated difference in annual and seasonal mean temperature (°F) for the Northeast region, for 2041-2070 with respect to the reference period of 1971-2000. These are multi-model means from 11 NARCCAP regional climate simulations for the high (A2) emissions scenario. Color with hatching (category 3) indicates that more than 50% of the models show a statistically significant change in temperature, and more than 67% agree on the sign of the change (see text). Note that the color scale is different from that of Fig. 16. Temperature changes for the NARCCAP simulations are of similar magnitude to those for the CMIP3 global models (Fig. 16, middle left panel). Seasonal changes are greatest in winter and summer, and lowest in spring, and are statistically significant for most models throughout the region.
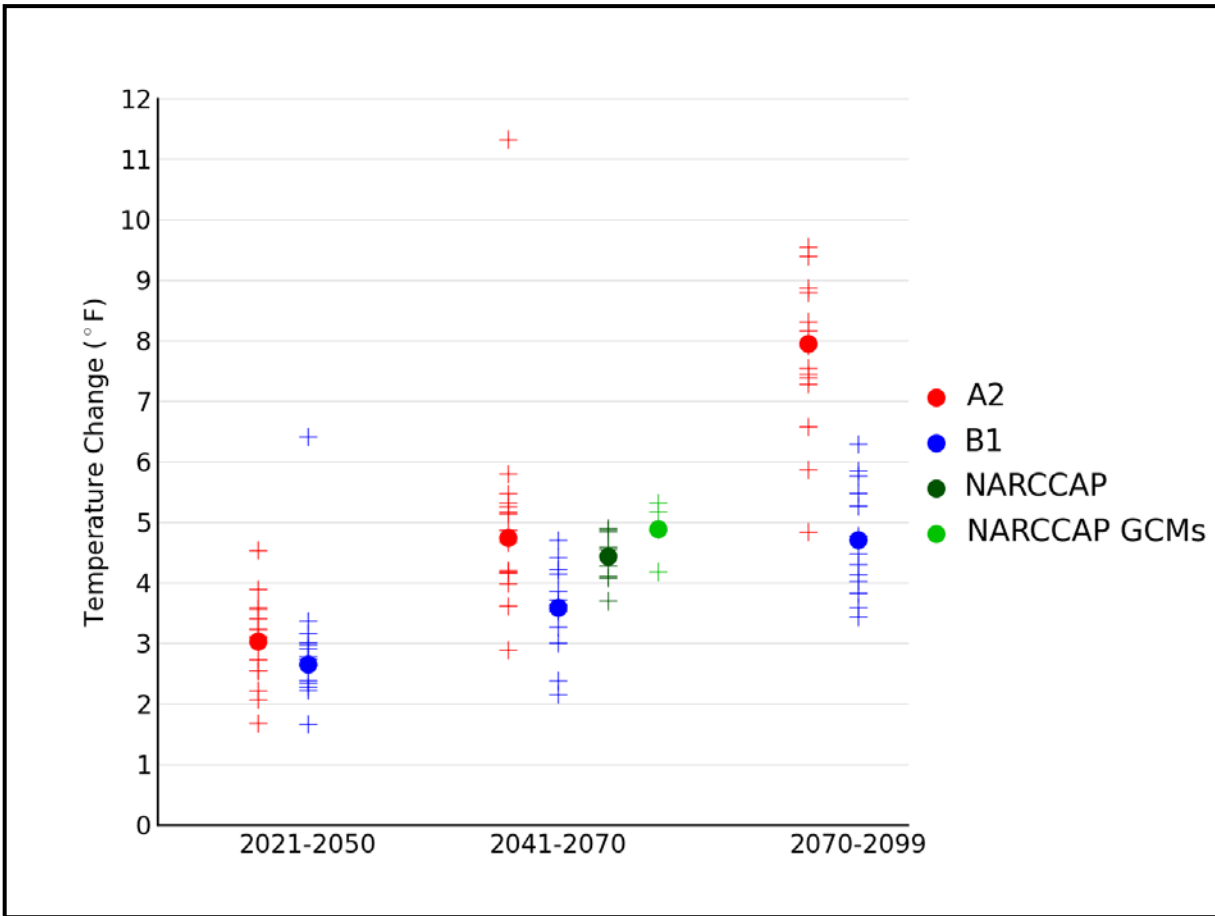
Figure 18. Simulated annual mean temperature change (°F) for the Northeast region, for each future time period (2021-2050, 2041-2070, and 2070-2099) with respect to the reference period of 1971-1999 for the CMIP3 models and 1971-2000 for the NARCCAP models. Values are given for the high (A2) and low (B1) emissions scenarios for the 14 (B1) or 15 (A2) CMIP3 models. Also shown for 2041-2070 (high emissions scenario only) are values for 9 NARCCAP models, as well as for the 4 GCMs used to drive the NARCCAP simulations. The small plus signs indicate each individual model and the circles depict the multi-model means. The range of model-simulated changes is large compared to the mean differences between A2 and B1 in the early and middle 21st century. By the end of the 21st century, the difference between A2 and B1 is comparable to the range of B1 simulations.

A key overall feature is that the simulated temperature changes are similar in value for the high and low emissions scenarios for 2035, but largely different for 2085. This indicates that early in the 21st century, the multi-model mean temperature changes are relatively insensitive to the emissions pathway, whereas late 21st century changes are quite sensitive to the emissions pathway. This arises because atmospheric CO_2 concentrations resulting from the two different emissions scenarios do not considerably diverge from one another until around 2050 (see Fig. 1). It can also be seen from Fig. 18 that the range of individual model changes is quite large, with considerable overlap between the A2 and B1 results, even for 2085. The range of temperature changes for the GCMs used to drive the NARCCAP simulations is small relative to the range for all CMIP3 models. This may be largely responsible for the relatively small range of the NARCCAP models.

Figure 19 shows the simulated change in seasonal mean temperature for each future time period with respect to 1971-1999 for the high (A2) emissions scenario, averaged over the entire Northeast region for the 15 CMIP3 models. Again, both the multi-model mean and individual model values are shown. Temperature increases are largest in the summertime, with means around 3°F in 2035, 5°F in 2055, and 8.5°F in 2085. The least amount of warming is simulated for the spring, the mean temperature change increasing from 2.8°F in 2035 to just over 7°F in 2085. The range of temperature changes for the individual models increases with each time period and is large relative to the differences between seasons and comparable to the differences between 2035 and 2085.

The distribution of changes in annual mean temperature for each future time period with respect to 1971-1999 for both emissions scenarios across the 14 (B1) or 15 (A2) CMIP3 models is shown in Table 4. Temperature changes simulated by the individual models vary from the lowest value of 1.7°F (in 2035 for the both scenarios) to the highest value of 11.3°F (in 2085 for the A2 scenario). Although the inter-model range of temperature changes (i.e., the difference between the highest and lowest model values) is seen to increase for each future time period, the interquartile range (the difference between the 75th and 25th percentiles) varies between 0.6 and 1.5°F across the three time periods. The NARCCAP simulated temperature changes have a smaller range than the comparable CMIP3 simulations, varying from 3.7°F to 4.9°F.

Table 4. Distribution of the simulated change in annual mean temperature (°F) from the 14 (B1) or 15 (A2) CMIP3 models for the Northeast region. The lowest, 25th percentile, median, 75th percentile and highest values are given for the high (A2) and low (B1) emissions scenarios, and for each future time period (2021-2050, 2041-2070, and 2070-2099) with respect to the reference period of 1971-1999. Also shown are values from the distribution of 9 NARCCAP models for 2041-2070, A2 only, with respect to 1971-2000.

Scenario	Period	Lowest	25th Percentile	Median	75th Percentile	Highest
A2	2021-2050	1.7	2.6	3.1	3.5	4.5
	2041-2070	2.9	4.1	4.9	5.3	6.4
	2070-2099	4.8	7.3	7.9	8.8	11.3
	NARCCAP (2041-2070)	*3.7*	*4.1*	*4.6*	*4.9*	*4.9*
B1	2021-2050	1.7	2.4	2.7	3.0	3.4
	2041-2070	2.2	3.3	3.6	4.1	4.7
	2070-2099	3.4	4.1	4.6	5.4	6.3

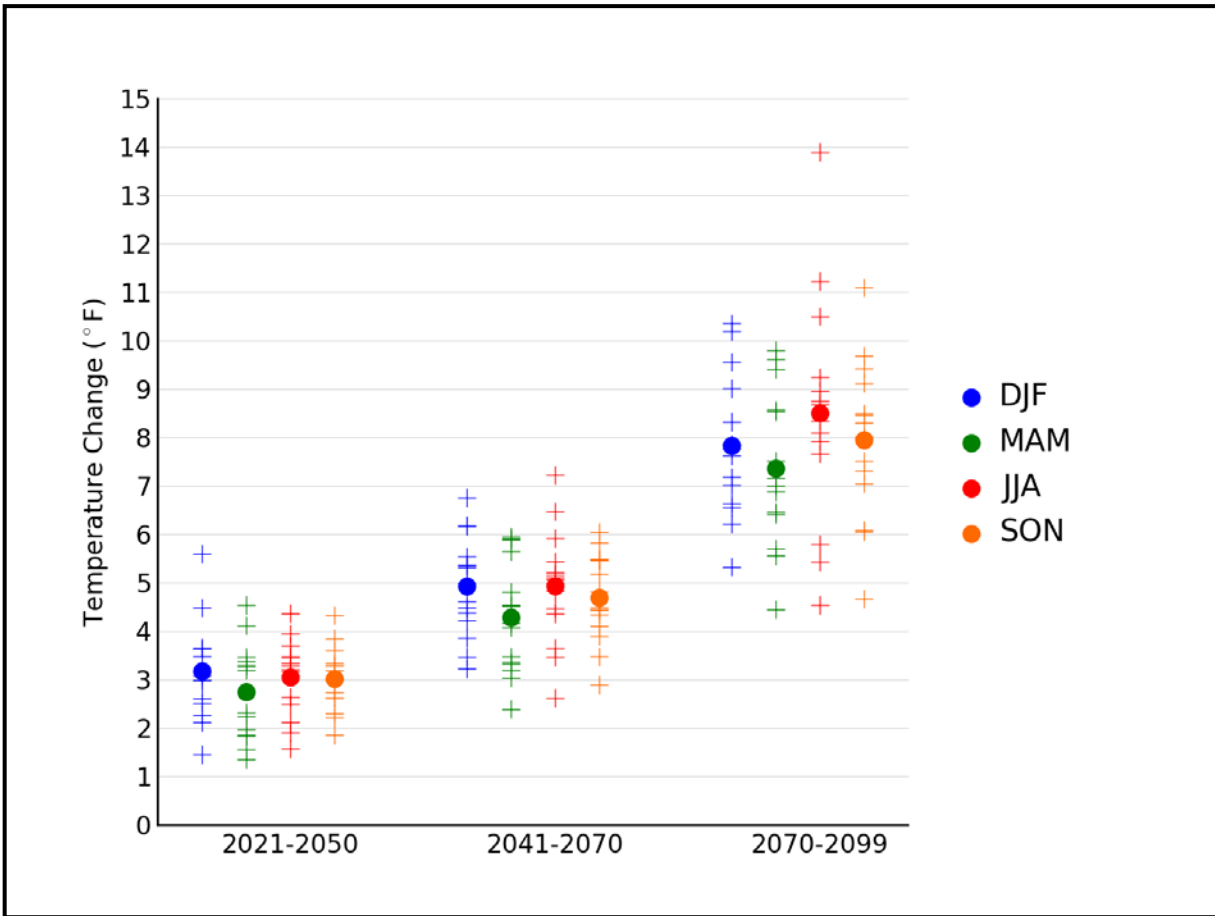*Figure 19. Simulated seasonal temperature change (°F) for the Northeast region, for each future time period (2021-2050, 2041-2070, and 2070-2099) with respect to the reference period of 1971-1999. Values are given for all 15 CMIP3 models for the high (A2) emissions scenario. The small plus signs indicate each individual model and the circles depict the multi-model means. Seasons are indicated as follows: winter (DJF, December-January-February), spring (MAM, March-April-May), summer (JJA, June-July-August), and fall (SON, September-October-November). The range of individual model-simulated changes is large compared to the differences among seasons and comparable to the differences between periods.*

This table also illustrates the overall uncertainty arising from the combination of model differences and emission pathway. For 2035, the simulated changes range from 1.7F to 4.5°F and are almost entirely due to differences in the models. By 2085, the range of simulated changes has increased to 4.8°F to 11.3°F, with roughly equal contributions to the range from model differences and emission pathway uncertainties.

3.4. Extreme Temperature

A number of metrics of extreme temperatures were calculated from the NARCCAP dynamically-downscaled and CMIP3 daily statistically-downscaled (Daily_CMIP3) data sets. Maps of a few select variables and a table summarizing all of the results follow. Each figure of NARCCAP data includes three map panels and the calculations used in each panel require some explanation. One panel (top) shows the difference between the 2055 period (2041-2070) simulation for the high (A2) emissions scenario and the 1980-2000 subset of the 1971-2000 simulation driven by the GCM. Since biases in the RCM simulations can arise from biases either in the driving global climate model or in the RCM, these two simulations include both sources of biases. It is usually assumed that such biases will be similar for historical and future periods. When taking the difference of these, the biases should at least partially cancel. As noted above, we were requested to include actual values of the variables, not just the future minus historical differences. We decided that the best model representation of the present-day values is the 1980-2000 simulation because it is driven by reanalysis data (NOAA 2012b) and thus will not include biases from a driving global climate model (although the reanalysis data used to drive the RCM is not a perfect representation of the actual state of the atmosphere). Any biases should be largely from the RCM. Thus, the lower left panel in the following figures shows the actual values from the 1980-2000 simulation. The lower right panel shows the actual values for the future period, calculated by adding the differences (the 2041-2070 simulation minus the 1980-2000 subset of the 1971-2000 simulation) to the 1980-2000 simulation. If our assumption that the differencing of present and future at least partially cancels out model biases is true, then the predominant source of biases in the future values in the lower right hand panel is from the RCM simulation of the present-day, 1980-2000. The agreement among models was once again assessed using the three categories described in Fig. 16.

The selection of threshold temperatures to calculate extremes metrics is somewhat arbitrary because impacts-relevant thresholds are highly variable due to the very diverse climate of the U.S., with the exception of the freezing temperature, which is a universal physical threshold. In terms of high temperature thresholds, the values of 90°F, 95°F, and 100°F have been utilized in various studies of heat stress, although it is obvious that these thresholds have very different implications for the impacts on northern, cooler regions compared to southern, warmer regions. The threshold of 95°F has physiological relevance for maize production because the efficiency of pollination drops above that threshold. The low temperature thresholds of 10°F and 0°F also have varying relevance on impacts related to the background climate of a region. Fortunately, our analysis results are not qualitatively sensitive to the chosen thresholds. Thus, the results for these somewhat arbitrary choices nevertheless provide general guidance into scenarios of future changes.

Figure 20 shows the spatial distribution of the multi-model mean change in the average annual number of days with a maximum temperature exceeding 95°F, between 2055 and the model reference period of 1980-2000, for the high (A2) emissions scenario, for 8 NARCCAP regional climate model simulations. The largest absolute increases of more than 18 days occur in the far

south and west of the region where the number of occurrences in the present climate is the highest with increases of up to 21 days in parts of West Virginia and Maryland. The smallest increases of less than 3 days occur in the northernmost areas of Maine, New Hampshire, Vermont and northern New York, where the general increase in temperature is not large enough to substantially increase the chances for such warm days. The NARCCAP model changes in the number of 95°F days across the majority of the Northeast are statistically significant. The models also agree on the sign of change, with these grid points satisfying category 3, i.e. the models are in agreement that the number of days above 95°F will increase throughout the region for this scenario. For northern portions of Vermont, New Hampshire, and Maine however, the changes are not statistically significant for most models (category 1). In these areas where the historical number of days is very small, the models are in agreement that the increases in temperature are not sufficiently large to substantially increase the number of such days under this scenario.

Figure 21 shows the NARCCAP multi-model mean change in the average annual number of days with a minimum temperature below 10°F between 2055 and the model reference period of 1980-2000, for the high (A2) emissions scenario. All parts of the region are simulated to experience a decrease in the number of days. The largest decreases occur in the north of the region with changes of 21 days or more. The smallest decreases occur in coastal and southern areas where the number of occurrences in the present-day climate is small. These simulated decreases in cold days are in line with the recent observed changes in the Northeast region; for example, the occurrence of cold waves has been seen to decrease in recent years. All grid points satisfy category 3, with the models indicating that the changes in the number days below 10°F across the Northeast are statistically significant. The models also agree on the sign of change, i.e. they are in agreement that the number of days with a minimum temperature of less than 10°F will decrease throughout the region under this scenario.

Figure 22 shows the NARCCAP multi-model mean change in the average annual number of days with a minimum temperature of less than 32°F between 2055 and the model reference period of 1980-2000, for the high (A2) emissions scenario. Model simulated decreases are between 18 and 26 days across most of the region, with smaller changes simulated along parts of the Atlantic coast. The NARCCAP model changes in the number of days below freezing across the Northeast are statistically significant. The models also agree on the sign of change, with all grid points satisfying category 3, i.e. the models are in agreement that the number of days below 32°F will decrease throughout the region under this scenario.
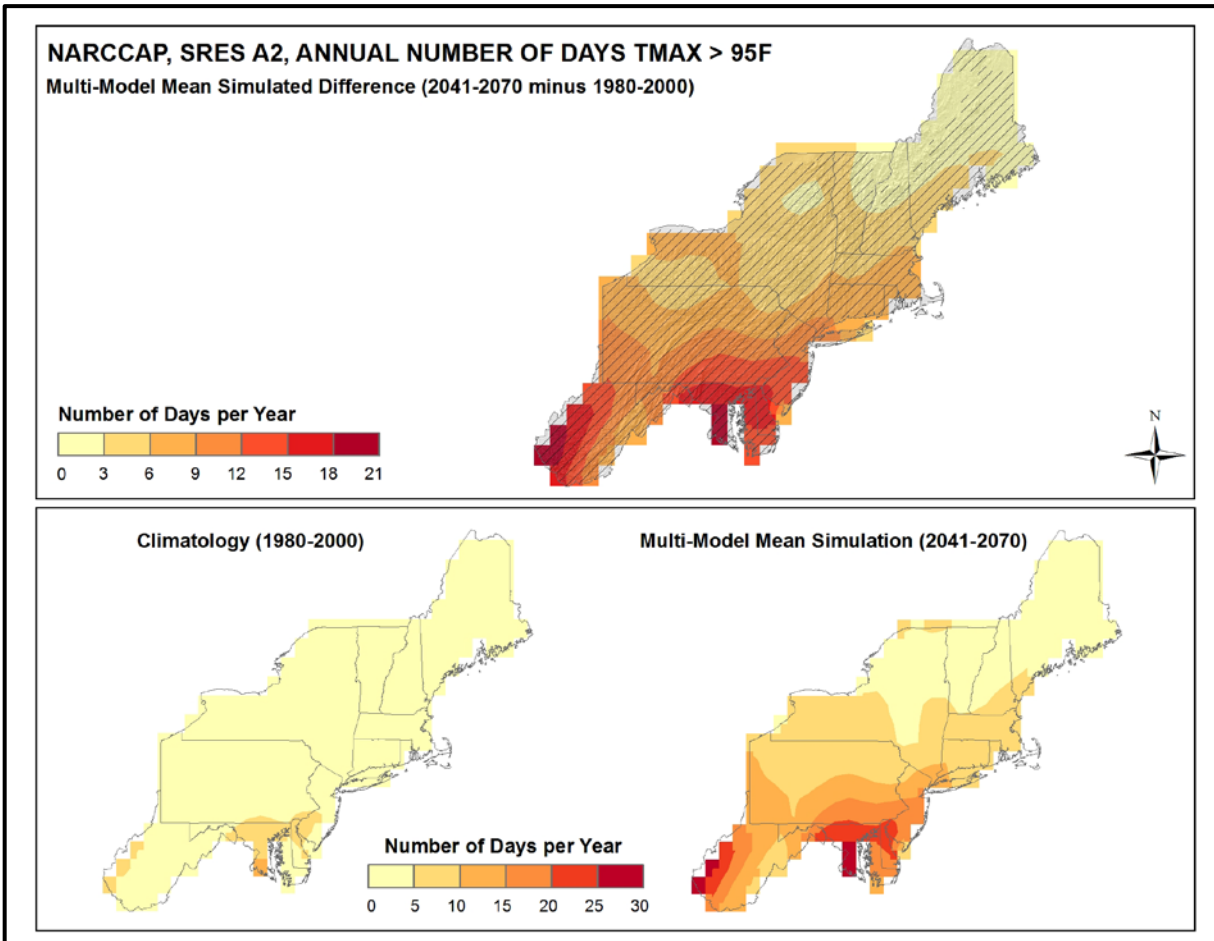
Figure 20. Simulated difference in the mean annual number of days with a maximum temperature greater than 95°F ($T_{max} > 95°F$) for the Northeast region, for the 2041-2070 time period with respect to the reference period of 1980-2000 (top). Color only (category 1) indicates that less than 50% of the models show a statistically significant change in the number of days. Color with hatching (category 3) indicates that more than 50% of the models show a statistically significant change in the number of days, and more than 67% agree on the sign of the change (see text). Mean annual number of days with $T_{max} > 95°F$ for the 1980-2000 reference period (bottom left). Simulated mean annual number of days with $T_{max} > 95°F$ for the 2041-2070 future time period (bottom right). These are multi-model means from 8 NARCCAP regional climate simulations for the high (A2) emissions scenario. Note that top and bottom color scales are different. The changes are upward everywhere. Increases are smallest in the far north, and largest in the south of the region.
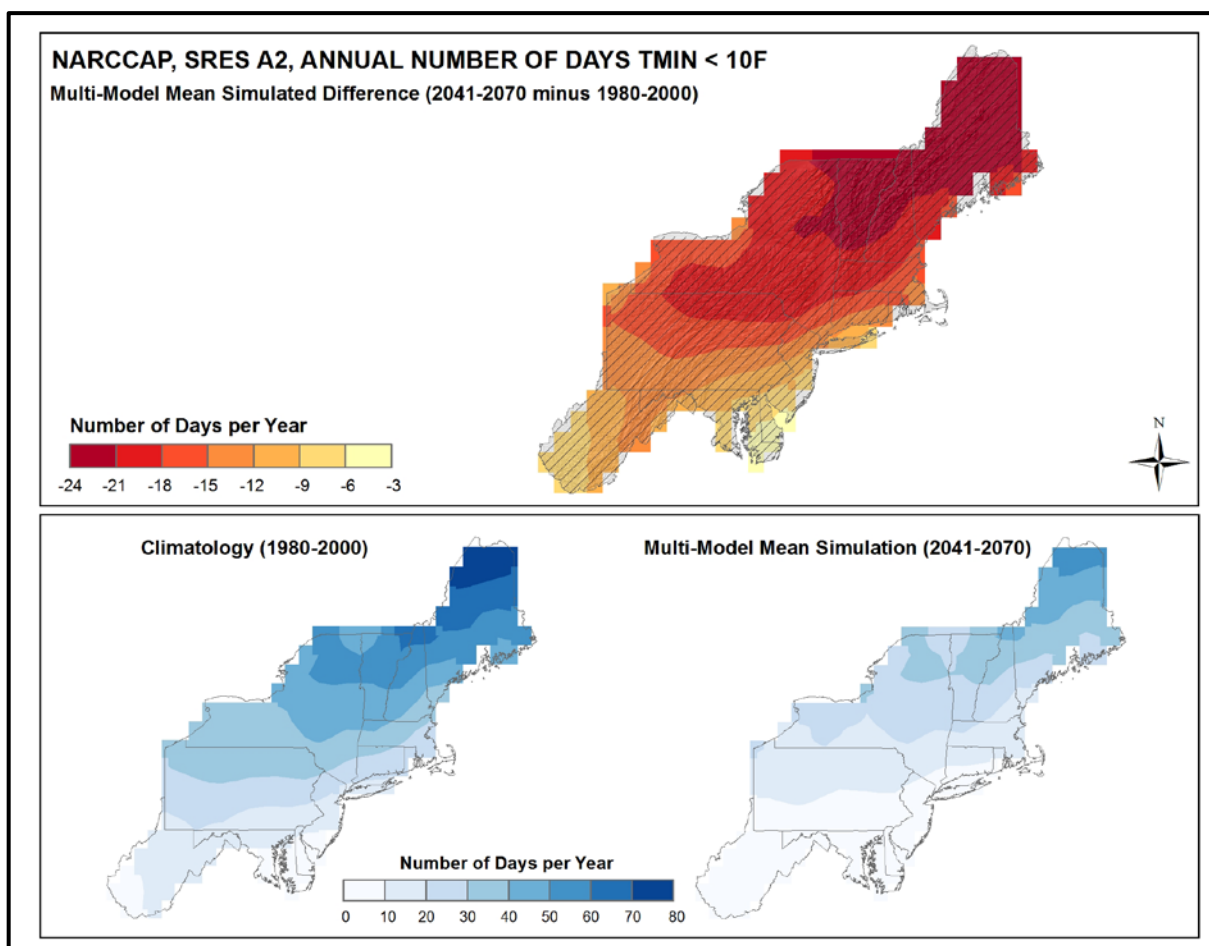
Figure 21. Simulated difference in the mean annual number of days with a minimum temperature less than 10°F ($T_{min} < 10°F$) for the Northeast region, for the 2041-2070 time period with respect to the reference period of 1980-2000 (top). Color with hatching (category 3) indicates that more than 50% of the models show a statistically significant change in the number of days, and more than 67% agree on the sign of the change (see text). Mean annual number of days with $T_{min} < 10°F$ for the 1980-2000 reference period (bottom left). Simulated mean annual number of days with $T_{min} < 10°F$ for the 2041-2070 future time period (bottom right). These are multi-model means from 8 NARCCAP regional climate simulations for the high (A2) emissions scenario. Decreases are largest in the north and become smaller southward, in a pattern similar to the present-day climatology.
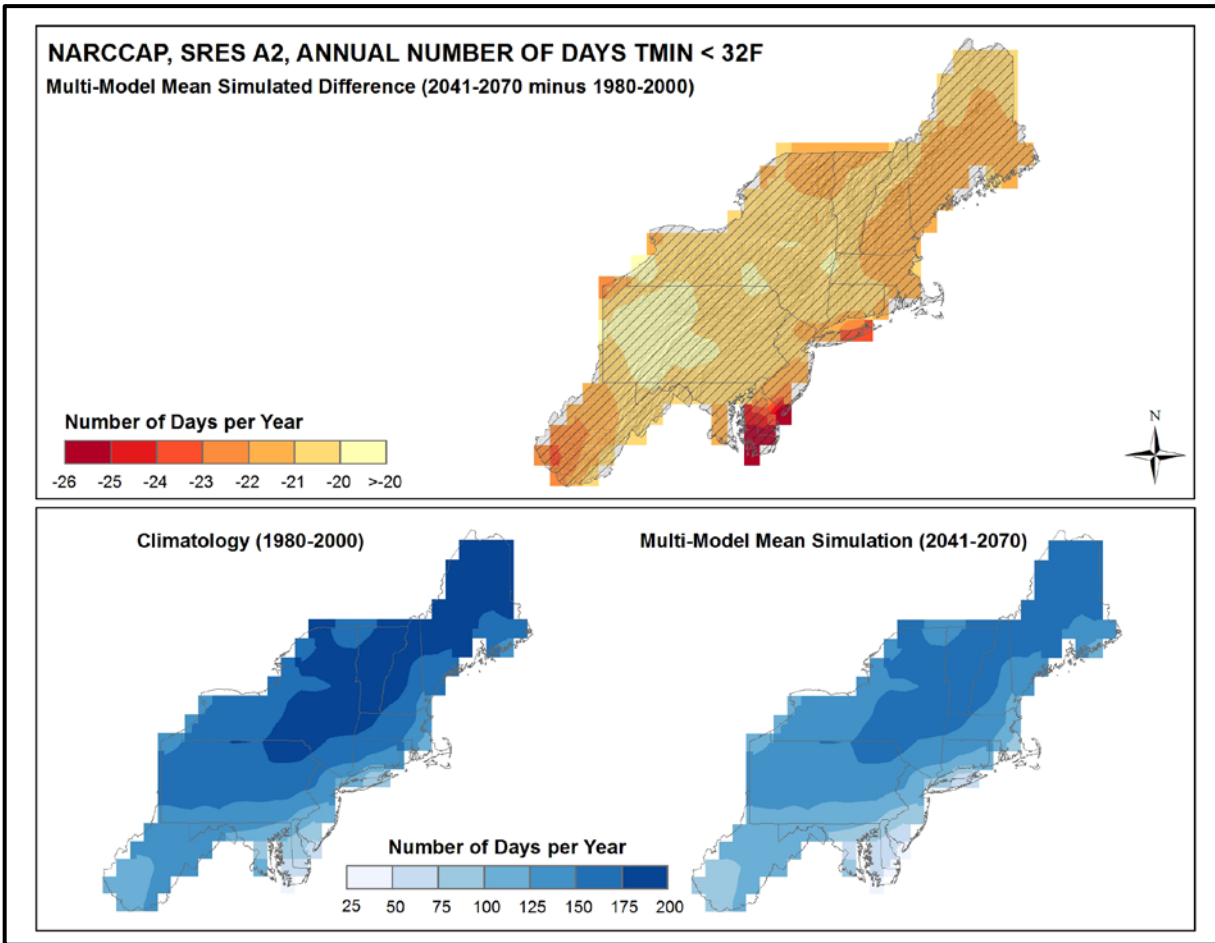
Figure 22. Simulated difference in the mean annual number of days with a minimum temperature less than 32°F ($T_{min} < 32°F$) for the Northeast region, for the 2041-2070 time period with respect to the reference period of 1980-2000 (top). Color with hatching (category 3) indicates that more than 50% of the models show a statistically significant change in the number of days, and more than 67% agree on the sign of the change (see text). Mean annual number of days with $T_{min} < 32°F$ for the 1980-2000 reference period (bottom left). Simulated mean annual number of days with $T_{min} < 32°F$ for the 2041-2070 future time period (bottom right). These are multi-model means from 8 NARCCAP regional climate simulations for the high (A2) emissions scenario. Changes are downward everywhere.

Consecutive warm days can have large impacts on a geographic area and its population, and are analyzed here as one metric of heat waves. Figure 23 shows the NARCCAP multi-model mean change in the average annual maximum number of consecutive days with maximum temperatures exceeding 95°F between 2055 and the model reference period of 1980-2000, for the high (A2) emissions scenario. The pattern is similar to the change in the total number of days exceeding 95°F for both the difference map, as well as its respective reference period. In most of New York and New England increases are small (less than 1 day), whereas changes for areas further south are generally in the range of 1-4 days. The greatest increases are in western West Virginia where the average annual longest string of days with such high temperatures is simulated to increase by up to 7 days. Changes in the number of consecutive days over 95°F are not statistically significant for northern areas of Maine and New Hampshire. All other grid points satisfy category 3, however, with the models indicating that changes across the Northeast are statistically significant. The models also agree on the sign of change, i.e. the models are in agreement that the number of consecutive days above 95°F will increase throughout the region under this scenario.

3.5. Other Temperature Variables

The spatial distribution of the NARCCAP multi-model mean change in the average length of the freeze-free season between 2055 and the model reference period of 1980-2000, for the high (A2) scenario, is shown in Fig. 24. The freeze-free season is defined as the period of time between the last spring frost (a daily minimum temperature of less than 32°F) and the first fall frost. The increases that have been seen climatologically over the last 30 years are simulated to continue, with the freeze-free season lengthening by at least 19 more days across the region by 2055 under this scenario. Most areas are simulated to see increases on the order of 3-4 weeks. All grid points satisfy category 3, with the models indicating that the changes in the length of the freeze-free season across the Northeast are statistically significant. The models also agree on the sign of change, i.e. the models are in agreement that the freeze-free season length will increase throughout the region under this scenario.

Cooling and heating degree days are accumulative metrics related to energy use, more specifically regarding the cooling and heating of buildings, with a base temperature of 65°F, assumed to be the threshold below which heating is required and above which cooling is required. Heating degree days provide a measure of the extent (in degrees), and duration (in days), that the daily mean temperature is below the base temperature. Cooling degree days measure the extent and duration that the daily mean temperature is above the base temperature.
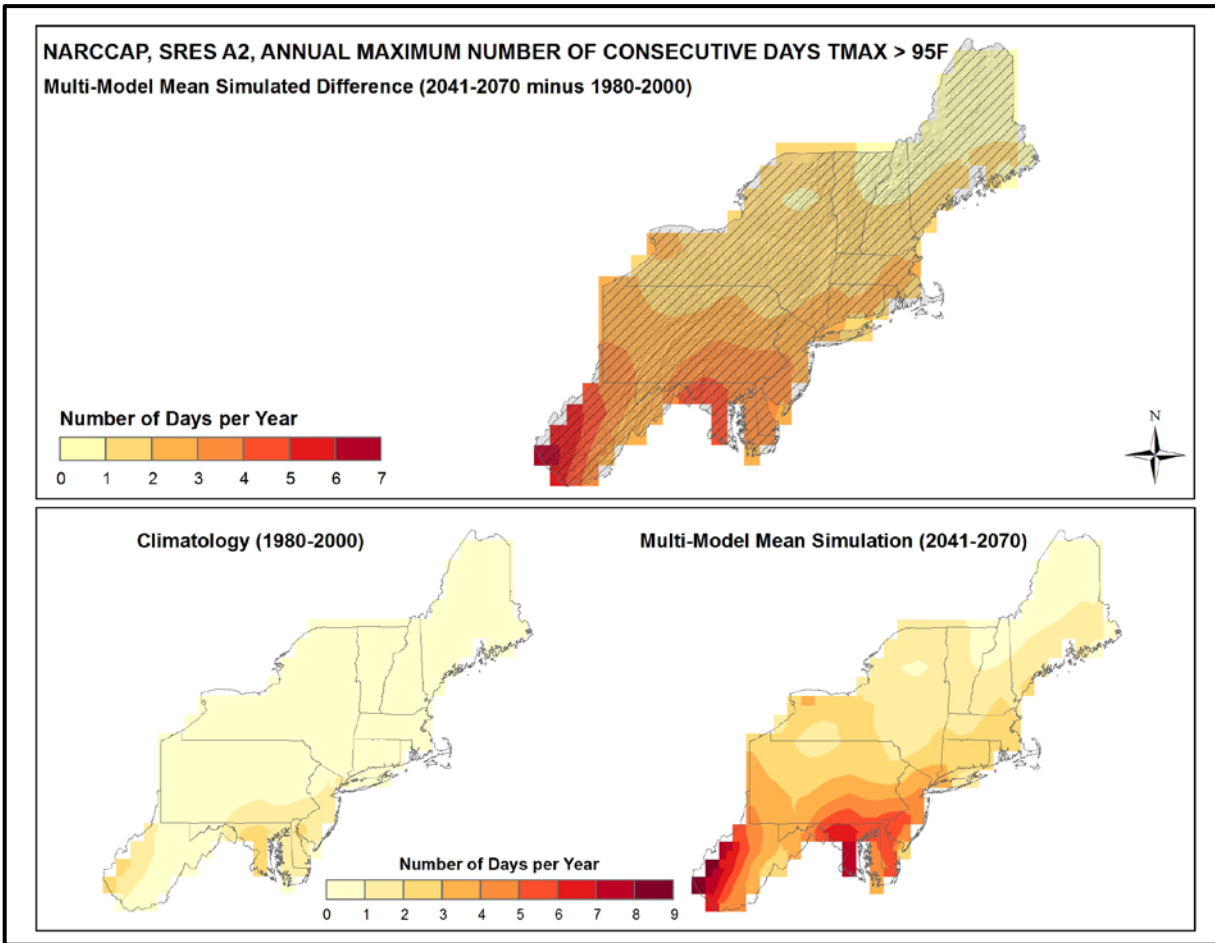
Figure 23. Simulated difference in the mean annual maximum number of consecutive days with a maximum temperature greater than 95°F ($T_{max} > 95°F$) for the Northeast region, for the 2041-2070 time period with respect to the reference period of 1980-2000 (top). Color only (category 1) indicates that less than 50% of the models show a statistically significant change in the number of consecutive days. Color with hatching (category 3) indicates that more than 50% of the models show a statistically significant change in the number of consecutive days, and more than 67% agree on the sign of the change (see text). Mean annual maximum number of consecutive days with $T_{max} > 95°F$ for the 1980-2000 reference period (bottom left). Simulated mean annual maximum number of consecutive days with $T_{max} > 95°F$ for the 2041-2070 future time period (bottom right). These are multi-model means from 8 NARCCAP regional climate simulations for the high (A2) emissions scenario. Note that top and bottom color scales are different. Increases are largest in the south and smallest in the north of the region, with a pattern similar to the present-day climatology.
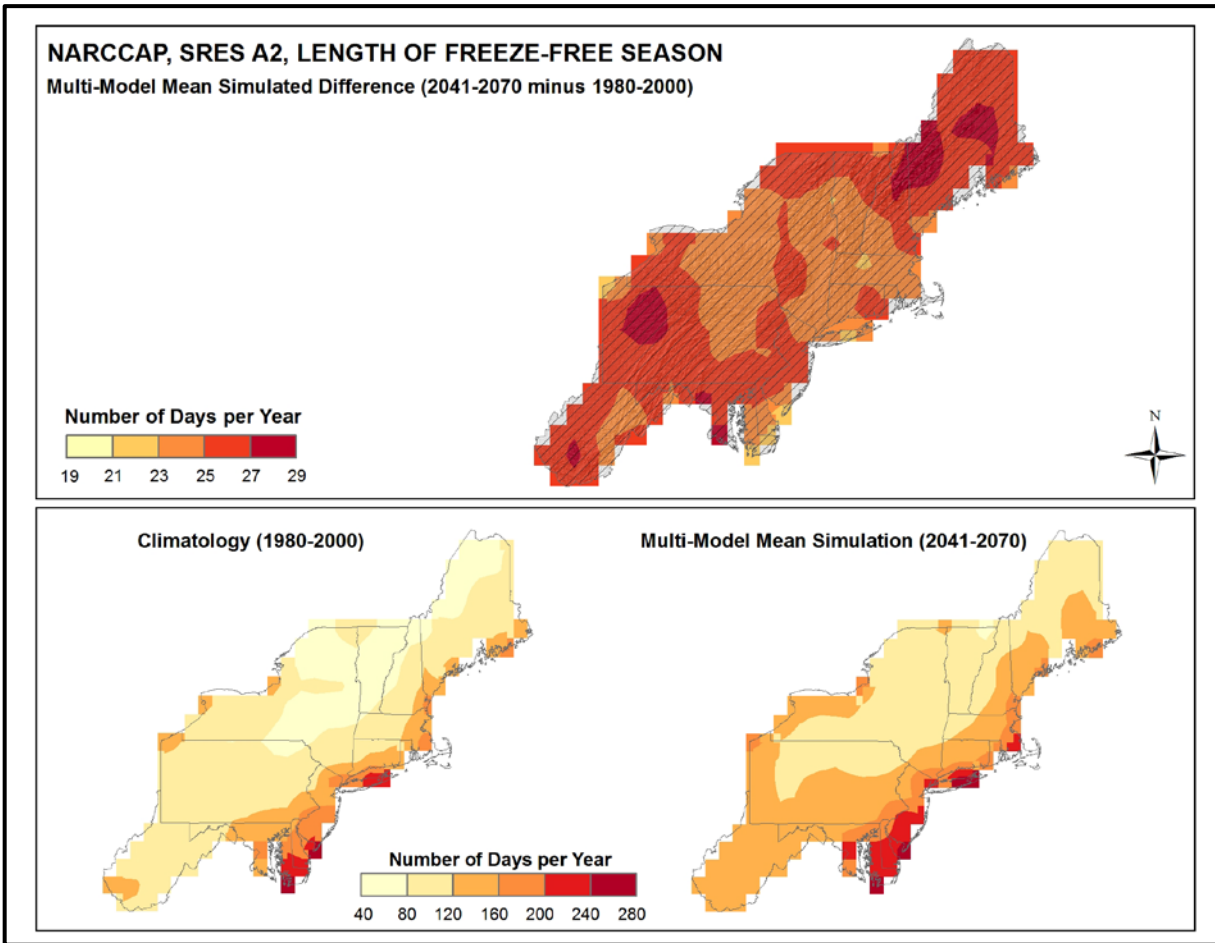
Figure 24. Simulated difference in the mean annual length of the freeze-free season for the Northeast region, for the 2041-2070 time period with respect to the reference period of 1980-2000 (top). Color with hatching (category 3) indicates that more than 50% of the models show a statistically significant change in the length of the freeze-free season, and more than 67% agree on the sign of the change (see text). Annual mean length of the freeze-free season for the 1980-2000 reference period (bottom left). Simulated mean annual length of the freeze-free season for the 2041-2070 future time period (bottom right). These are multi-model means from 8 NARCCAP regional climate simulations for the high (A2) emissions scenario. Note that top and bottom color scales are different. The length of the freeze-free season is simulated to increase throughout the region, with changes mostly in the 23-27 day range.

Figure 25 shows the NARCCAP multi-model mean change in the average annual number of cooling degree days (a climatic metric related to the energy required for cooling in the warm season, as previously described) between 2055 and the model reference period, for the high (A2) emissions scenario. In general, the simulated changes are quite closely related to mean temperature with the warmest (coolest) areas showing the largest (smallest) changes. The southernmost areas of West Virginia and Maryland are simulated to have the largest increases of up to 700 cooling degree days (CDDs) per year. The farthest northern portions of the region, including northern Maine and New Hampshire, will see the smallest increases of less than 200 CDDs. The models indicate that the changes in cooling degree days across the Northeast are statistically significant. The models also agree on the sign of change, with all grid points satisfying category 3, i.e. the models are in agreement that the number of CDDs will increase throughout the region under this scenario.

The NARCCAP multi-model mean change in the average annual number of heating degree days (a climatic metric related to the energy required for heating in the cold season, as previously described) between 2055 and the model reference period, for the high (A2) emissions scenario, is shown in Fig. 26. In general, the entire region is simulated to experience a decrease of at least 600 heating degree days (HDDs) per year. The areas simulated to have the greatest increase in CDDs have the smallest decrease in HDDs, and vice versa. The largest changes occur in northern areas, with decreases of up to 1,500 HDDs. Areas south of Pennsylvania and New Jersey are simulated to experience the smallest decrease in HDDs per year. The models once again indicate that the changes across the Northeast are statistically significant. All grid points satisfy category 3, with the models also agreeing on the sign of change, i.e. the models are in agreement that the number of HDDs will decrease throughout the region under this scenario.

3.6. Tabular Summary of Selected Temperature Variables

The mean changes for selected temperature-based derived variables from 8 NARCCAP simulations for 2055 with respect to the model reference period of 1971-2000, for the high (A2) emissions scenario, are summarized in Table 5. These were determined by first calculating the derived variable at each grid point. The spatially-averaged value of the variable was then calculated for the reference and future period. Finally, the difference or ratio between the two periods was calculated from the spatially-averaged values. In addition, these same variables were calculated from the 8 CMIP3 daily statistically-downscaled data set (Daily CMIP3) simulations for comparison.

For the NARCCAP simulations, the multi-model mean freeze-free period over the Northeast region is simulated to increase by 26 days, comparable to the 25 days calculated for the CMIP3 daily statistically-downscaled data. The number of days with daily maximum temperatures greater than 90°F, 95°F, and 100°F are simulated to increase by 13, 8, and 4 days, respectively, for the NARCCAP models. For the Daily CMIP3 data, corresponding increases are 15, 4, and 0 days, with the values decreasing by a greater amount as the thresholds become more extreme.
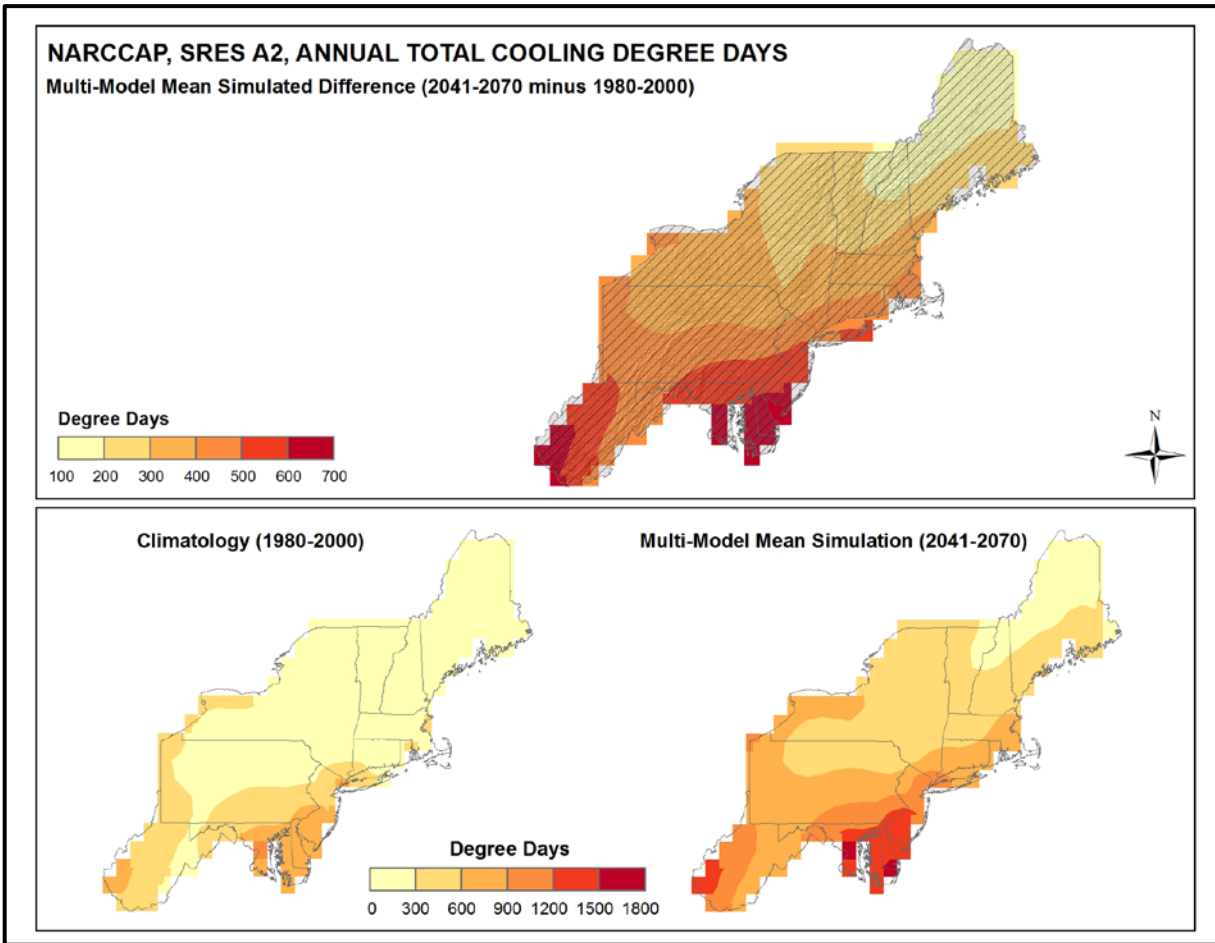
Figure 25. Simulated difference in the mean annual number of cooling degree days for the Northeast region, for the 2041-2070 time period with respect to the reference period of 1980-2000 (top). Color with hatching (category 3) indicates that more than 50% of the models show a statistically significant change in the number of cooling degree days, and more than 67% agree on the sign of the change (see text). Mean annual number of cooling degree days for the 1980-2000 reference period (bottom left). Simulated mean annual number of cooling degree days for the 2041-2070 future time period (bottom right). These are multi-model means from 8 NARCCAP regional climate simulations for the high (A2) emissions scenario. Note that top and bottom color scales are different. There are increases everywhere with the changes becoming larger from north to south.
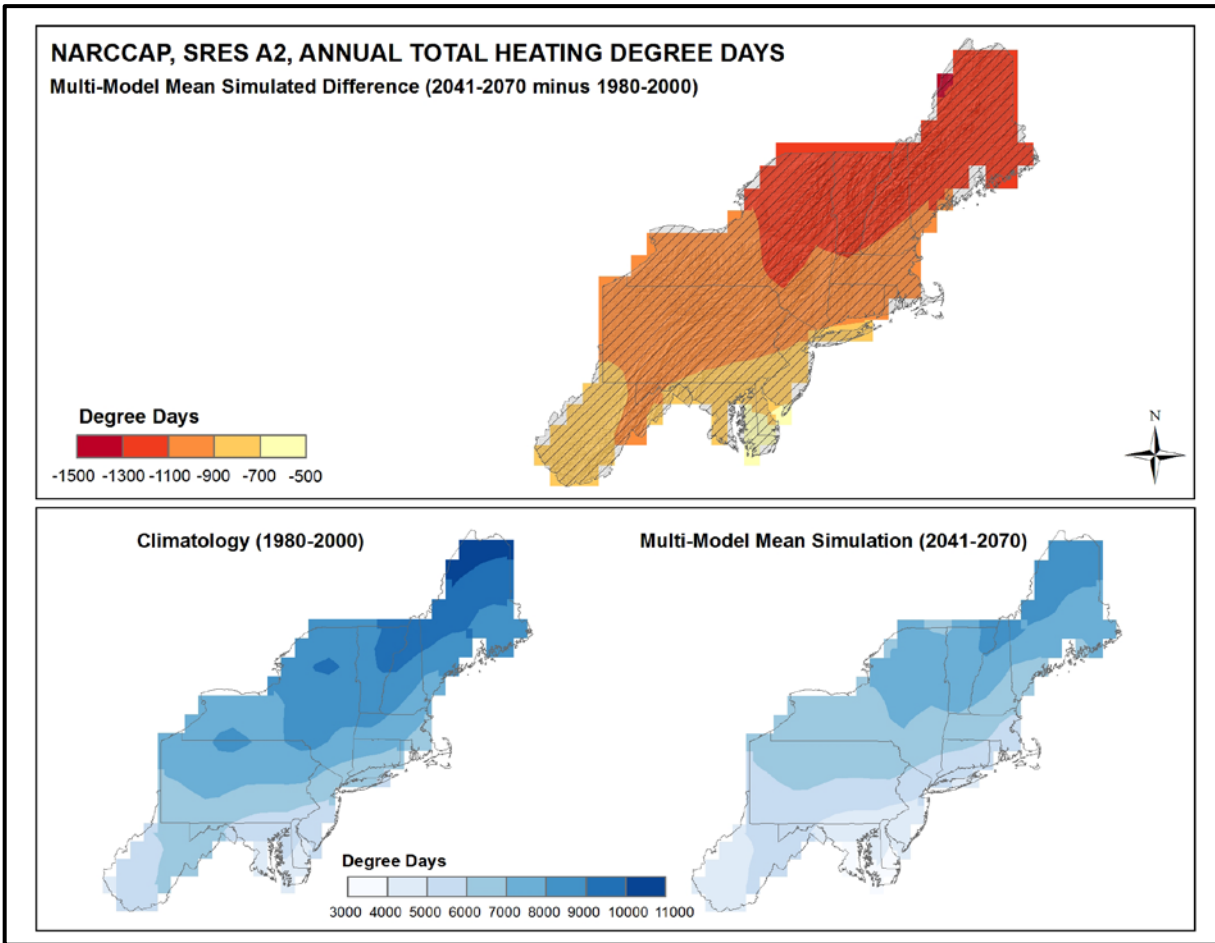
Figure 26. Simulated difference in the mean annual number of heating degree days for the Northeast region, for the 2041-2070 time period with respect to the reference period of 1980-2000 (top). Color with hatching (category 3) indicates that more than 50% of the models show a statistically significant change in the number of heating degree days, and more than 67% agree on the sign of the change (see text). Mean annual number of heating degree days for the 1980-2000 reference period (bottom left). Simulated mean annual number of heating degree days for the 2041-2070 future time period (bottom right). These are multi-model means from 8 NARCCAP regional climate simulations for the high (A2) emissions scenario. There are decreases everywhere with the largest changes in the north.

Table 5. Multi-model means and standard deviations of the simulated annual mean change in select temperature variables from 8 NARCCAP simulations for the Northeast region. Multi-model means from the 8 Daily_CMIP3 simulations are also shown for comparison. Analyses are for the 2041-2070 time period with respect to the reference period of 1971-2000, for the high (A2) emissions scenario.

Temperature Variable	NARCCAP Mean	NARCCAP Standard Deviation	Daily_CMIP3 Mean
Freeze-free period	+26 days	5 days	+25 days
#days $T_{max} > 90°F$	+13 days	7 days	+15 days
#days $T_{max} > 95°F$	+8 days	6 days	+4 days
#days $T_{max} > 100°F$	+4 days	5 days	0 days
#days $T_{min} < 32°F$	-26 days	3 days	-32 days
#days $T_{min} < 10°F$	-17 days	4 days	-13 days
#days $T_{min} < 0°F$	-9 days	4 days	-6 days
Consecutive #days > 95°F	+171%	105%	+309%
Consecutive #days > 100°F	+237%	212%	+786%
Heating degree days	-16%	1%	-18%
Cooling degree days	+99%	32%	+91%
Growing degree days (base 50°F)	+41%	6%	+35%

The number days with minimum temperatures of less than 32°F, 10°F, and 0°F are simulated to decrease by 26, 17, and 9 days, respectively, for the NARCCAP models. Corresponding values for the Daily CMIP3 simulations are comparable decreases of 32, 13, and 6 days.

The multi-model mean annual maximum number of consecutive days exceeding 95°F and 100°F (our heat wave metric) are simulated to increase by 171% and 237%, respectively, for the NARCCAP data, a substantial increase in the length of such hot periods. These increases are greater for the Daily CMIP3 simulations, with values of 309% for the 95°F and 786% for the 100°F threshold.

Table 5 indicates that, for the high (A2) emissions scenario, the number of heating degree days are simulated by the NARCCAP simulations to decrease by 16% (18% for Daily CMIP3), while the number of cooling degree days are simulated to increase by 99% (91% for Daily CMIP3). The number of growing degree days are also comparable for both data sets, increasing by 41% and 35% for NARCCAP and Daily CMIP3, respectively.

3.7. Mean Precipitation

Figure 27 shows the spatial distribution of multi-model mean simulated differences in average annual precipitation for the three future time periods (2035, 2055, 2085) with respect to 1971-1999, for both emissions scenarios, for the 14 (B1) or 15 (A2) CMIP3 models. The far northern regions show the largest simulated increases while southern and coastal areas show less of an increase. This gradient increases in magnitude as the time progresses, particularly for the high (A2) emissions scenario. The largest north-south differences are for the A2 scenario in 2085, varying from an increase of around 0-3% in southern West Virginia to an increase of 6-9% in northern New England and New York. The smallest simulated differences occur for both scenarios in 2035, with increases of less than 0 to 6% throughout the region. The agreement between models was once again assessed

using the three categories described in Fig. 16. It can be seen that for the 2035 time period the changes in precipitation are not significant for most models (category 1) over the majority of grid points. This means that most models are in agreement that any changes will be smaller than the normal year-to-year variations that occur. However, for both emissions scenarios in 2055 and 2085, most models indicate changes that are larger than these normal variations (category 3), i.e., the models are mostly in agreement that precipitation will increase over the entire region. There is a small area in the south of the region for the A2 scenario in 2035 where the models are in disagreement about the sign of the changes (category 2).

Table 6 shows the distribution of simulated changes in annual mean precipitation for each future time period with respect to 1971-1999, for both emissions scenarios, across the 14 (B1) or 15 (A2) CMIP3 models. The distribution of 9 NARCCAP simulations (for 2055, A2 scenario only) is also shown for comparison, with respect to 1971-2000. For all three time periods and both scenarios, the CMIP3 suite includes model simulations with both increases and decreases in precipitation. All the median values are greater than zero. The inter-model range of changes in precipitation (i.e., the difference between the highest and lowest model values) varies from 12% to 24%. The range of the NARCCAP values is 11%. The interquartile range (the difference between the 75th and 25th percentiles) of precipitation changes across all the GCMs is less than 8% for all execept the A2, 2085 simulation.

Table 6. Distribution of the simulated change in annual mean precipitation (%) from the 14 (B1) or 15 (A2) CMIP3 models for the Northeast region. The lowest, 25th percentile, median, 75th percentile and highest values are given for the high (A2) and low (B1) emissions scenarios, and for each future time period (2021-2050, 2041-2070, and 2070-2099) with respect to the reference period of 1971-1999. Also shown are values from the distribution of 9 NARCCAP models for 2041-2070, A2 only, with respect to 1971-2000.

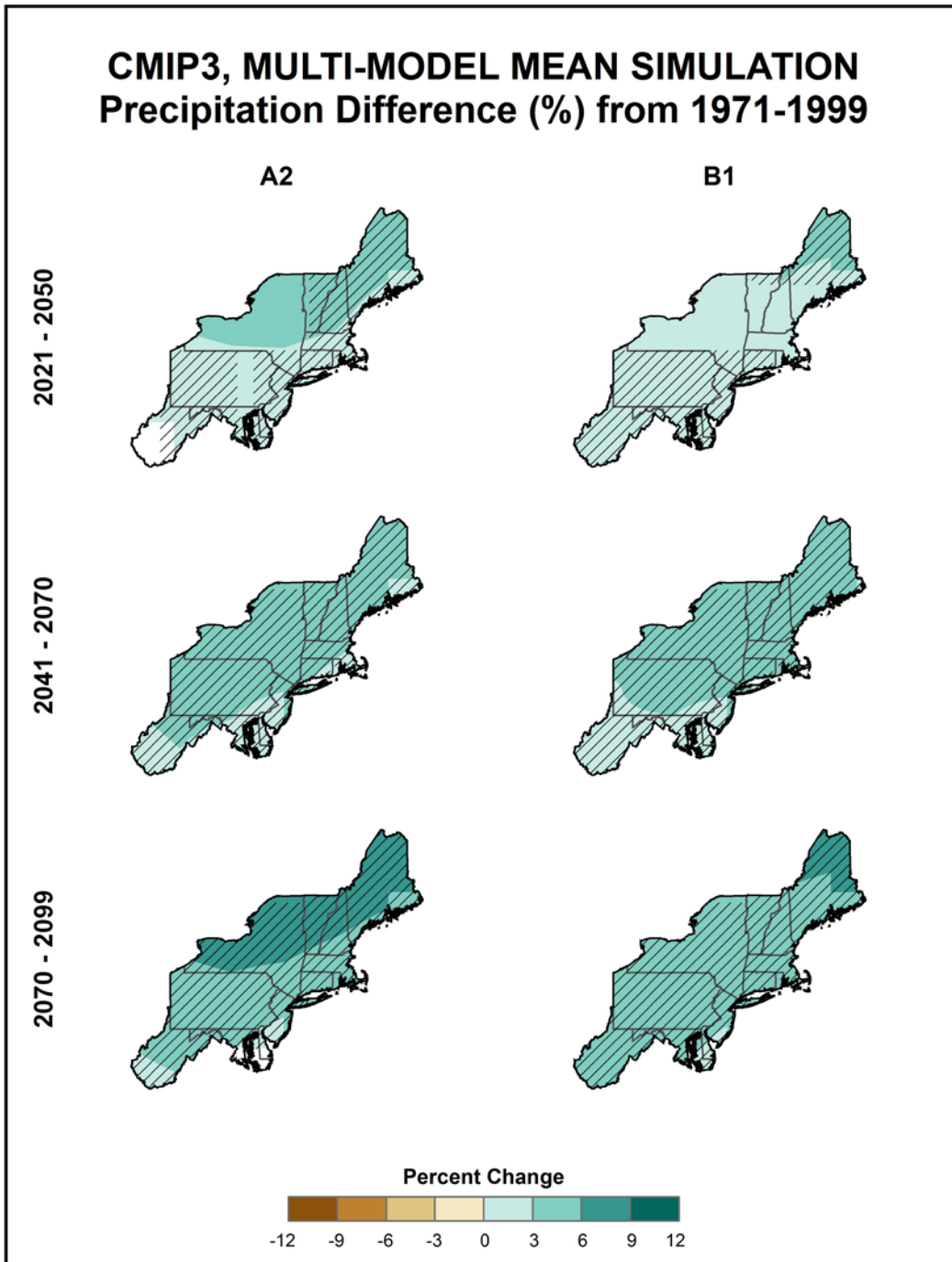| Scenario	Period	Lowest	25th Percentile	Median	75th Percentile	Highest
A2	2021-2050	-5	1	4	5	7
	2041-2070	-6	1	5	8	10
	2070-2099	-8	-1	9	11	16
	NARCCAP (2041-2070)	*-1*	*4*	*6*	*6*	*10*
B1	2021-2050	-5	1	3	5	9
	2041-2070	-4	-2	4	6	8
	2070-2099	-2	2	6	8	10

Figure 27. Simulated difference in annual mean precipitation (%) for the Northeast region, for each future time period (2021-2050, 2041-2070, and 2070-2099) with respect to the reference period of 1971-1999. These are multi-model means for the high (A2) and low (B1) emissions scenarios from the 14 (B1) or 15 (A2) CMIP3 global climate simulations. Color only (category 1) indicates that less than 50% of the models show a statistically significant change in precipitation. Color with hatching (category 3) indicates that more than 50% of the models show a statistically significant change in precipitation, and more than 67% agree on the sign of the change. Whited out areas (category 2) indicate that more than 50% of the models show a statistically significant change in precipitation, but less than 67% agree of the sign of the change (see text). The models simulate increases across the entire region.

54

Figure 28 shows the multi-model mean annual and seasonal 30-year average precipitation change between 2041-2070 and 1971-2000 for the high (A2) emissions scenario, for 11 NARCCAP regional climate model simulations. The simulated annual changes are upward throughout the region, with increases of less than 7% everywhere. Winter shows the greatest simulated increases of up to 20%. Spring and fall changes are mostly upward, varying between -4 and 12%. Simulated precipitation changes in the summertime are mostly downward, ranging from +4 to -12%. The agreement between models was again assessed using the three categories described in Fig. 16. It can be seen that annually, and for the fall season, the simulated changes in precipitation are not statistically significant for most models over all grid points (category 1). This is also the case for the other seasons, with the exception of a few areas where the models are in agreement (category 3). These are: northern Vermont and northwestern Pennsylvania for the winter simulation, parts of central New York for spring, and an area of western Pennsylvania for summer.

Table 7 shows the distribution of simulated changes in seasonal mean precipitation among the 14 (B1) or 15 (A2) CMIP3 models, between 2070-2099 and 1971-1999 for both emissions scenarios. On a seasonal basis, the range of model-predicted changes is quite large. For example, in the high (A2) emissions scenario, the simulated change in summer precipitation varies from a decrease of 26% to an increase of 26%. In the low (B1) emissions scenario, the range of changes in precipitation is generally smaller, with a tendency towards slightly wetter conditions (i.e., more models indicate an increase in precipitation than for the A2 scenario). The central feature of the results in Table 7 is the large uncertainty in seasonal precipitation changes.

Table 7. Distribution of the simulated change in seasonal mean precipitation (%) from the 14 (B1) or 15 (A2) CMIP3 models for the Northeast region. The lowest, 25th percentile, median, 75th percentile and highest values are given for the high (A2) and low (B1) emissions scenarios, and for the 2070-2099 time period with respect to the reference period of 1971-1999.

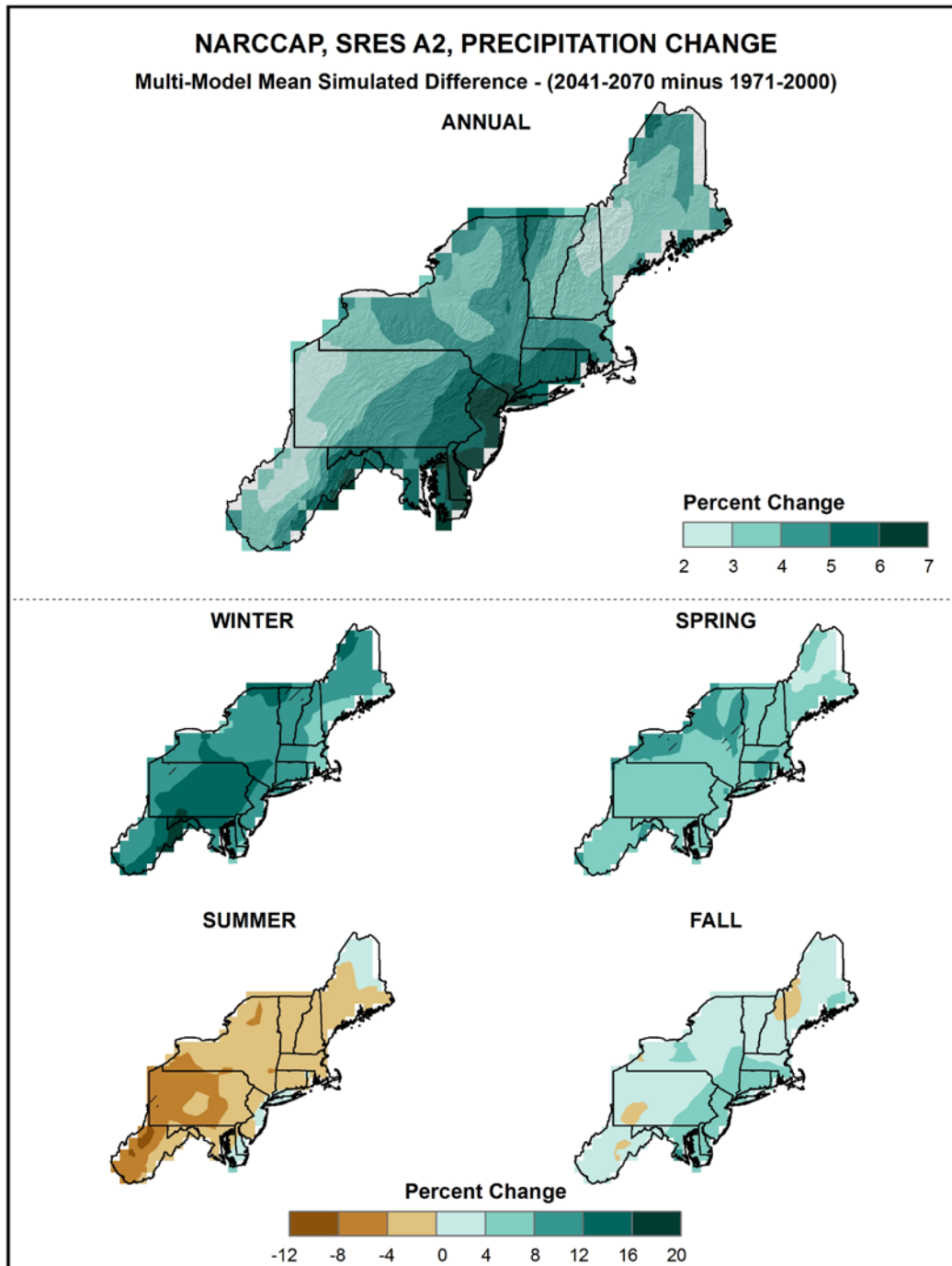| Scenario	Period	Season	Lowest	25th Percentile	Median	75th Percentile	Highest
A2	2070-2099	DJF	1	5	14	19	29
		MAM	-5	-3	8	16	26
		JJA	-26	-5	2	6	26
		SON	-13	-8	3	9	15
B1	2070-2099	DJF	-2	4	8	14	20
		MAM	-1	6	7	8	21
		JJA	-6	-2	3	6	6
		SON	-9	-3	0	6	10

Figure 28. Simulated difference in annual and seasonal mean precipitation (%) for the Northeast region, for 2041-2070 with respect to the reference period of 1971-2000. These are multi-model means from 11 NARCCAP regional climate simulations for the high (A2) emissions scenario. Color only (category 1) indicates that less than 50% of the models show a statistically significant change in precipitation. Color with hatching (category 3) indicates that more than 50% of the models show a statistically significant change in the number of days, and more than 67% agree on the sign of the change (see text). Note that the top and bottom color scales are unique, and different from that of Fig. 27. The annual change is upward everywhere, with increases of 2-7% throughout the region. Changes are mostly upward in winter, spring, and fall, and downward in summer.

Figure 29 shows the simulated change in annual mean precipitation for each future time period with respect to 1971-1999, for both emissions scenarios, averaged over the entire Northeast region for the 14 (B1) or 15 (A2) CMIP3 models. In addition, averages for 9 of the NARCCAP (relative to 1971-2000) simulations and the 4 GCMs used in the NARCCAP experiment are shown for 2055 (A2 scenario only). Both the multi-model mean and individual model values are shown. The multi-model mean changes for the CMIP3 models are both positive and negative, with the majority of models simulating increases in precipitation. For the high (A2) emissions scenario, the models simulate mean increases of between 3 and 6%. Simulations for the low (B1) emissions scenario indicate less of an increase for each time period, reaching +5% by 2085. The multi-model mean of the NARCCAP simulations is larger than that of the associated CMIP3 simulations, with the mean of the 4 GCMs used in the NARCCAP experiment being even greater. The inter-model range of changes in Fig. 29 is large compared to the differences in the multi-model means, as also illustrated in Table 6. In fact, for both emissions scenarios, the individual model range is much larger than the differences in the CMIP3 multi-model means between time periods.

Figure 30 shows the simulated change in seasonal mean precipitation for each future time period with respect to 1971-1999, for the high (A2) emissions scenario, averaged over the entire Northeast region for the 15 CMIP3 models, as well as the NARCCAP models for 2055, relative to 1971-2000. Again, both the multi-model mean and individual model values are shown. The CMIP3 models simulate mean increases for all seasons, except summer for 2085. The NARCCAP models, which are displayed for 2055 only, simulate slightly larger increases in precipitation than the CMIP3 models for winter, spring, and fall, and indicate a decrease for summer. As was the case for the annual totals in Fig. 29, the model ranges in Fig. 30 are large compared to the multi-model mean differences. This illustrates the large uncertainty in the precipitation estimates using these simulations.

3.8. Extreme Precipitation

Figure 31 shows the spatial distribution of the multi-model mean change in the average annual number of days with precipitation exceeding 1 inch, for 8 NARCCAP regional climate model simulations. Again this is the difference between the period of 2041-2070 and the 1980-2000 model reference period, for the high (A2) emissions scenario. In addition to this difference map, maps of the model simulations of the actual values for historical conditions (NARCCAP models driven by the NCEP Reanalysis II) and for the future are also displayed for comparison. All areas exhibit increases, the greatest being up to 30% in parts of New York. The smallest simulated increases of 9 to 12% are mainly in coastal regions, as well as western Pennsylvania and West Virginia. It can be seen that changes in days exceeding 1 inch are not statistically significant for most models (category 1) over the majority of grid points in the south and east of the region. This means that most models are in agreement that any changes will be smaller than the normal year-to-year variations that occur under this scenario. However, in the central portion of the region (where simulated increases are largest), most models indicate increases in days with precipitation of more than 1 inch that are larger than these normal variations (category 3).
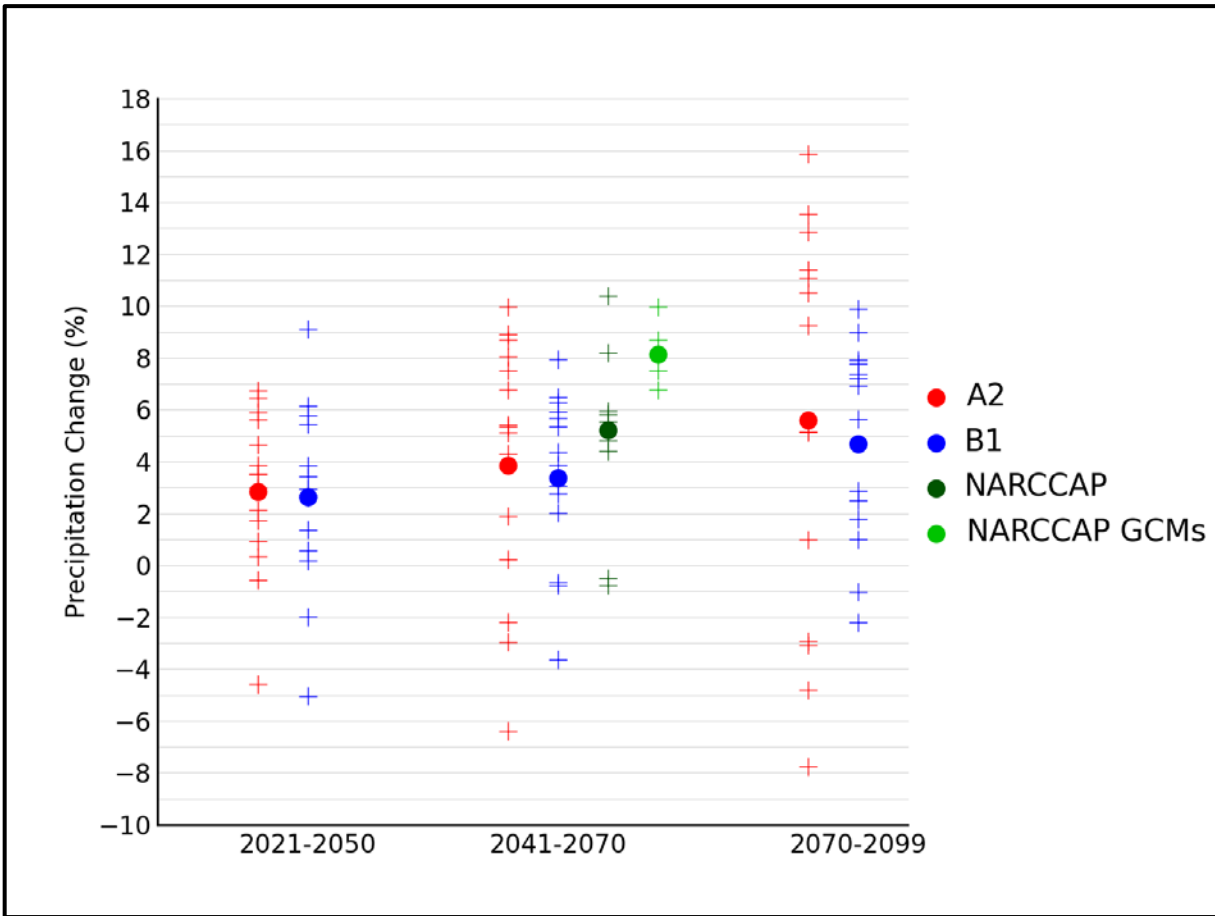
Figure 29. Simulated annual mean precipitation change (%) for the Northeast region, for each future time period (2021-2050, 2041-2070, and 2070-2099) with respect to the reference period of 1971-1999. Values are given for the high (A2) and low (B1) emissions scenarios for the 14 (B1) or 15 (A2) CMIP3 models. Also shown for 2041-2070 (high emissions scenario only) are values (relative to 1971-2000) for 9 NARCCAP models, as well as for the 4 GCMs used to drive the NARCCAP simulations. The small plus signs indicate each individual model and the circles depict the multi-model means. The ranges of model-simulated changes are very large compared to the mean changes and to differences between the A2 and B1 scenarios.
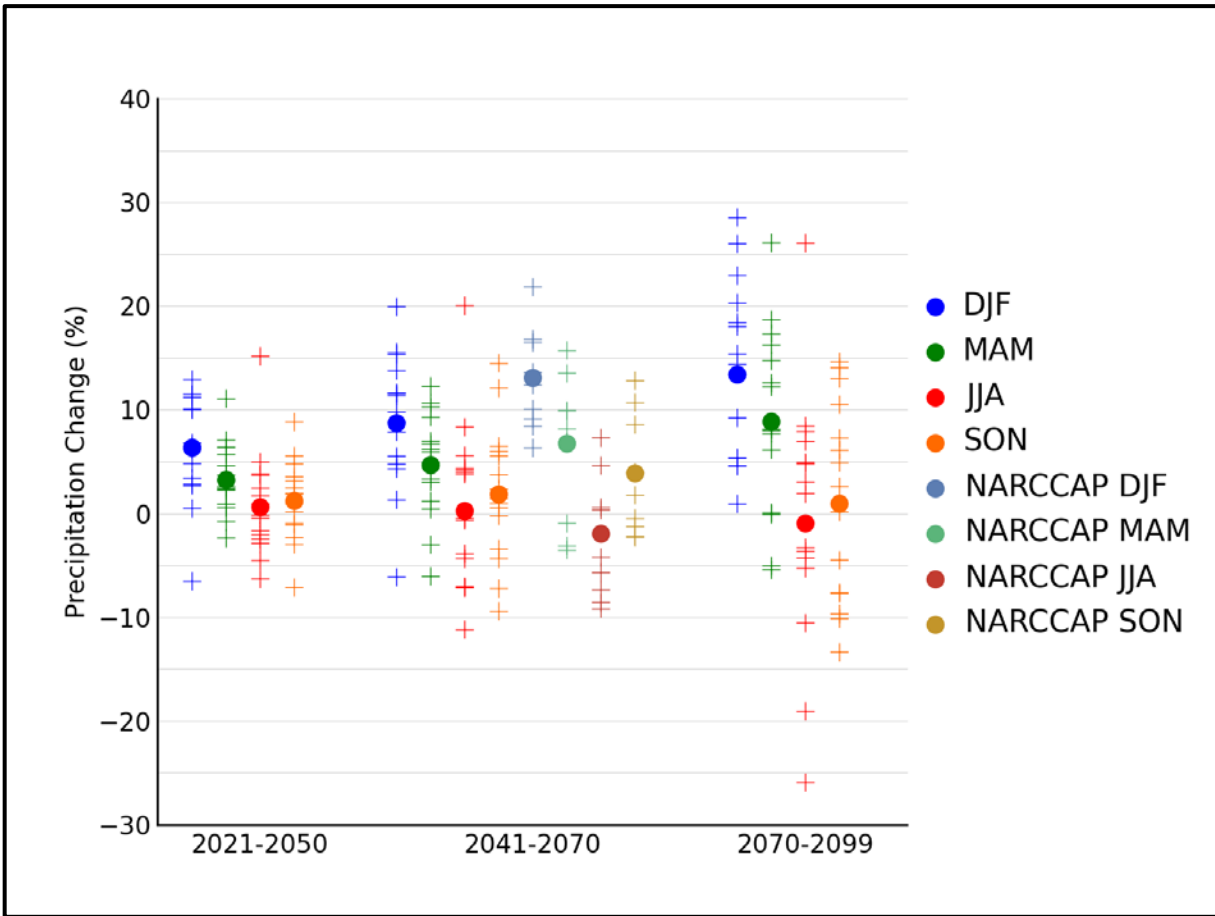
Figure 30. Simulated seasonal mean precipitation change (%) for the Northeast region, for each future time period (2021-2050, 2041-2070, and 2070-2099) with respect to the reference period of 1971-1999. Values are given for all 15 CMIP3 models for the high (A2) emissions scenario. Also shown are values (relative to 1971-2000) for 9 NARCCAP models for 2041-2070. The small plus signs indicate each individual model and the circles depict the multi-model means. Seasons are indicated as follows: winter (DJF, December-January-February), spring (MAM, March-April-May), summer (JJA, June-July-August), and fall (SON, September-October-November). The ranges of model-simulated changes are large compared to the mean changes and compared to differences between the seasons.
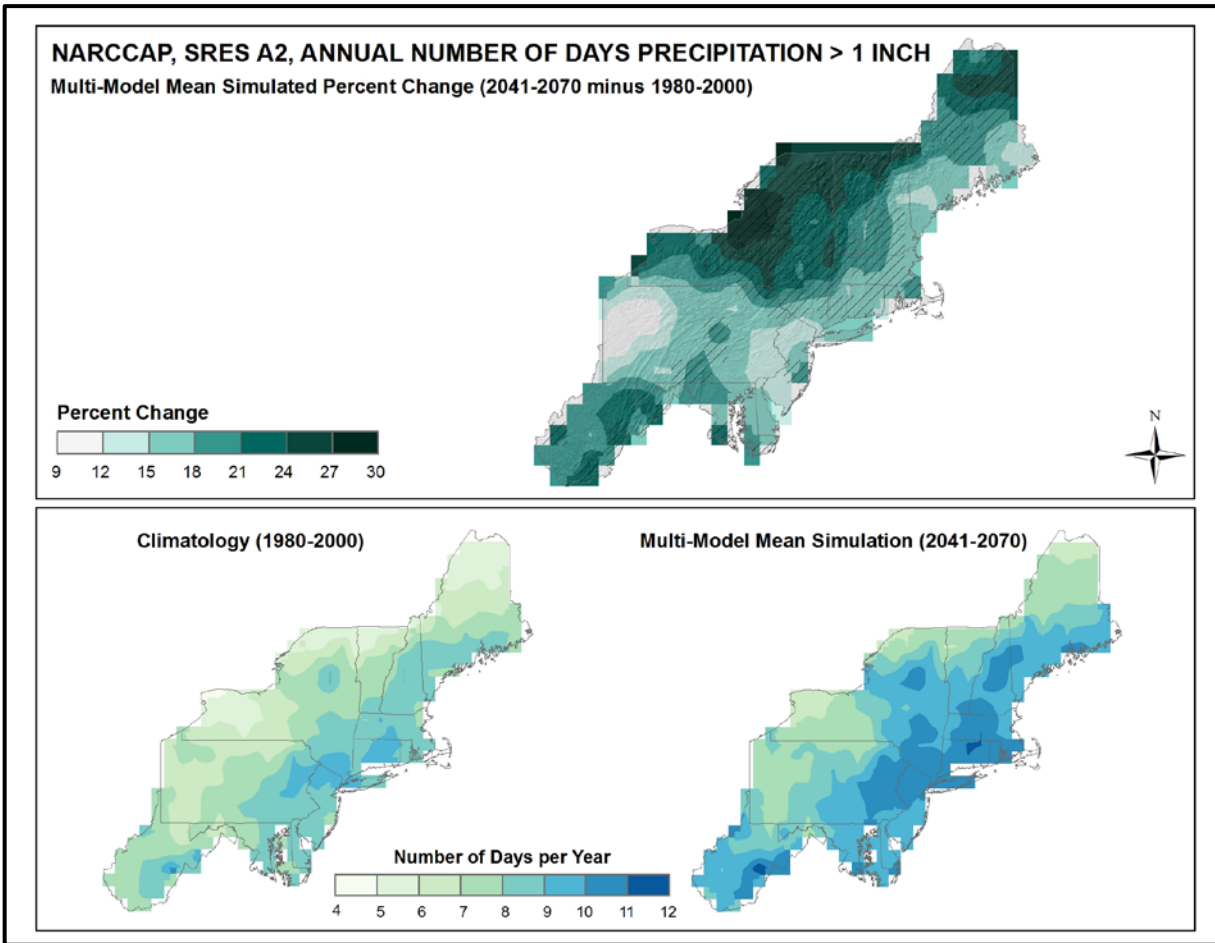
Figure 31. Simulated percentage difference in the mean annual number of days with precipitation of greater than one inch for the Northeast region, for the 2041-2070 time period with respect to the reference period of 1980-2000 (top). Color only (category 1) indicates that less than 50% of the models show a statistically significant change in the number of days. Color with hatching (category 3) indicates that more than 50% of the models show a statistically significant change in the number of days, and more than 67% agree on the sign of the change (see text). Mean annual number of days with precipitation of greater than one inch for the 1980-2000 reference period (bottom left). Simulated mean annual number of days with precipitation of greater than one inch for the 2041-2070 future time period (bottom right). These are multi-model means from 8 NARCCAP regional climate simulations for the high (A2) emissions scenario. The models simulate general increases with the largest changes in the north.

Consecutive days with little or no precipitation reduce soil moisture levels and put stress on plants. Figure 32 shows the NARCCAP multi-model mean change in the average annual maximum number of consecutive days with precipitation less than 0.1 inches (3 mm) between 2055 and the model reference period of 1980-2000, for the high (A2) emissions scenario. Most areas are simulated to see small increases or no change over time (0 to 3 days per year). There are some areas in the northern portion of the region that show simulated decreases in consecutive dry days, but these values are also relatively small (less than 2 days). Changes in the number of consecutive days with precipitation of less than 0.1 inches are not statistically significant for most models (category 1) over the majority of grid points. This means that most models are in agreement that any changes will be smaller than the normal year-to-year variations that occur under this scenario. However, for small areas of Pennsylvania, New Jersey, Maryland, and Delaware, most models indicate statistically significant increases (category 3).

3.9. Tabular Summary of Selected Precipitation Variables

The mean changes for select precipitation-based variables derived from 8 NARCCAP simulations for 2055 with respect to the model reference period of 1971-2000, for the high (A2) emissions scenario, are summarized in Table 8. The same variables from the 8 CMIP3 statistically-downscaled (Daily_CMIP3) simulations are also shown for comparison. These spatially-averaged values were calculated as described for Table 5.

Table 8. Multi-model means and standard deviations of the simulated mean annual change in select precipitation variables from 8 NARCCAP simulations for the Northeast region. Multi-model means from the 811 Daily_CMIP3 simulations are also shown for comparison. Analyses are for the 2041-2070 time period with respect to the reference period of 1971-2000, for the high (A2) emissions scenario.

Precipitation Variable	NARCCAP Mean	NARCCAP Standard Deviation	Daily_CMIP3 Mean
#days > 1 inch	+21%	7%	+21%
#days > 2 inches	+41%	24%	+40%
#days > 3 inches	+56%	45%	+53%
#days > 4 inches	+65%	70%	+79%
Consecutive #days < 0.1 inches	+1 day	+2 days	+1 day

Climatologically, extreme precipitation events have increased in recent years, a trend which is simulated to continue. For the NARCCAP data, the multi-model mean number of days with precipitation greater than certain thresholds increases for all threshold values (+21% for 1 inch, +41% for 2 inches, +56% for 3 inches, and +65% for 4 inches). The increases are higher for the more extreme thresholds. The average annual maximum number of consecutive days with precipitation less than 0.1 inches increases by only 1 day. The CMIP3 daily statistically-downscaled simulations are comparable to their NARCCAP counterparts, with the number of days also increasing for each threshold. The change in the average maximum number of consecutive days with precipitation less than 0.1 inches is the same as the NARCCAP value.
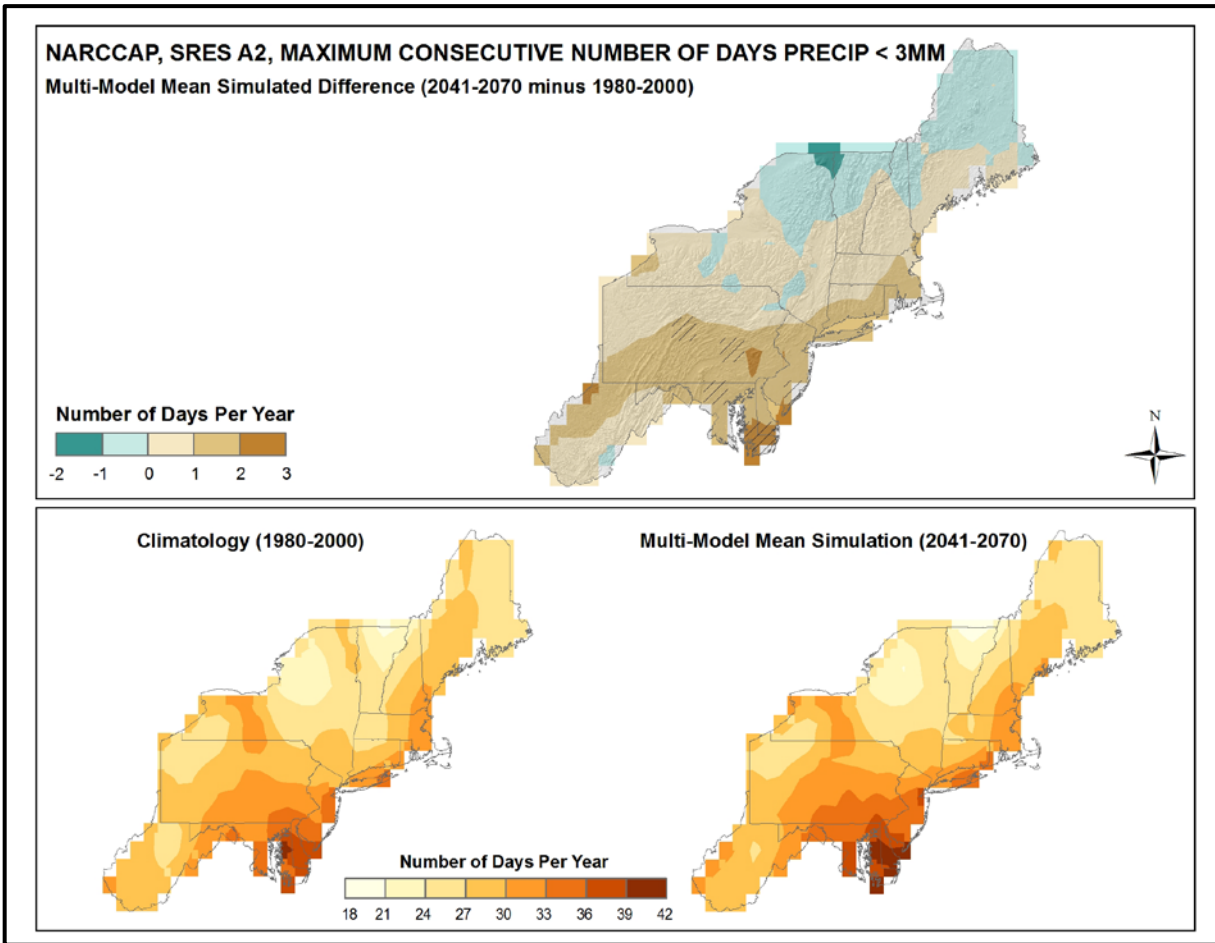
Figure 32. Simulated difference in the mean annual maximum number of consecutive days with precipitation of less than 0.1 inches/3 mm for the Northeast region, for the 2041-2070 time period with respect to the reference period of 1980-2000 (top). Color only (category 1) indicates that less than 50% of the models show a statistically significant change in the number of consecutive days. Color with hatching (category 3) indicates that more than 50% of the models show a statistically significant change in the number of consecutive days, and more than 67% agree on the sign of the change (see text). Mean annual maximum number of consecutive days with precipitation of less than 0.1 inches/3 mm for the 1980-2000 reference period (bottom left). Simulated mean annual maximum number of consecutive days with precipitation of less than 0.1 inches/3 mm for the 2041-2070 future time period (bottom right). These are multi-model means from 8 NARCCAP regional climate simulations for the high (A2) emissions scenario. The models simulate little change over the majority of the region, with slight decreases in the south.

### 3.10. Comparison Between Model Simulations and Observations

In this section, some selected comparisons between CMIP3 model simulations and observations are presented. These are limited to annual and seasonal temperature and precipitation. The model simulations of the 20th century that are shown herein are based on estimated historical forcings of the climate systems, including such factors as greenhouse gases, volcanic eruptions, solar variations, and aerosols. Also shown are the simulations of the 21st century for the high (A2) emissions scenario.

In these comparisons, both model and observational data are expressed as deviations from the 1901-1960 average. As explained in Section 2.4 (Climatic Trends), acceleration of the anthropogenic forcing occurs shortly after 1960. Thus, for the purposes of comparing net warming between periods of different anthropogenic forcing, 1960 is a rational choice for the ending date of a reference period. It is not practical to choose a beginning date earlier than about 1900 because many model simulations begin in 1900 or 1901 and the uncertainties in the observational time series increase substantially prior to 1900. Therefore, the choice of 1901-1960 as the reference period is well suited for this purpose (comparing the net warming between periods of different anthropogenic forcing). However, there are some uncertainties in the suitability of the 1901-1960 reference period for this purpose. Firstly, there is greater uncertainty in the natural climate forcings (e.g., solar variations) during this time period than in the latter half of the 20th century. If there are sizeable errors in the estimated natural forcings used in climate models, then the simulations will be affected; this type of error does not represent a model deficiency. Secondly, the 1930s "Dust Bowl" era is included in this period. The excessive temperatures experienced then, particularly during the summers, are believed to be caused partially by poor land management through its effects on the surface energy budget. Climate models do not incorporate land management changes and there is no expectation that models should simulate the effects of such. Thirdly, there are certain climate oscillations that occur over several decades. These oscillations have important effects on regional temperatures. A 60-year period is too short to sample entire cycles of some of these, and thus only represents a partial sampling of the true baseline climate.

Figure 33 shows observed (using the same data set as shown in Fig. 5) and simulated decadal mean annual temperature changes for the Northeast U.S. from 1900 to 2100, expressed as deviations from the 1901-1960 average (see later discussion for the rationale for use of this period). The observed rate of warming is similar to that of the models, with temperature values being contained within the envelope of 20th century modeled temperatures for the entire period.

The results for the four seasons are shown in Fig. 34. For most time periods, the observed temperature anomalies are within the envelope of the model simulations, with a few exceptions. For the summer season, observed temperatures for the 1930s are higher than any model simulation. The observed temperatures for winter are higher than any modeled value during the 1950s. The overall warming for the entire observational record is within the range of model simulations for winter, spring, and fall, however, the models overestimate the warming for the summer season due to the high temperatures of the 1930s.

The 21st century portions of the time series indicate that the simulated future warming is much larger than the observed and simulated temperature changes for the 20th century.
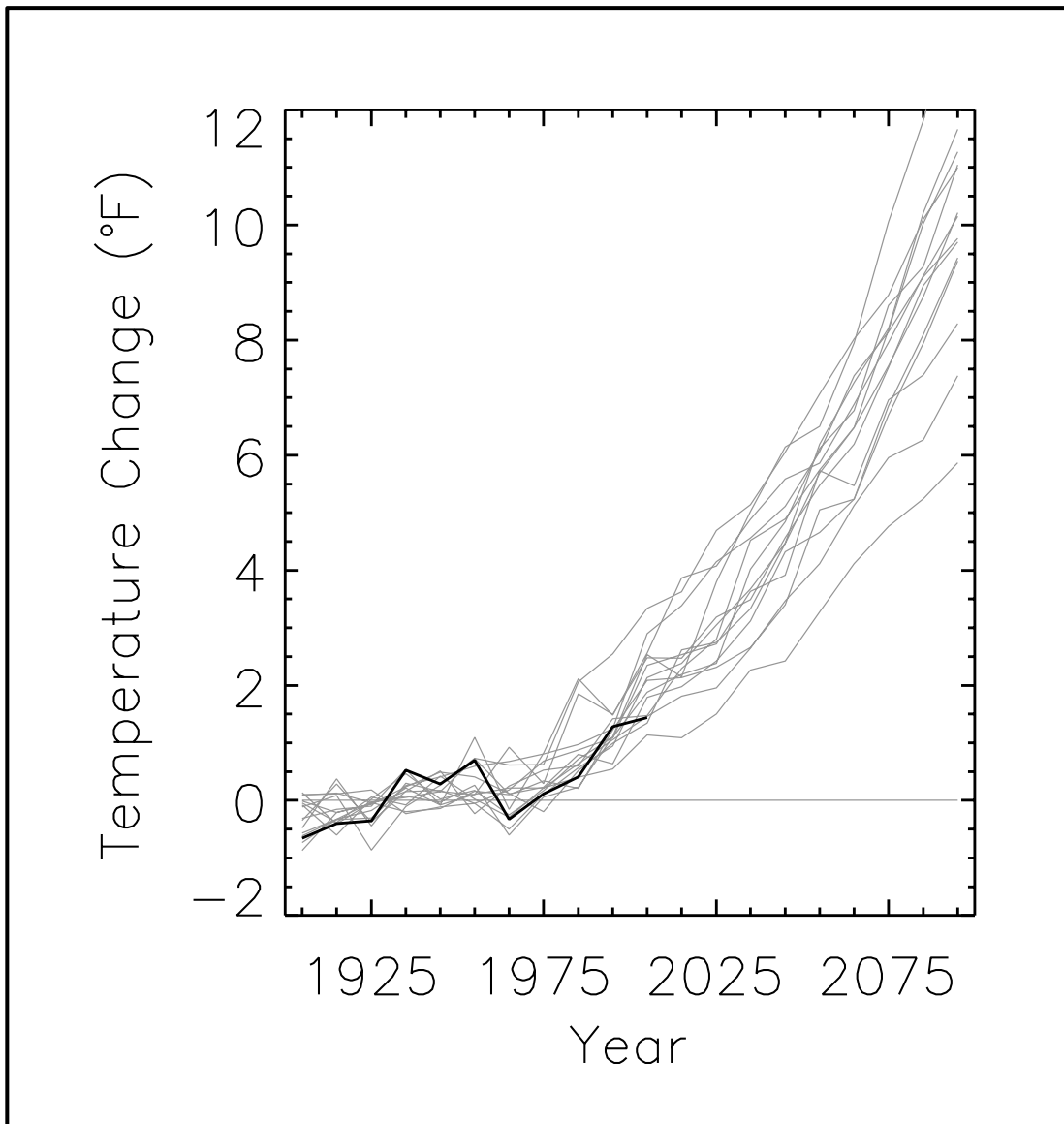
Figure 33. Observed decadal mean annual temperature change (deviations from the 1901-1960 average, °F) for the Northeast U.S. (black line). Based on a new gridded version of the COOP data from the National Climatic Data Center, the CDDv2 data set (R. Vose, personal communication, July 27, 2012). Gray lines indicate the 20th and 21st century simulations from 15 CMIP3 models, for the high (A2) emissions scenario. The observed rate of warming is within the envelope of model simulations.
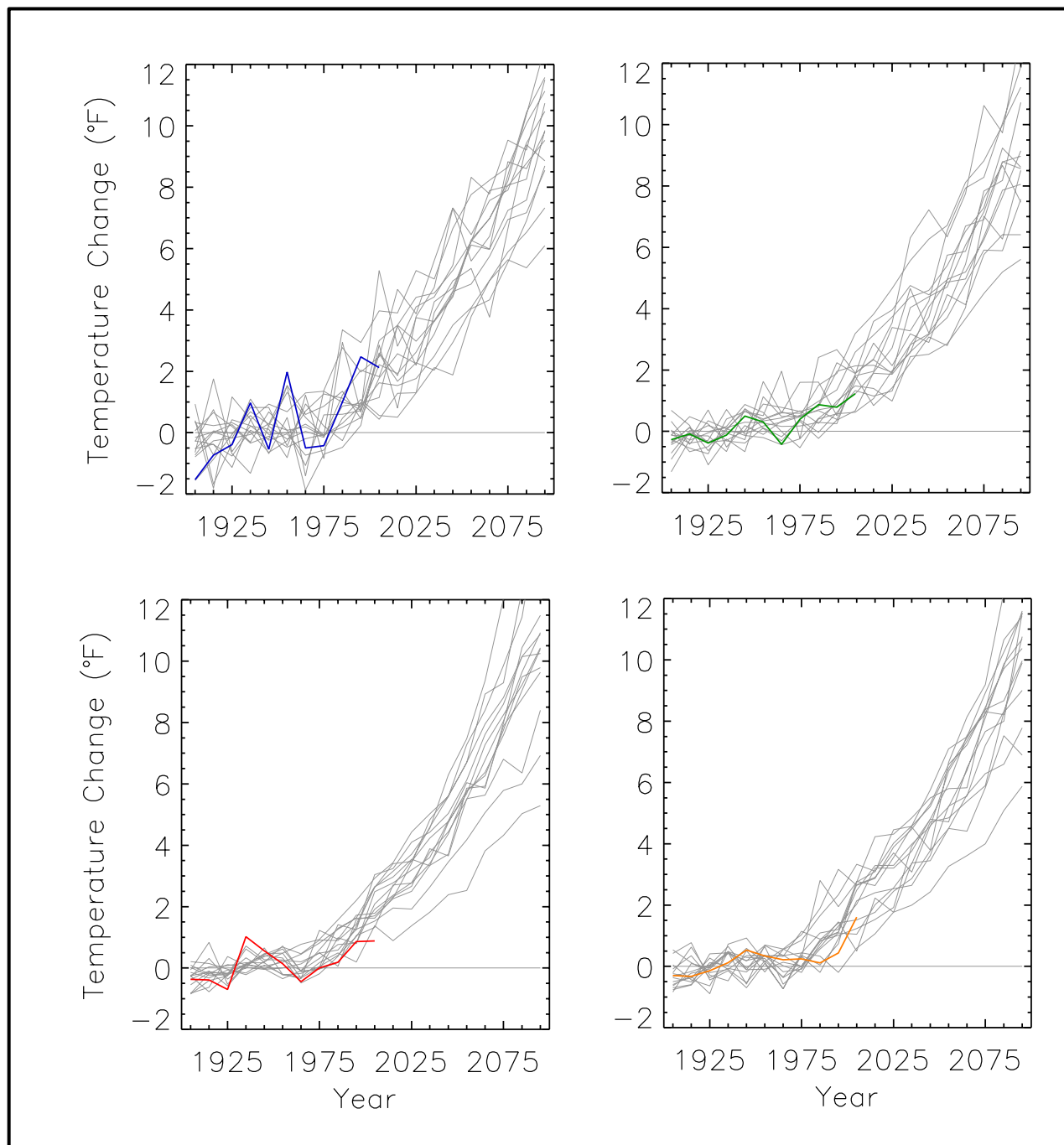
Figure 34. Observed decadal mean temperature change (deviations from the 1901-1960 average, °F) for the Northeast U.S. for winter (top left, blue line), spring (top right, green line), summer (bottom left red line), and fall (bottom right, orange line). Based on a new gridded version of the COOP data from the National Climatic Data Center, the CDDv2 data set (R. Vose, personal communication, July 27, 2012). Gray lines indicate 20th and 21st century simulations from 15 CMIP3 models, for the high (A2) emissions scenario. The observed amount of 20th century warming is generally within the envelope of model simulations.

Observed and model-simulated decadal mean precipitation changes (using the same data set as shown in Fig. 6) can be seen in Fig. 35 for annual and Fig. 36 for seasonal values. Observed variability is generally higher than the model simulations. As a result, a number of decadal values are outside the range of the model simulations. For example, the 1960s are drier than any model simulation for annual, winter, spring, and summer. Summer and fall are wetter than any model simulation in the 2000s. For the 21st century it can be seen that the majority of the models simulate an overall increase in precipitation annually, as well as for the winter and spring seasons, and indicate an overall decrease for summer. These 21st century portions of the time series show increased variability among the model simulations.

The CMIP3 archive contains a total of 74 simulations of the 20th century, 40 simulations of the 21st century for the high (A2) emissions scenario, and 32 simulations of the 21st century for the low (B1) emissions scenario from a total of 23 different models (many models performed multiple simulations for these periods). An exploratory analysis of the entire archive was performed, limited to temperature and to the year as a whole. As before, the data were processed using 1901-1960 as the reference period to calculate anomalies.

Figure 37 compares observations of annual temperature with the entire suite of model simulations. For each model, the annual anomalies were first calculated using the 1901-1960 period as the reference. Then the mean 1901-1960 value from the observations was added to each annual anomaly, essentially removing the model mean bias. In this presentation, the multi-model mean and the 5th and 95th percentile bounds of the model simulations are shown. The mean and percentile values were calculated separately for each year. Then, the curves were smoothed with a 10-year moving boxcar average. The observational time series is not smoothed. During the first half of the 20th century, the observed annual values vary around the model mean because that is the common reference period. These values occasionally fall outside the 5th/95th percentile bounds for the model simulations. After about 1960, the observed values are entirely within the 5th/95th percentile bounds. The rate of observed warming after 1960 is similar to that of the multi-model mean, a similar result to that found in Fig. 33 for a subset of the CMIP3 models.

On decadal time scales, climate variations arising from natural factors can be comparable to or larger than changes arising from anthropogenic forcing. An analysis of change on such time scales was performed by examining the decadal changes simulated by the CMIP3 models with respect to the most recent historical decade of 2001-2010. Figure 38 shows the simulated change in decadal mean values of annual temperature for each future decadal time period with respect to the most recent historical decade of 2001-2010, averaged over the entire Northeast region for the 14 (B1) or 15 (A2) CMIP3 models. For the 2011-2020 decade, the temperature increases are not statistically significant relative to the 2001-2010 decade for most of the models. As the time period increases into the future, more of the individual models simulate statistically significant temperature changes, with all being significant at the 95% confidence level by 2055 for the high emissions scenario (2075 for the low emissions scenario). By this point, all of the model decadal mean values lie outside the 10-90th percentile range of the historical annual temperature anomalies. As also shown in Fig. 33, the model simulations show increased variability over time, with the inter-model range of temperature changes for 2091-2100 being more than double that for 2061-2070 (for the high emissions scenario).
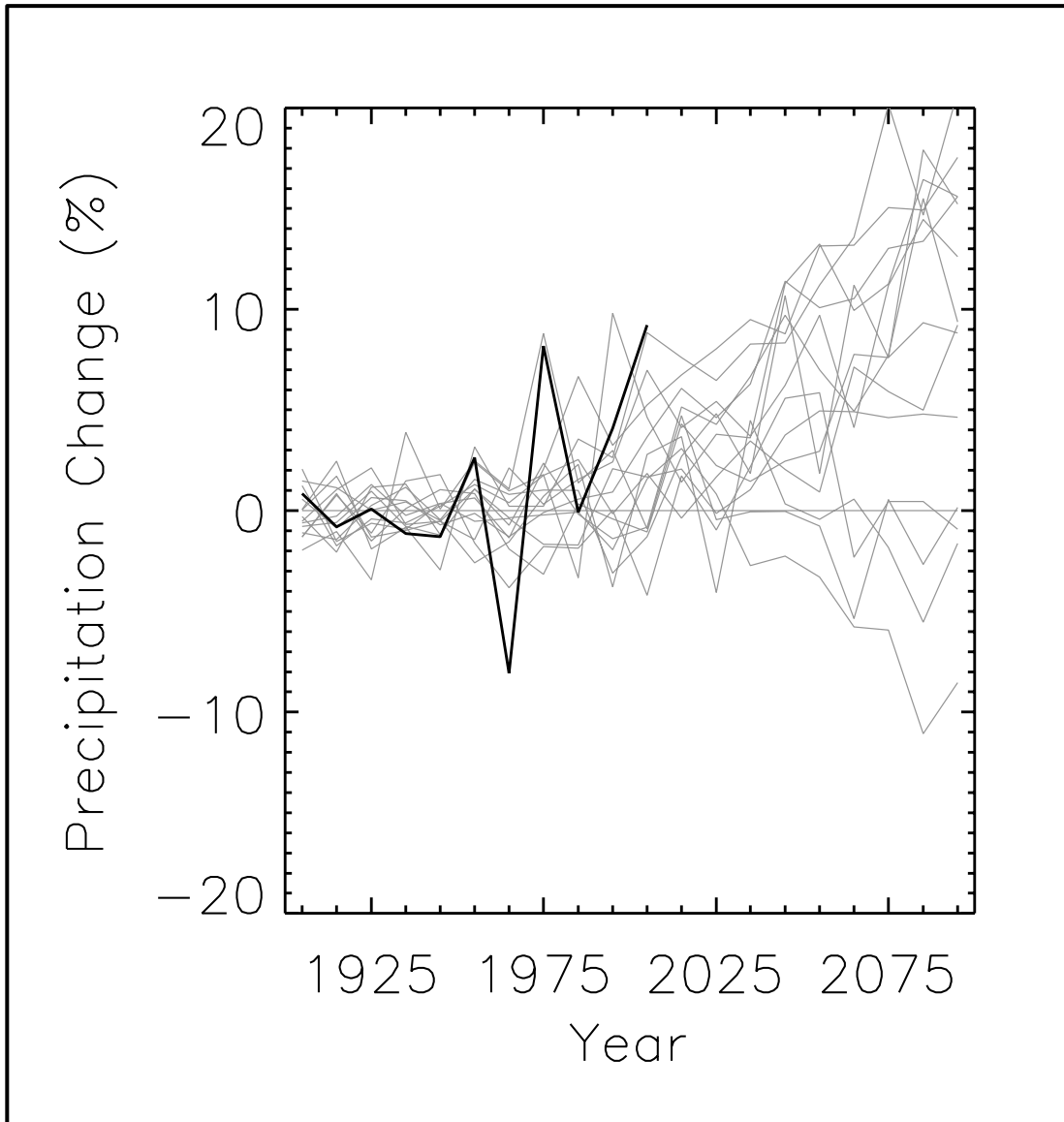
Figure 35. Observed decadal mean annual precipitation change (deviations from the 1901-1960 average, %) for the Northeast U.S. (black line Based on a new gridded version of the COOP data from the National Climatic Data Center, the CDDv2 data set (R. Vose, personal communication, July 27, 2012). Gray lines indicate the 20th *and 21*[st] *century simulations from 15 CMIP3 models, for the high (A2) emissions scenario. Observed precipitation variations are within the model simulations.*
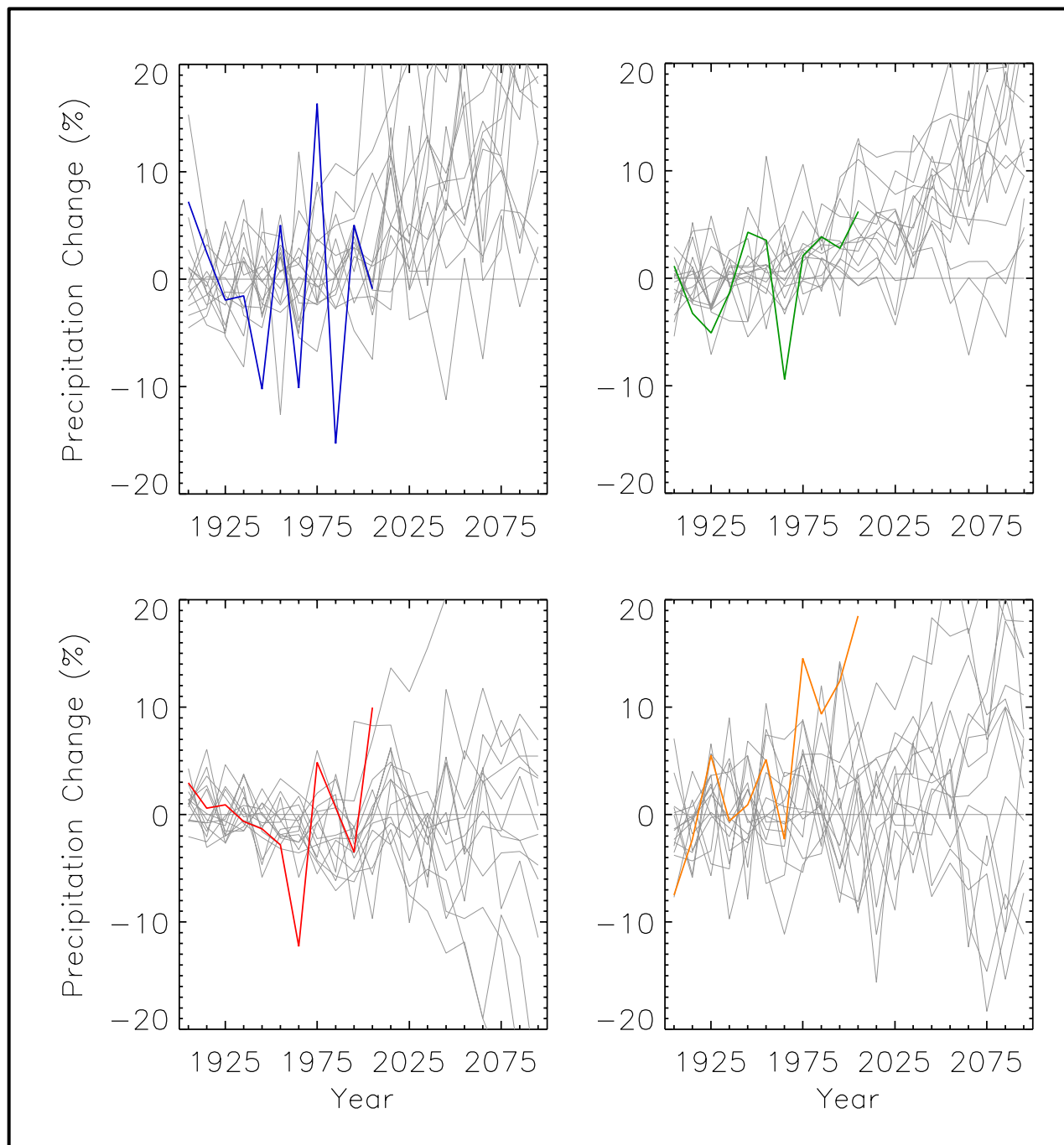
Figure 36. Observed decadal mean precipitation change (deviations from the 1901-1960 average, %) for the Northeast U.S. for winter (top left, blue line), spring (top right, green line), summer (bottom left red line), and fall (bottom right, orange line). Based on a new gridded version of the COOP data from the National Climatic Data Center, the CDDv2 data set (R. Vose, personal communication, July 27, 2012). Gray lines indicate 20th and 21st century simulations from 15 CMIP3 models, for the high (A2) emissions scenario. Observed seasonal precipitation variations are within model simulations for all seasons.
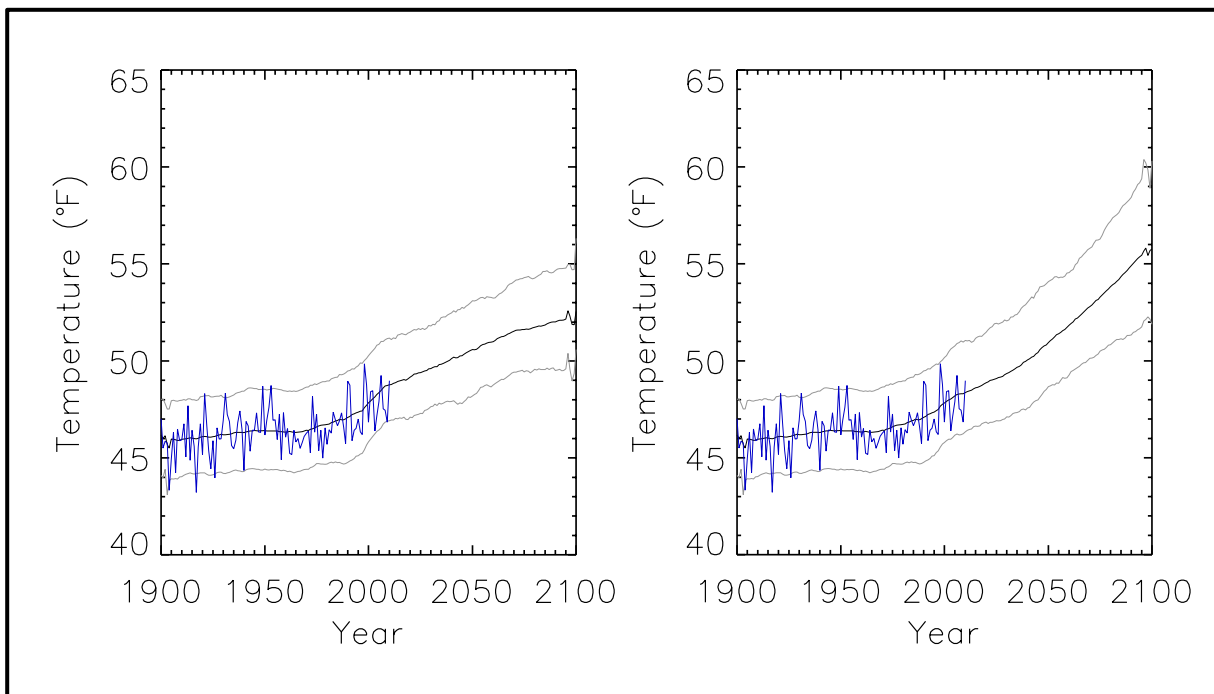
Figure 37. Time series of mean annual temperature for the Northeast region from observations (blue) and from all available CMIP3 global climate model simulations (black and grey). Black represents the mean and grey indicates the 5 and 95% limits of the model simulations. Model mean and percentile limits were calculated for each year separately and then smoothed. Results are shown for the low (B1) emissions scenario (left) and the high (A2) emissions scenario (right). A total of 74 simulations of the 20th century were used. For the 21st century, there were 40 simulations for the high emissions scenario and 32 for the low emissions scenario. For each model simulation, the annual temperature values were first transformed into anomalies by subtracting the simulation's 1901-1960 average from each annual value. Then, the mean bias between model and observations was removed by adding the observed 1901-1960 average to each annual anomaly value from the simulation. For each year, all available model simulations were used to calculate the multi-model mean and the 5th and 95th percentile bounds for that year. Then, the mean and 5th and 95th percentile values were smoothed with a 10-year moving boxcar average.

The corresponding simulated change in decadal mean values of annual precipitation can be seen in Fig. 39. Unlike for temperature, many of the model values of precipitation change are not statistically significant in all decades out to 2091-2099. Increases in multi-model mean precipitation are simulated for all time periods, for both emissions scenarios. An increase in variability over time is seen for the high (A2) emissions scenario, however little change in variability is seen for the low (B1) scenario, with a large number of models lying outside the 10-90th percentile range for all time periods.
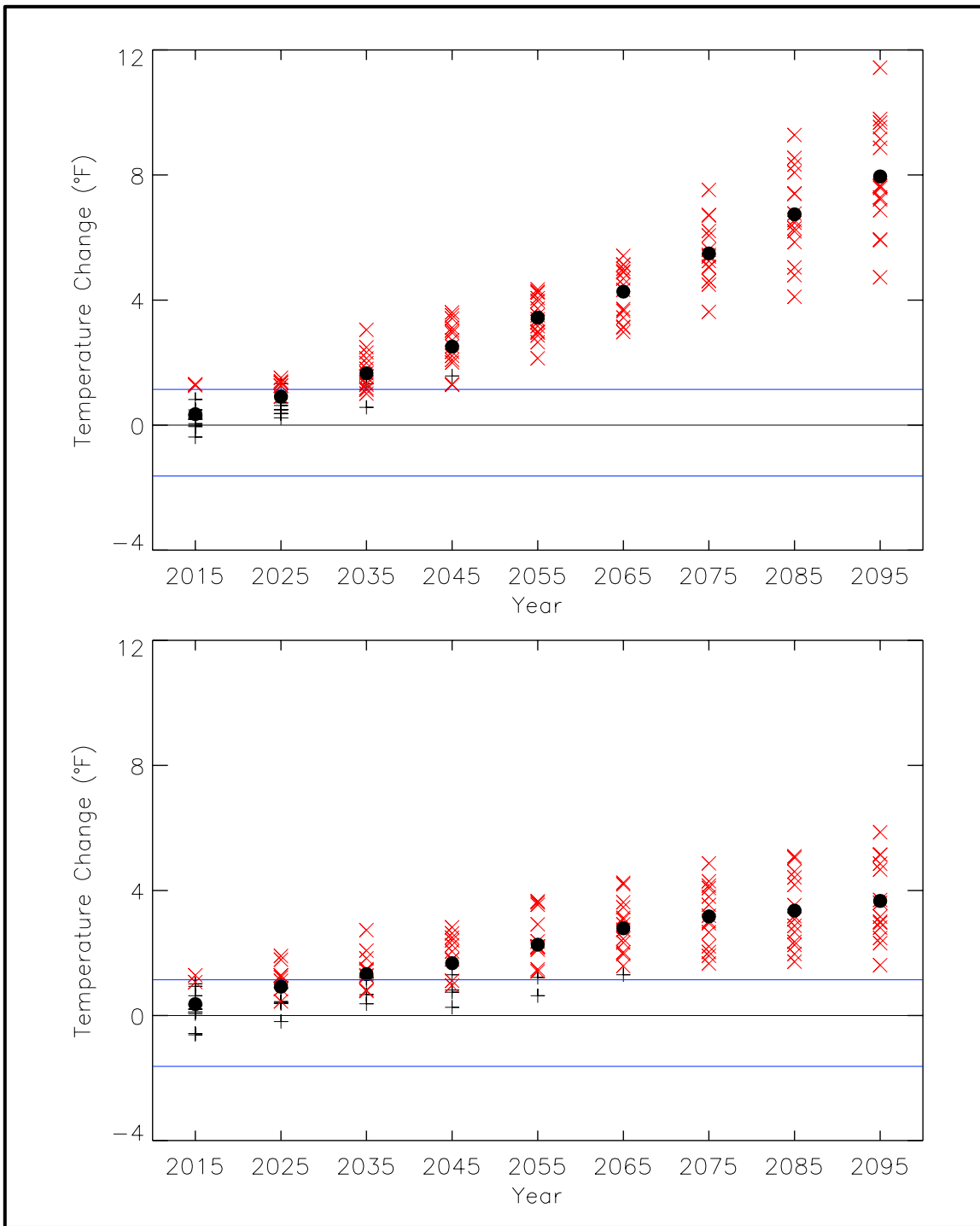
Figure 38. Simulated decadal mean change in annual temperature (°F) for the Northeast U.S. for each future decadal time period (represented by their approximate midpoints, e.g., 2015 = 2011-2020), with respect to the reference period of 2001-2010. Values are given for the high (A2, top) and low (B1, bottom) emissions scenarios for the 14 (B1) or 15 (A2) CMIP3 models. Large circles depict the multi-model means. Each individual model is represented by a black plus sign (+), or a red x if the value is statistically significant at the 95% confidence level. Blue lines indicate the 10th and 90th percentiles of 30 annual anomaly values from 1981-2010. The model simulated warming by 2015 is not statistically significant but by mid-21st century, all models simulate statistically significant warming.
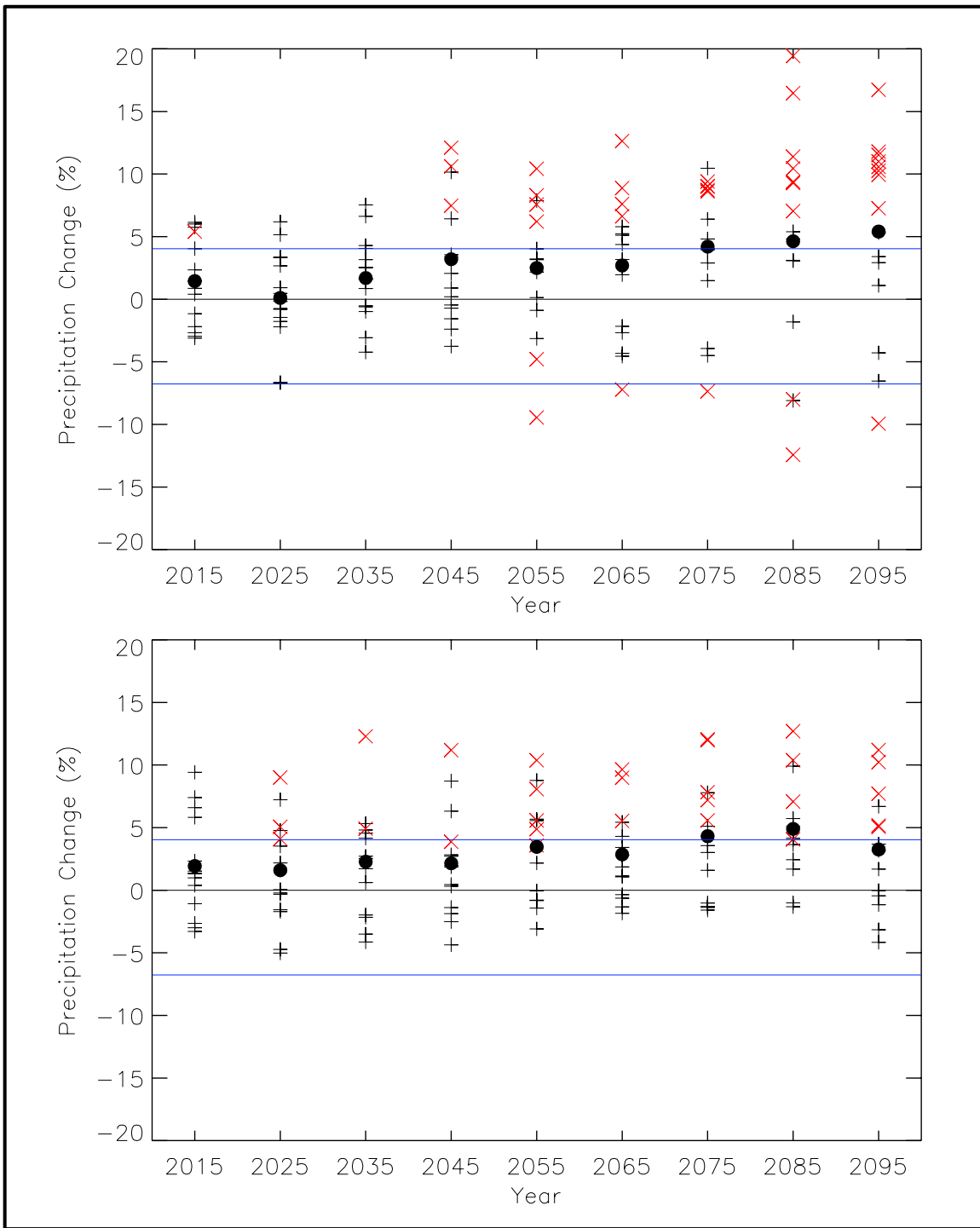
70

Figure 39. Simulated decadal mean change in annual precipitation (%) for the Northeast U.S. for each future decadal time period (represented by their approximate midpoints, e.g., 2015 = 2011-2020), with respect to the reference period of 2001-2010. Values are given for the high (A2, top) and low (B1, bottom) emissions scenarios for the 14 (B1) or 15 (A2) CMIP3 models. Large circles depict the multi-model means. Each individual model is represented by a black plus sign (+), or a red x if the value is statistically significant at the 95% confidence level. Blue lines indicate the 10th and 90th percentiles of the 30 annual anomaly values from 1981-2010. Many models simulate precipitation changes that are not statistically significant out to the end of the 21st century.

71

4. SUMMARY

The primary purpose of this document is to provide physical climate information for potential use by the authors of the 2013 National Climate Assessment report. The document contains two major sections. One section summarizes historical conditions in the U.S. Northeast and primarily focuses on trends in temperature and precipitation metrics that are important in the region. The core observational data set used is that of the National Weather Service's Cooperative Observer Network (COOP).

The second section summarizes climate model simulations for two scenarios of the future path of greenhouse gas emissions: the IPCC SRES high (A2) and low (B1) emissions scenarios. These simulations incorporate analyses from multiple sources, the core source being Coupled Model Intercomparison Project 3 (CMIP3) simulations. Additional sources consist of statistically- and dynamically-downscaled data sets, including simulations from the North American Regional Climate Change Assessment Program (NARCCAP). Analyses of the simulated future climate are provided for the periods of 2021-2050, 2041-2070, and 2070-2099), with changes calculated with respect to an historical climate reference period (1971-1999, 1971-2000, or 1980-2000). The resulting climate conditions are to be viewed as scenarios, not forecasts, and there are no explicit or implicit assumptions about the probability of occurrence of either scenario. The basis for these climate scenarios (emissions scenarios and sources of climate information) were considered and approved by the National Climate Assessment Development and Advisory Committee.

Some key characteristics of the historical climate include:

- Climatic phenomena that have major impacts on the Northeast include flood-producing extreme precipitation, winter storms (Nor'easters), lake-effect snow, ice storms, heat waves, drought, tropical cyclones, and fog.

- Temperatures have generally remained above the 1901-1960 average over the last 30 years. Warming has been more pronounced during the winter and spring seasons. Trends are upward and statistically significant for each season, as well as the year as a whole, with magnitudes ranging from +0.11 to + 0.24°F per decade.

- Annual precipitation shows a clear shift towards greater variability and higher totals since 1970. While summer precipitation exhibits no overall trend, there have been a few very wet summers over the past decade. The two wettest summers on record occurred in 2006 and 2009. Precipitation trends are statistically significant for fall and for the year as a whole.

- The frequency of extreme cold events was high early in the record, followed by a quieter period, and has been generally less than average since a peak in the 1970s and early 1980s. Since 1985, the cold wave index has averaged about 30% below the long-term average.

- The late 19th century into the 1950s was characterized by a moderately high number of heat waves. From the late 1950s into the early 1980s, there were few intense heat waves. Since the late 1980s, the frequency of heat waves has been similar to that of the first half of the 20th century.

- There is substantial decadal-scale variability in the number of extreme precipitation events since about 1935. The index has been quite high since the 1990s, with the highest value occurring in 2008.

- There has been a generally increasing trend in the length of the freeze-free season since the mid-1980s. The average freeze-free season length during 1991-2010 was about 10 days longer than during 1961-1990.

- Over the last 30 years, the spring center-of-volume dates (a measure of the seasonality of river flow volume) have come 1-2 weeks earlier on average.

- Overall warming is further evidenced by later ice-in dates on northeastern lakes, decreases in average snow depth, and an increase in the rate of sea-level rise along the coast. Sea level rose by an average of 1.2 inches per decade during the 20th century.

- Significant trends toward warmer temperatures are apparent in 3 of 4 sub basins of Lake Ontario. Temperatures have increased by more than 5°F across the four basins. Surface water temperatures in Lake Erie have also increased, but at a much lower rate.

The climate characteristics simulated by climate models for the two emissions scenarios have the following key features:

- Models indicate an increase in temperature for all three future periods, with little spatial variation. Changes along coastal areas are slightly smaller than inland areas, and the warming tends to be slightly larger in the north. CMIP3 models indicate that temperature changes across the region are statistically significant for all three future time periods and both emissions scenarios.

- Simulated temperature changes are similar in value for the high and low emissions scenarios for the near future, whereas late in the 21st century, the high (A2) emissions scenario indicates nearly twice the amount of warming.

- The range of model-simulated temperature changes is substantial, indicating substantial uncertainty in the magnitude of warming associated with each scenario. However, in each model simulation, the warming is unequivocal and large compared to historical variations. This is also true for all of the derived temperature variables described below.

- Increases in the number of days with a maximum temperature above 95°F are simulated to occur throughout the region, with the largest increases occurring in the southern and western areas (for the A2 scenario at mid-century).

- Simulated decreases in the average annual number of days with a minimum temperature below 10°F are largest (21 days or more) in northern areas. Decreases in the number of days with a minimum temperature below 32°F are 20-23 days across most of the region (for the A2 scenario at mid-century).

- The freeze-free season is simulated to lengthen by at least 19 days across the region by mid-21st century (for the A2 scenario at mid-century). Simulated increases in most areas are 3-4 weeks.

- Cooling degree days are simulated to increase throughout most of the region, with the largest increases (up to 700) occurring in the southernmost areas of West Virginia and Maryland and the smallest increases (less than 200) occurring in the northernmost areas (for the A2 scenario at mid-century).

- Heating degree days are simulated to decrease throughout the region, with all areas experiencing a decrease of at least 500 heating degree days per year (for the A2 scenario at mid-century). The largest simulated changes of up to 1,500 are in northern areas.

- The far northern regions show the largest simulated increases in average annual precipitation, while southern and coastal areas show less of an increase. Models are mostly in agreement that precipitation will increase over the entire region under these scenarios, other than a small area in the south where models do not agree about the sign of the change. Simulated seasonal changes are mostly upward in winter, spring, and fall, and downward in summer. However, the range of model-simulated precipitation changes is considerably larger than the multi-model mean change. Thus, there is great uncertainty associated with future precipitation changes in these scenarios.

- All areas see simulated increases in the number of days with precipitation totals exceeding 1 inch, with the greatest increases (up to 30%) occurring in parts of New York (for the A2 scenario at mid-century). The simulated increases are statistically significant in most northern areas. The changes in the average annual maximum number of consecutive days with precipitation of less than 0.1 inches are not statistically significant in any area.

- Most models do not indicate a statistically significant change in temperature (with respect to 2001-2010) for the near future; however, as the time period increases, a greater number of models simulate statistically significant temperature changes, with all being significant at the 95% confidence level by 2055 (for the high emissions scenario).

- Many of the modeled values of decadal precipitation change are not statistically significant, with respect to 2001-2010, out to 2091-2099.

A comparison of model simulations of the 20th century with observations indicates the following:

- For most time periods, the observed temperature changes are within the envelope of model simulated changes, with a few exceptions. For the summer season, the observed increase in temperature from the 1920s to the Dust Bowl era of the 1930s and the subsequent decrease from the 1930s to the 1960s are not simulated by any model. For then annual time series, the decrease from the 1950s to the 1960s is greater than any model. Simulations of temperature in the 21st century indicate that future warming is much larger than the observed and simulated values for the 20th century.

- The variability in observed precipitation change tends to be somewhat higher than that of the models.

5. REFERENCES

AchutaRao, K., and K.R. Sperber, 2002: Simulation of the El Niño Southern Oscillation: Results from the Coupled Model Intercomparison Project. *Clim. Dyn.,* **19,** 191–209.

Arakawa, A., 2004: The cumulus parameterization problem: Past, present, and future. *J. Climate,* **17**, 2493-2525.

Bader D. C., C. Covey, W. J. Gutowski Jr., I. M. Held, K. E. Kunkel, R. L. Miller, R. T. Tokmakian, and M. H. Zhang, 2008: *Climate models: An Assessment of Strengths and Limitations*. U.S. Climate Change Science Program Synthesis and Assessment Product 3.1. Department of Energy, Office of Biological and Environmental Research, 124 pp.

Blake, E. S., C. W. Landsea, and E. J. Gibney, 2011: The Deadliest, Costliest and Most Intense United States Tropical Cyclones from 1851 to 2010 (and other Frequently Requested Hurricane Facts). NOAA Technical Memorandum NWS NHC-6, 47 pp. [Available online at http://www.nhc.noaa.gov/pdf/nws-nhc-6.pdf.]

Cortinas Jr, J. V., B. C. Bernstein, C. C. Robbins, and J. Walter Strapp, 2004: An Analysis of freezing rain, freezing drizzle, and ice pellets across the United States and Canada: 1976-90. *Weather Forecast.*, **19,** 377-390.

DeGaetano, A. T., 2000: Climatic perspective and impacts of the 1998 northern New York and New England ice storm. *Bull. Am Meteorol. Soc.*, **81,** 237-254.

——, 2009: Time-Dependent Changes in Extreme-Precipitation Return-Period Amounts in the Continental United States. *J. Appl. Meteorol. Climatol.*, **48,** 2086-2099.

Dobiesz, N. E., and N. P. Lester, 2009: Changes in mid-summer water temperature and clarity across the Great Lakes between 1968 and 2002. *J. Great Lakes Res.*, **35,** 371-384.

Dufresne, J.-L., and S. Bony. 2008: An assessment of the primary sources of spread of global warming estimates from coupled ocean–atmosphere models. *J. Climate,* **21**, 5135-5144.

Dupigny-Giroux, L.-A., 2002: Climate variability and socioeconomic consequences of Vermont's natural hazards: A historical perspective. *Vermont History.*, **70,** 19-39.

Fall, S., A. Watts, J. Nielsen-Gammon, E. Jones, D. Niyogi, J. R. Christy, and R. A. Pielke Sr, 2011: Analysis of the impacts of station exposure on the US Historical Climatology Network temperatures and temperature trends. *J. Geophys. Res.*, **116,** D14120.

Hayhoe, K., and Coauthors, 2004: Emission pathways, climate change, and impacts on California. *P. Natl. Acad. Sci. USA*, **101,** 12422-12427.

Hayhoe, K., and Coauthors, 2008: Regional climate change projections for the Northeast USA. *Mitig. Adapt. Strateg. Glob. Change*, **13,** 425-436.

Hayhoe, K. A., 2010: A standardized framework for evaluating the skill of regional climate downscaling techniques. Ph.D. thesis, University of Illinois, 153 pp. [Available online at https://www.ideals.illinois.edu/handle/2142/16044.]

Hodgkins, G., R. Dudley, and T. Huntington, 2003: Changes in the timing of high river flows in New England over the 20th century. *J. Hydrol.*, **278,** 244-252.

Hodgkins, G. A., and R. W. Dudley, 2006: Changes in late-winter snowpack depth, water equivalent, and density in Maine, 1926–2004. *Hydrol. Process.*, **20,** 741-751.

Hubbard, K., and X. Lin, 2006: Reexamination of instrument change effects in the US Historical Climatology Network. *Geophys. Res. Lett.*, **33,** L15710.

IPCC, 2000: *Special Report on Emissions Scenarios: A Special Report of Working Group III of the Intergovernmental Panel on Climate Change,* N. Nakicenovic, and R. Swart, Eds., Cambridge University Press, 570 pp.

——, 2007: *Climate Change 2007: Synthesis Report. Contribution of Working Groups I, II and III to the Fourth Assessment Report of the Intergovernmental Panel on Climate Change,* Pachauri, R. K, and Reisinger, A., Eds., IPCC, 104 pp.

——, cited 2012: IPCC Data Distribution Centre. [Available online at http://www.ipcc-data.org/ddc_co2.html.]

Jarrell, J. D., P. J. Hebert, and M. Mayfield, 1992: Hurricane Experience Levels of Coastal County Populations from Texas to Maine. NOAA Technical Memorandum NWS NHC-46, 152 pp. [Available online at http://www.nhc.noaa.gov/pdf/NWS-NHC-1992-46.pdf.]

Jones, P. D., P. Y. Groisman, M. Coughlan, N. Plummer, W. C. Wang, and T. R. Karl, 1990: Assessment of urbanization effects in time series of surface air temperature over land. *Nature*, **347,** 169-172.

Karl, T. R., C. N. Williams Jr, P. J. Young, and W. M. Wendland, 1986: A model to estimate the time of observation bias associated with monthly mean maximum, minimum and mean temperatures for the United States. *J. Appl. Meteorol.*, **25,** 145-160.

Karl, T. R., H. F. Diaz, and G. Kukla, 1988: Urbanization: Its detection and effect in the United States climate record. *J. Climate*, **1,** 1099-1123.

Karl, T. R., J. M. Melillo, and T. C. Peterson, Eds, 2009: *Global Climate Change Impacts in the United States.* Cambridge University Press, 188 pp.

Knutti, R., 2010: The end of model democracy? *Climatic Change*, **102,** 395-404.

Kocin, P. J., and L. W. Uccellini, 2004a: A Snowfall Impact Scale Derived from Northeast Storm Snowfall Distributions. *Bull. Am. Meteorol. Soc.*, **85,** 177-194.

——, 2004b: *Northeast Snowstorms.* American Meterorological Society, 818 pp.

LSU, cited 2012: Climate Trends. [Available online at http://charts.srcc.lsu.edu/trends/.]

Maurer, E. P., A. W. Wood, J. C. Adam, D. P. Lettenmaier, and B. Nijssen, 2002: A long-term hydrologically based dataset of land surface fluxes and states for the conterminous United States. *J. Climate*, **15,** 3237–3251.

Meehl, G. A., W. M. Washington, T. M. L. Wigley, J. M. Arblaster, and A. Dai, 2003: Solar and greenhouse gas forcing and climate response in the twentieth century. *J. Climate*, **16,** 426-444.

Meehl, G. A., and Coauthors, 2007: Global climate projections. *Climate Change 2007: The Physical Basis. Contribution of Working Group I to the Fourth Assessment Report of the Intergovernmental Panel on Climate Change*, Solomon, S., D. Qin, M. Manning, Z. Chen, M. Marquis, K.B. Averyt, M. Tignor, and H.L. Miller, Eds., Cambridge University Press, 747-845.

Menne, M. J., C. N. Williams, and R. S. Vose, 2009: The US Historical Climatology Network monthly temperature data, version 2. *Bull. Am. Meteorol. Soc.*, **90,** 993-1007.

Menne, M. J., C. N. Williams, and M. A. Palecki, 2010: On the reliability of the U.S. surface temperature record. *J. Geophys. Res.*, **115,** D11108.

Monahan, A.H., and A. Dai, 2004: The spatial and temporal structure of ENSO nonlinearity. *J. Climate,* **17,** 3026–3036.

NARCCAP, cited 2012: North American Regional Climate Change Assessment Program. [Available online at http://www.narccap.ucar.edu/.]

NOAA, cited 2012a: Cooperative Observer Program. [Available online at http://www.nws.noaa.gov/om/coop/.]

——, cited 2012b: NCEP/DOE AMIP-II Reanalysis. [Available online at http://www.cpc.ncep.noaa.gov/products/wesley/reanalysis2/.]

NOAA GLERL, cited 2012: Great Lakes Water Level Observations. [Available online at http://www.glerl.noaa.gov/data/now/wlevels/levels.html.]

Norton, C. W., P.-S. Chu, and T. A. Schroeder, 2011: Projecting changes in future heavy rainfall events for Oahu, Hawaii: A statistical downscaling approach. *J. Geophys. Res*., **116,** D17110.

NWS, 1993: Cooperative Program Operations. National Weather Service Observing Handbook No. 6, 56 pp. [Available online at http://www.srh.noaa.gov/srh/dad/coop/coophb6.pdf.]

NWS, cited 2012a: Dates of Lake Champlain Closing. [Available online at http://www.erh.noaa.gov/btv/climo/lakeclose.shtml.]

——, cited 2012b: Tropical Cyclone Climatology. [Available online at http://www.nhc.noaa.gov/climo/#usl.]

Overland, J. E., M. Wang, N. A. Bond, J. E. Walsh, V. M. Kattsov, and W. L. Chapman, 2011: Considerations in the selection of global climate models for regional climate projections: The Arctic as a case study. *J. Climate*, **24,** 1583-1597.

PCMDI, cited 2012: CMIP3 Climate Model Documentation, References, and Links. [Available online at http://www-pcmdi.llnl.gov/ipcc/model_documentation/ipcc_model_documentation.php.]

PSMSL, cited 2012: Permanent Service for Mean Sea Level. [Available online at http://www.psmsl.org/data/obtaining/.]

Quayle, R. G., D. R. Easterling, T. R. Karl, and P. Y. Hughes, 1991: Effects of recent thermometer changes in the cooperative station network. *Bull. Am. Meteorol. Soc.*, **72,** 1718-1723.

Randall, D.A., and Coauthors, 2007: Climate models and their evaluation. *Climate Change 2007: The Physical Basis. Contribution of Working Group I to the Fourth Assessment Report of the Intergovernmental Panel on Climate Change*, Solomon, S., D. Qin, M. Manning, Z. Chen, M. Marquis, K.B. Averyt, M. Tignor, and H.L. Miller, Eds., Cambridge University Press, 590-662.

Tebaldi, C., J. M. Arblaster, and R. Knutti, 2011: Mapping model agreement on future climate projections. *Geophys. Res. Lett.*, **38,** L23701.

U.S. Census Bureau, cited 2011: Metropolitan and Micropolitan Statistical Areas. [Available online at http://www.census.gov/popest/data/metro/totals/2011/.]

Vose, R. S., C. N. Williams, Jr., T. C. Peterson, T. R. Karl, and D. R. Easterling, 2003: An evaluation of the time of observation bias adjustment in the U.S. Historical Climatology Network. *Geophys. Res. Lett.*, **30,** 2046.

Wilby, R. L., and T. Wigley, 1997: Downscaling general circulation model output: a review of methods and limitations. *Prog. Phys. Geog.*, **21,** 530.

Williams, C. N., M. J. Menne, and P. W. Thorne, 2011: Benchmarking the performance of pairwise homogenization of surface temperatures in the United States. *J. Geophys. Res.*, **52,** 154-163.

6. ACKNOWLEDGEMENTS

A partial listing of reports appears below:

NESDIS 102 NOAA Operational Sounding Products From Advanced-TOVS Polar Orbiting Environmental Satellites. Anthony L. Reale, August 2001.

NESDIS 103 GOES-11 Imager and Sounder Radiance and Product Validations for the GOES-11 Science Test. Jaime M. Daniels and Timothy J. Schmit, August 2001.

NESDIS 104 Summary of the NOAA/NESDIS Workshop on Development of a Coordinated Coral Reef Research and Monitoring Program. Jill E. Meyer and H. Lee Dantzler, August 2001.

NESDIS 105 Validation of SSM/I and AMSU Derived Tropical Rainfall Potential (TRaP) During the 2001 Atlantic Hurricane Season. Ralph Ferraro, Paul Pellegrino, Sheldon Kusselson, Michael Turk, and Stan Kidder, August 2002.

NESDIS 106 Calibration of the Advanced Microwave Sounding Unit-A Radiometers for NOAA-N and NOAA-N=. Tsan Mo, September 2002.

NESDIS 107 NOAA Operational Sounding Products for Advanced-TOVS: 2002.   Anthony L. Reale, Michael W. Chalfant, Americo S. Allegrino, Franklin H. Tilley, Michael P. Ferguson, and Michael E. Pettey, December 2002.

NESDIS 108 Analytic Formulas for the Aliasing of Sea Level Sampled by a Single Exact-Repeat Altimetric Satellite or a Coordinated Constellation of Satellites. Chang-Kou Tai, November 2002.

NESDIS 109 Description of the System to Nowcast Salinity, Temperature and Sea nettle (*Chrysaora quinquecirrha*) Presence in Chesapeake Bay Using the Curvilinear Hydrodynamics in 3-Dimensions (CH3D) Model.   Zhen Li, Thomas F. Gross, and Christopher W. Brown, December 2002.

NESDIS 110 An Algorithm for Correction of Navigation Errors in AMSU-A Data. Seiichiro Kigawa and Michael P. Weinreb, December 2002.

NESDIS 111 An Algorithm for Correction of Lunar Contamination in AMSU-A Data. Seiichiro Kigawa and Tsan Mo, December 2002.

NESDIS 112 Sampling Errors of the Global Mean Sea Level Derived from Topex/Poseidon Altimetry. Chang-Kou Tai and Carl Wagner, December 2002.

NESDIS 113 Proceedings of the International GODAR Review Meeting: Abstracts. Sponsors: Intergovernmental Oceanographic Commission, U.S. National Oceanic and Atmospheric Administration, and the European Community, May 2003.

NESDIS 114 Satellite Rainfall Estimation Over South America: Evaluation of Two Major Events. Daniel A. Vila, Roderick A. Scofield, Robert J. Kuligowski, and J. Clay Davenport, May 2003.

NESDIS 115 Imager and Sounder Radiance and Product Validations for the GOES-12 Science Test. Donald W. Hillger, Timothy J. Schmit, and Jamie M. Daniels, September 2003.

NESDIS 116 Microwave Humidity Sounder Calibration Algorithm. Tsan Mo and Kenneth Jarva, October 2004.

NESDIS 117 Building Profile Plankton Databases for Climate and EcoSystem Research. Sydney Levitus, Satoshi Sato, Catherine Maillard, Nick Mikhailov, Pat Cadwell, Harry Dooley, June 2005.

NESDIS 118 Simultaneous Nadir Overpasses for NOAA-6 to NOAA-17 Satellites from 1980 and 2003 for the Intersatellite Calibration of Radiometers. Changyong Cao, Pubu Ciren, August 2005.

NESDIS 119 Calibration and Validation of NOAA 18 Instruments. Fuzhong Weng and Tsan Mo, December 2005.

NESDIS 120 The NOAA/NESDIS/ORA Windsat Calibration/Validation Collocation Database. Laurence Connor, February 2006.

NESDIS 121 Calibration of the Advanced Microwave Sounding Unit-A Radiometer for METOP-A. Tsan Mo, August 2006.

NESDIS 122   JCSDA Community Radiative Transfer Model (CRTM). Yong Han, Paul van Delst, Quanhua
             Liu, Fuzhong Weng, Banghua Yan, Russ Treadon, and John Derber, December 2005.
NESDIS 123   Comparing Two Sets of Noisy Measurements. Lawrence E. Flynn, April 2007.
NESDIS 124   Calibration of the Advanced Microwave Sounding Unit-A for NOAA-N'. Tsan Mo, September
             2007.
NESDIS 125   The GOES-13 Science Test: Imager and Sounder Radiance and Product Validations. Donald
             W. Hillger, Timothy J. Schmit, September 2007.
NESDIS 126   A QA/QC Manual of the Cooperative Summary of the Day Processing System. William E.
             Angel, January 2008.
NESDIS 127   The Easter Freeze of April 2007: A Climatological Perspective and Assessment of Impacts and
             Services. Ray Wolf, Jay Lawrimore, April 2008.
NESDIS 128   Influence of the ozone and water vapor on the GOES Aerosol and Smoke Product (GASP)
             retrieval. Hai Zhang, Raymond Hoff, Kevin McCann, Pubu Ciren, Shobha Kondragunta, and
             Ana Prados, May 2008.
NESDIS 129   Calibration and Validation of NOAA-19 Instruments. Tsan Mo and Fuzhong Weng, editors,
             July 2009.
NESDIS 130   Calibration of the Advanced Microwave Sounding Unit-A Radiometer for METOP-B. Tsan
             Mo, August 2010.
NESDIS 131   The GOES-14 Science Test: Imager and Sounder Radiance and Product Validations. Donald
             W. Hillger and Timothy J. Schmit, August 2010.
NESDIS 132   Assessing Errors in Altimetric and Other Bathymetry Grids. Karen M. Marks and Walter
             H.F. Smith, January 2011.
NESDIS 133   The NOAA/NESDIS Near Real Time CrIS Channel Selection for Data Assimilation and
             Retrieval Purposes. Antonia Gambacorta, Chris Barnet, Walter Wolf, Thomas King, Eric
             Maddy, Murty Divakarla, Mitch Goldberg, April 2011.
NESDIS 134   Report from the Workshop on Continuity of Earth Radiation Budget (CERB) Observations:
             Post-CERES Requirements. John J. Bates and Xuepeng Zhao, May 2011.
NESDIS 135   Averaging along-track altimeter data between crossover points onto the midpoint gird:
             Analytic formulas to describe the resolution and aliasing of the filtered results. Chang-Kou
             Tai, August 2011.
NESDIS 136   Separating the Standing and Net Traveling Spectral Components in the Zonal-Wavenumber
             and Frequency Spectra to Better Describe Propagating Features in Satellite Altimetry. Chang-
             Kou Tai, August 2011.
NESDIS 137   Water Vapor Eye Temperature vs. Tropical Cyclone Intensity. Roger B. Weldon, August 2011.
NESDIS 138   Changes in Tropical Cyclone Behavior Related to Changes in the Upper Air Environment.
             Roger B. Weldon, August 2011.
NESDIS 139   Computing Applications for Satellite Temperature Datasets: A Performance Evaluation of
             Graphics Processing Units. Timothy F.R. Burgess and Scott F. Heron, December 2011.
NESDIS 140   Microburst Nowcasting Applications of GOES. Kenneth L. Pryor, September 2011.
NESDIS 141   The GOES-15 Science Test: Imager and Sounder Radiance and Product Validations. Donald
             W. Hillger and Timothy J. Schmit, November 2011.

NOAA SCIENTIFIC AND TECHNICAL PUBLICATIONS

The National Oceanic and Atmospheric Administration was established as part of the Department of Commerce on October 3, 1970. The mission responsibilities of NOAA are to assess the socioeconomic impact of natural and technological changes in the environment and to monitor and predict the state of the solid Earth, the oceans and their living resources, the atmosphere, and the space environment of the Earth.

The major components of NOAA regularly produce various types of scientific and technical information in the following types of publications

PROFESSIONAL PAPERS – Important definitive research results, major techniques, and special investigations.

CONTRACT AND GRANT REPORTS – Reports prepared by contractors or grantees under NOAA sponsorship.

ATLAS – Presentation of analyzed data generally in the form of maps showing distribution of rainfall, chemical and physical conditions of oceans and atmosphere, distribution of fishes and marine mammals, ionospheric conditions, etc.

TECHNICAL SERVICE PUBLICATIONS – Reports containing data, observations, instructions, etc. A partial listing includes data serials; prediction and outlook periodicals; technical manuals, training papers, planning reports, and information serials; and miscellaneous technical publications.

TECHNICAL REPORTS – Journal quality with extensive details, mathematical developments, or data listings.

TECHNICAL MEMORANDUMS – Reports of preliminary, partial, or negative research or technology results, interim instructions, and the like.

U.S. DEPARTMENT OF COMMERCE
National Oceanic and Atmospheric Administration
National Environmental Satellite, Data, and Information Service
Washington, D.C. 20233